BEHAVIOUR OF STRIP FOOTING RESTING ON PRETENSIONED GEOGRID REINFORCED FERROCHROME SLAG SUBGRADE

Thesis submitted in partial fulfillment of the requirements for the award of the degree of

MASTER OF TECHNOLOGY

in

GEOTECHNICAL ENGINEERING

by

ATUL KUMAR
(2016PGCEGE08)

Under the esteemed guidance of

Dr. A. K. CHOUDHARY

DEPARTMENT OF CIVIL ENGINEERING

NATIONAL INSTITUTE OF TECHNOLOGY, JAMSHEDPUR
JHARKHAND, INDIA-831014

JUNE, 2018

© NATIONAL INSTITUTE OF TECHNOLOGY JAMSHEDPUR, 2017

ALL RIGHTS RESERVED

NATIONAL INSTITUTE OF TECHNOLOGY JAMSHEDPUR

CANDIDATE'S DECLARATION

I hereby certify that this work is being proposed in the dissertation entitled **"Behaviour of Strip Footing Resting on Pretensioned Geogrid Reinforced Ferrochrome Slag Subgrade"** in partial fulfillment for the award of degree of Master of Technology and submitted in Civil Engineering Department, National Institute of Technology Jamshedpur is an authentic record of my own work carried out during a period from August 2017 to June 2018 under the supervision of Dr. Anil Kumar Choudhary, Professor, Department of Civil Engineering, National Institute of Technology Jamshedpur.

The matter embodied in this dissertation has not been submitted by me for the award of any other degree.

(ATUL KUMAR)

Reg. No.: 2016PGCEGE08

This is to certify that the above statement made by the candidate is true and correct to the best of my/our knowledge and belief.

(Dr. Anil Kumar Choudhary)
Professor
Department of Civil Engineering
NIT Jamshedpur

Date:.....

The viva-voce examination of **Mr. Atul Kumar,** Master of Technology, has been held on.....

Signature of Supervisor

External Examiner

Head of the Department
Civil Engineering
NIT Jamshedpur

This work is dedicated to my beloved family....

ACKNOWLEDGEMENT

This thesis would not have been possible without the inspiration and support of a number of wonderful individuals — my thanks and appreciation to all of them for being part of this journey and making this thesis possible.

I owe my deepest gratitude to my supervisor **Dr. Anil Kumar Choudhary**. Without their enthusiasm, support encouragement, and continuous optimism this thesis would hardly have been completed.

I thank Prof. Karunesh Kumar Shukla, Director, NIT Jamshedpur for the support extended towards the work. I thank Dr. R.P. Singh, Head of the institute, Department of Civil Engineering, for the appreciation of my work.

I thank all teaching and non-teaching staff of the Department of Civil Engineering for their constant support.

My special thanks to Dr. Sanjay Kumar Shukla, Professor, Edith Cowan University, Australia. I thank him for spending his valuable time to give important feedbacks over the entire course of work.

I express my warmest gratitude to my senior Ujjwal Kumar. His guidance and motivation for this project from starting to end has put a significant influence in shaping many of the concepts presented in this thesis.

I also want to express my gratitude to my colleague and friend Madhumita Mohanti, Ashish tyagi and GRK Reddy. They have made available his support in a number of ways, especially towards the completion of experimental work.

I gratefully acknowledge the contributions of Manjeet Singh Saini who helped me in fixing the instruments of the test setup. I would like to thank all my friends especially Krishna, Madhumita, for his frequent help and support. Finally, my deep and sincere gratitude to my family for their continuous and unparalleled love, help and support. They selflessly encouraged me to explore new directions in life and seek my own destiny. This journey would not have been possible if not for them, and I dedicate this milestone to them.

ABSTRACT

Since last few decades, India has witnessed rapid industrialization and urbanization. To fuel the need for infrastructural development, a large number of steel plants have been set up which generate large amount of industrial wastes in the form of fly-ash, slag etc. without proper disposal solutions. Ferrochrome slag is one such industrial waste obtained during the manufacturing of high carbon ferrochromium alloy which is the vital component in the manufacture of stainless steel. Ferrochrome slag resembles coarse dark colored sand. Use of ferrochrome slag as a substitute for natural soil shall not only mitigate the problems of waste disposal but also reduce the problem of environmental degradation.

Further; It is well established that reinforce earth technique is quite beneficial for improving the strength and deformation characteristics of soil especially the granular soils. It has been previously observed that, for low levels of settlement, strains in the soil are insufficient to mobilize tensile load in the reinforcement. This may not be a desirable feature for shallow footings where deformation allowed is very limited. To overcome this problem, reinforcement can be pre-tensioned.

The paper presents the results of a series of model footing tests conducted with a strip footing resting on ferrochrome slag subgrade. The tests were conducted in a tank of size 100cm x 50cm x 70cm. A rigid strip footing of size 50cm x 10cm was used. The model footing tests were conducted with unreinforced ferrochrome slag subgrade, subgrade reinforced with a single layer of geogrid without pre-tension as well as pre-tensioned geogrid. Embedment depth for the geogrid was varied corresponding to the width of the footing for both the cases. For pre- tensioned geogrid; pre-tension force on the geogrid was varied as 1% 2% 3% of tensile strength of geogrid. It is concluded that pre tensioning of the geogrid is quite beneficial in enhancing the reinforcement efficiency.

Keywords: *Bearing capacity, Ferrochrome slag, Model strip footing, Pre-tensioned geogrid.*

INDEX

CONTENT	Page
CANDIDATE'S DECLARATION	i
ACKNOWLEDGEMENT	iii
ABSTRACT	iv
Contents	v
LIST OF TABLES	ix
LIST OF FIGURES	x
LIST OF SYMBOLS	xiii
CHAPTER -1	1
INTRODUCTION	1
1.1 GENERAL	1
1.1.1 Composition of Ferrochrome Slag	3
1.1.2 Production of ferrochrome slag	3
1.1.3 Utilization of ferrochrome slag	4
1.1.4 Issues preventing broader recycling	5
1.2 GEOGRID	7
1.2.1 Graphical symbol proposed by IGS	8
1.2.2 Raw materials used for production of types of geosynthetics	9
1.2.3 Definitions, Manufacturing and Classification	11
1.2.4 Types of geogrid	14

1.2.5 Function and Working of geogrid 14

1.2.6 Application of geogrid 16

1.2.7 Advantage of geogrid 18

1.3 PROBLEM STATEMENT 19

1.4 RESEARCH OBJECTIVE 19

1.5 STUDY LAYOUT 19

CHAPTER-2 20

LITERATURE REVIEW 20

2.1 INTRODUCTION 20

2.2 STUDY ON FERROCHROME SLAG 20

2.3 LITERATURE REVIEW ON MODEL FOOTING TESTS 21

CHAPTER-3 30

MATERIALS AND METHODOLOGY 30

3.1 INTRODUCTION 30

3.2 MATERIALS 30

3.2.1 Ferrochrome slag 30

3.2.2 Preparation of sample 31

3.2.3 Grain size analysis test 31

3.2.4 Specific gravity of solids 31

3.2.5 Direct shear test 31

3.2.6 Relative density test 32

3.2.7 Geogrid 33

3.3 METHODOLOGY 34

3.3.1 Test setup 34

3.3.2 Preparation of test bed 36

3.3.3 Test procedure 37

3.3.4 Test variables 38

CHAPTER-4 40

RESULT AND DISCUSSION 40

4.1 TEST SERIES A (UNREINFORCED) 40

4.2 TEST SERIES B (VARYING DEPTH OF GEOGRID) 41

4.2.1 Depth of geogrid= 0.2B 41

4.2.2 Depth of geogrid= 0.3B 44

4.2.3 Depth of geogrid= 0.4B 46

4.2.4 Depth of geogrid= 0.5B 48

4.2.5 Optimum depth of geogrid 50

4.3 TEST SERIES C (PRETENSION CONDITION) 50

4.3.1 Pretensioning at 1% 50

4.3.2 Pretensioning at 2% 52

4.3.3 Pretensionong at 3% 55

4.3.4 Comparison curve for test series C 57

4.4 OVERALL COMPARISION 58

4.5 IMPROVEMENT FACTOR 59

4.6 TEST SERIES 1 (UNREINFORCED) 62

4.7 TEST SERIES 2 (REINFORCED) 63

4.8 TEST SERIES 3 (PRETENSIONED CONDITION) 65

4.8.1 Pretension at 1% 65

4.8.2 Pretensioning at 2% 67

4.8.3 Pretensioning at 3% 69

4.8.4 Comparison curve for test series 3 72

4.9 OVERALL COMPARISION 72

4.10 IMPROVEMENT FACTOR 73

CHAPTER-5 76

CONCLUSION 76

CHAPTER-6 77

FUTURE SCOPE 77

REFERENCES 78

PUBLICATION 81

LIST OF TABLES

Table	Title	Page
Table 1.1	Composition of Ferrochrome slag	3
Table 1.2	Representation of geosynthesis	8
Table 3.1	Physical property of ferrochrome slag	33
Table 3.2	Basic property of geogrid	33
Table 3.3	Series of test at different-2 relative density of ferrochrome slag	39
Table 4.1	Readings of test series A (Unreinforced)	40
Table 4.2	Readings of test series B (u=0.2B)	41
Table 4.3	Readings of test series B (u=0.3B)	44
Table 4.4	Readings of test series B (u=0.4B)	46
Table 4.5	Readings of test series B (u=0.5B)	48
Table 4.6	Readings of test series C (1% prestensioning)	50
Table 4.7	Readings of test series C (2% prestensioning)	52
Table 4.8	Readings of test series C (3% prestensioning)	55
Table 4.9	Readings of test series 1 (Unreinforced)	62
Table 4.10	Readings of test series 2 (Reinforced)	63
Table 4.11	Readings of test series 3 (1% prestensioning)	65
Table 4.12	Readings of test series 3 (2% prestensioning)	67
Table 4.13	Readings of test series 3 (3% prestensioning)	69

LIST OF FIGURES

Figure	Title	Page
Figure 1.1	Ferrochrome plant around the world (www.ferro-alloys.net)	1
Figure 1.2	Ferrochrome Slag, Balasore Ferro Alloys Ltd., Somonathpur	2
Figure 1.3	Dumping yard of ferrochrome slag, Balasore Ferro Alloys Ltd	2
Figure 1.4	Utilization of ferrochrome slag	6
Figure 1.5	Directions in geogrid	11
Figure 1.6	Processing of geogrid	12
Figure 1.7	Extruded geogrid(www.tradekey.com)	13
Figure 1.8	Knitted Geogrid	13
Figure 1.9	Tension membrane effect	15
Figure 1.10	Improvement in bearing capacity	15
Figure 1.11	Lateral strain capability	16
Figure 1.12	A typical arrangement of geogrid in retaining wall	17
Figure 3.1	Ferrochrome slag	30
Figure 3.2	Grain size distribution curve	31
Figure 3.3	Elevation, and plan of the test setup(dimension in mm)	34
Figure 3.4	Test setup of the experiment	36
Figure 3.5	Test arrangement	37
Figure 3.6	Placement of geogrid	38
Figure 3.7	Geometry of the pre-tensioned geogrid-reinforced foundation bed	39

Figure 4.1 Bearing pressure versus normalized settlement curves in unreinforced case 41

Figure 4.2 Bearing pressure versus normalized settlement curves with geogrid at u/B=0.2 43

Figure 4.3 Bearing pressure versus normalized settlement curves with geogrid at u/B=0.3 45

Figure 4.4 Bearing pressure versus normalized settlement curves with geogrid at u/B=0.4 47

Figure 4.5 Bearing pressure versus normalized settlement curves with geogrid at u/B=0.5 49

Figure 4.6 Comparison curve of test series B 50

Figure 4.7 Bearing pressure v/s normalize settlement curve with 1% pre-tension force 52

Figure 4.8 Bearing pressure v/s normalize settlement curve with 2% pre-tension force 54

Figure 4.9 Bearing pressure v/s normalize settlement curve with 3% pre-tension force 56

Figure 4.10 Comparison curve for the test series C 57

Figure 4.11 Bearing pressure versus normalize settlement curve for the test series A,B,C 58

Figure 4.12 Improvement factor versus settlement curve 59

Figure 4.13 Variation in allowable bearing capacity ratio 60

Figure 4.14 Settlement curve corresponding to 200kPa 60

Figure 4.15 percentage reduction in settlement of footing for test series B,C 61

Figure 4.16 Bearing pressure versus normalized settlement curves in unreinforced case 63

Figure 4.17 Bearing pressure v/s normalized settlement curves with geogrid at u/B=0.4 65

Figure 4.18 Bearing pressure v/s normalize settlement curve with 1% pre-tension force 67

Figure 4.19 Bearing pressure v/s normalize settlement curve with 2% pre-tension force 69

Figure 4.20 Bearing pressure v/s normalize settlement curve with 3% pre-tension force 71

Figure 4.21 Comparison curve test series3 72

Figure 4.22 Overall comparison curve for test series 1,2,3 72

Figure 4.23 Improvement factor v/s settlement curve 73

Figure 4.24 Allowable bearing capacity curve corresponding to 5mm settlement 73

Figure 4.25 Settlement curve corresponding to 200kpa 74

Figure 4.26 Percentage reduction in settlement curve for test series 2,3 75

LIST OF SYMBOLS

MDD	**:** Maximum Dry Density
UR	**:** Unreinforced
G_s	**:** Specific Gravity of Soil Solids
PL	**:** Plastic Limit
LL	**:** Liquid Limit
PI	**:** Plasticity Index
PRS	**:** Percentage reduction settlement
Φ	**:** Angle of Internal Friction
C	**:** Cohesion
u	**:** Depth of geogrid below the foundation level

CHAPTER-1

INTRODUCTION

1.1 GENERAL

We all know that, traditionally we used the natural material for the construction of road, embankment and civil engineering structures, but due scarcity of natural material it is essential to find the some substitute material for civil engineering works, which replace the conventional materials. With rapid industrialization, increasing quantities of pollutants are being spewed into the atmosphere and water sources in solid liquid and gaseous form. These pose the major health hazard in most urban and semi- urban areas. There is an vital need to find a solution to this problem. The sustainability of industries now depends upon the effective management and utilization of its by-products. In order to use the industrial waste in huge quantities efforts are being made to use the same as a substitute of natural resources. A variety of efforts have been made to utilize industrial wastes like fly ash, blast furnace slag, red mud etc. in some civil engineering construction works. Ferrochrome slag is a waste material obtained from the manufacturing of high carbon ferrochromium alloy. This slag is formed as a liquid at 1700 °C and its main components are SiO_2, Al_2O_3 and MgO. Moreover it consists of chrome, ferrous/ferric oxides and CaO. . Worldwide production of Ferrochrome slag is 6.4 to 9.6 million tons and increased by 2.8 to 3 % per annum (Kauppi and Peka, 2007).

Figure:1.1 Ferrochrome plant around the world (www.ferro-alloys.net)

Figure: 1.2 Ferrochrome Slag, Balasore Ferro Alloys Ltd., Somonathpur

Figure 1.3Dumping yard of ferrochrome slag, Balasore Ferro Alloys Ltd.,

Stainless steel industry utilize the huge amount of ferrochrome slag. Around the world's Ferrochrome is produced in South Africa, Kazakhstan and India. High carbon ferrochrome is produced by carbothermic reduction process. Rate of ferrochromium slag production is 1.1 to 1.5 times that of ferrochrome metal produced. Worldwide ferrochromium slag production is approximately 12 to16 million tons per year (Richard 2015). The slag composition is an important part in ferrochrome smelting technology .Bulk of ferrochromium slag is throwing away and sent

for land filling which will create a huge waste deposit over the years. Many researchers addressed the oxidation of Cr (+3) to Cr (+6) in presence of strong oxidants in laboratory conditions and there exists a controversy regarding the possibility of slowly releasing of Cr (+6) to environment in long run term practice. Therefore profitable utilization of these wastes in an environmentally safe manner is still a challenge for the ferrochrome producers. Worldwide ferroalloy producers are striving hard to add value to these wastes which will solve the environment issue and will reduce the overall cost of their production.

1.1.1 Composition of Ferrochrome Slag

Chromite is the raw material which is used in the production of ferrochrome , which is chromeand iron oxides containing mineral. Chromite is used as lumpy ores or fine concentrates, which must be generally agglomerated to make them useable charge for the furnace. The smelted products obtained from the smelting furnaces are ferrochrome alloy and slag.

Table 1.1 Composition of ferrochrome slag

Composition	**Percentage**
SiO_2	15-29%
Al_2O_3	19-32%
MgO	14-26%
CaO	1-4%
Cr	1-5%
Fe	1-12%

Ferrochrome slag consists mainly of SiO_2, Al_2O_3 and MgO in unlike ratios but also smaller amounts of CaO, chromium and iron oxides, with significant quantities of chromium in the form of PAC (Partially activated chromium) and entrained alloy. Table 1.1 gives Ferrochrome slag composition.

1.1.2 Production of ferrochrome slag

The production of ferrochrome slag is in carbothermic smelt reduction of chromite ores in submerged arc furnace. This course of action usually generates about 1.0-1.1 ton of slag per ton of the alloy produced. The molten slag and metal is tapped from them furnace at 1650-17000C into a ladle. The molten slag is permitted to overflow to granulation pit where it is granulated to below

10mm size by water quenching. It contains 28-30% of SiO2, 23-29% of MgO, 23-29% of Al2O3, 1.4-2.5% of CaO, 8-16% of Chromium, 2-3% of Iron and other minerals. Its true density is 3.21g/cc and cold crushing strength(CCS) is 100-200kg/cm^2.

There is two type of quenching is done for molten ferrochrome slag a) water quenching b) naturally cooled by air. The proposed studies need to be carried out using water granulated slag. In both water cooled and air-cooled slag, there are three main phases namely i) bulk slag phase, ii) partially reduced chromite particles, iii) entrapped ferrochrome metallic droplets rich in iron. The lime (CaO) in Ferrochrome slag is present in the bulk slag phase in combined phases with Mg-Al silicates. Thus, ferrochrome slag do not have any puffiness properties at atmosphere temperatures.

In both water cooled and air-cooled slag, chromium is present in all the above three phases. The major chromium is contributed from (a) partially reduced chromite (b) entrapped metallic granules (c) and minimal chromium amount in bulk slag phase. Chromium present in partially reduced chromite (a) and bulk slag phase (b) are in stable trivalent (Cr^{+3} or Cr_2O_3) state contributed from stable combined spinel members of chromite ore particles left out unsmelted in slag. In melted slag, Cr is mainly in Cr^{+2} or CrO form, which is not stable at room temperature and therefore solidifies in most oxide i.e. Cr_2O_3 or Cr^{+3} valance state. Cr^{+3} or Cr_2O_3 is not soluble in water and also not expected to oxidize at atmospheric temperature range to Cr^{+6} which is highly soluble in water. The chromium contributed from metallic granules of iron rich ferrochrome (b) is in dispersed state in the bulk slag (i.e. covered with bulk slag phase) and therefore not expected to leach out when in contact with water. Therefore, we expect that the Ferrochrome slag, chromium is present in stable trivalent state (Cr^{3+} or Cr_2O_3 form) which is present as spinel member in unreduced chromite mineral particles left in slag. The bulk phase in slag contains very minimal chromium which is also present as Cr^{+3}phases. Cr^{+3} is not soluble in water and not expected to oxidize in normal atmospheric temperature range, therefore, the slag does not have any health effect.

1.1.3 Utilization of ferrochrome slag

Generally, Finland, Sweden and Russia have effectively utilized these waste materials in road making and building material applications. In South Africa Ferrochromium slagis safely used in landfills. Due to excellent combination of high strength and refractory phases,the ferrochromium slag can be treated in many possible ways such as: road making material, building material, refractory material and simply land filling.

Many researchers around the world are broadly discussed under following categories as:

- In ceramic and refractory application.
- In road and building construction application.
- In hazardous hexavalent Cr treatment

1.1.4 Issues preventing broader recycling

In South Africa Ferrochromium slag is safely used in landfills Ferrochrome producers from Finland utilized these waste materials in road making and building material applications. There isno such hazardous incident in terms of Cr (+6) leaching had been reported with such usage despite many years of practice. Although air cooled ferrochromium slag is an excellent construction material due to its superior mechanical properties, yet their potential utilisation in public domain is limited due to many reasons such as:

a) Government/legislation

Government/legislation/bureaucratic obstacles are deterrent for the utilisation of ferrochromium slag in public domain as construction material. The waste management policy for utilisation of ferrochromium slag is different in countries and not all countries classify ferrochromium slag as hazardous or as a waste. According to the guidelines laid by Department of Water Affairs and Forestry (DWAF) of South Africa for handling, classification and disposal of hazardous waste, wastes to be considered as hazardous waste if there is any doubt regarding its potential danger to human or environment. So based on the precautionary principle, Ferrochromium slag is classified under waste category in South Africa (Department of Water Affairs & Forestry, 1998). However it is not a hazardous waste in Finland according to the verdict of highest administrative court of Finland in 2005. (Erdem et al., 2005).

b) Environmental issue

In both water cooled and air cooled ferrochromium slag, chromium is present in stable spinel phase and entrapped metallic granules. In molten slag, Cr is mainly in Cr+2 or CrO form, which is not stable at room temperature and therefore solidifies in most stable oxide i.e. Cr2O3 or Cr+3 valance state. Cr in solidified ferrochromium slag is in stable Cr+3 or Cr2O3 form which is insoluble in water and also not expected to oxidize at atmospheric temperature range to highly soluble and carcinogenic Cr+6 form. The Cr present in entrapped metallic granules is in dispersed state in the bulk slag (i.e. covered with bulk slag phase) and therefore not expected to leach out when in contact with water. However many researchers addressed the oxidation of Cr (+3) to Cr

(+6) in presence of strong oxidants in laboratory conditions and there exists a controversy regarding the possibility of slow releasing of Cr (+6) to environment in long run practice. Leachability of heavy metals is the main environmental concern of government due to the possible impacts on human health and environmental impacts.L

c) Geographical and Economic factors

A huge amount of slag is generated in ferrochrome smelting process and it is not possible to consume whole volume locally. Also metallurgical waste like ferrochromium slag generally generates in remote areas where the demand for construction material is not high. So transportation of this raw material to other location makes it uneconomical compared to the natural resources and only a small fraction of waste is utilised. Further processing and modification of ferrochromium slag for specific use sometimes makes the end product or process uneconomical. For example the basic processing steps the ferrochromium slag has to undergo for ceramics and refractory application are grinding and milling, shaping and high temperature firing. So a techno economics aspect of this process/product compared to the existing competitive products affects its extent of utilization. We can utilize the ferrochrome slag for many construction works shown in figure 1.4.

Figure 1.4Utilization of ferrochrome slag

From the above, although ferrochrome slag is a waste inorganic material but it can be utilized in various work to develop on economical point of view and making the environment as pollution

free. In the present study, characterization of ferrochrome slag to be used as a fill and embankment material. However, it has the potential to be used as an alternate civil engineering material for filling and embankment as well as pavement material for road construction.

The present work focuses on the utilization of industrial waste such as ferrochrome slag in the geotechnical applications and to determine the applicability of industrial waste as fill in Geotechnical structures such as embankment and other similar structures etc. An effort is being carried out to characterize the local ferrochrome slag as an alternate civil engineering material. The findings based on the limited laboratory tests of the basic material properties, physical properties suggest that ferrochrome slag has the potential to be used as an alternate geotechnical material.

1.2 GEOGRID

Never in the history of civil engineering has any material developed and used so rapidly as the geosynthetics. The reason being they are really needed and can, with proper design, replace difficult conventional designs: and they are being aggressively marketed. The professional group taking active role in using it are geotechnical engineers in heavy construction, thus the prefix "geo" is indeed appropriate. In the geosynthetics, one can include any man made material used with soil and rock related activities, however the following specific materials which can be used in field: Geotextile, Geogrid, Geocomposites and Geomembrane etc. The most important reason of the utilization of geosynthetics offers excellent technical, economic, environment friendly and energy-efficient alternative to the conventional solutions for many civil engineering problems, and thus allow sustainable development of infrastructure projects. Different function of geosynthetics.

- Drainage
- Surface erosion control
- Filtration
- Protection
- Reinforcement
- Seperation
- Barrier

1.2.1 Graphical symbols proposed by IGS

Table 1.2 Representation of geosynthesis

Letter Symbol	Graphical Symbol	Geosynthetic Name
GT		Geotextile
GM		Geomembrance
GG	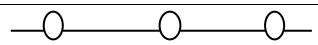	Geogrid
GN	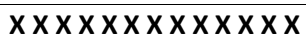	Geonet
GC		Geocell
GA		Geomat
GCL	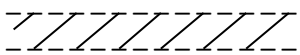	Geo composite clay liner

For the centuries engineers have had difficulties in constructing road, railways over low bearing capacity soils, controlling the erosion caused by water, draining flat low lying land and securing the growth of vegetation. Traditionally, construction over poor soils entailed its removal and replacement by suitable granular soils or the punching in of large rock to eventually provide a stable platform. Both conventional methods are expensive, and due to imprecise construction techniques used it is extremely difficult to estimate the cost of such procedures. Initially brushwood fascines were used to “FLOAT” the pavement over the soft marshy land , later “FABRICS” made from hessian or natural fibres were attempted as they were more economics. However the development of non-woven fabrics and polymer grids in the 1960’s offered the engineer a factory controlled synthetic man made fabric to act as a separator, reinforcement and to aid drainage.

Manmade fabrics, therefore, replace the gap in non-availability of natural fabrics form needed for geotechnical purpose. Natural fabrics or membrane like animal hides or fascines made of brushwood, mats or jute/ coir fabrics, have been used in soil structures since ages. They are mostly

biodegradable or have inherent problems of large continuous form to manufactured and handle and are uneconomical because of being labour intensive and limited life.

Synthetic nets by Nelton Limited, U.K. were used for the first time for reinforcement of soft ground in Japan in 1967. Since then this has inspired the development of geogrids. Actually, "Geogrid" is a trade name used by Nelton Limited, U.K. , to demonstrate a synthetics net developed through their in-house research facilities. Meshes/Geogrids are, therefore, defined as synthetic nets either extruded un-oriented or punched and oriented polymer based fabrics with fused/integral strand joint. The former is better known as NELTON and the later is a high strength version and is called TENSAR. Because of polymeric origin they are non- biodegradable, anti-toxic inert product and are UV protected for long term application. During their development, the geogrids have come a long way in encompassing various application while developing the design practices and standard. They are used today with confidence in many structures around the world including India and provide cost- effective long term solution to many civil engineering problems.

1.2.2 Raw materials used for the production of various types of geosynthetics

- Polypropylene (PP)
- Polyethylene (PE)
- Polyamide/ Nylon (PA)
- High Density Polyethylene (HDPE)
- Low Density Polyethylene (LDPE)
- Linear Low Density Polyethylene (LLDPE)
- Medium Density Polyethylene (MDPE)
- Very Low Density Polyethylene (VLDPE)
- Chlorinated Polyethylene (CPE)
- Polystyrene (PS)
- Polyvinyl chloride (PVC)
- Geo Jute (GJ)
- Geo Coir (GC)
- Bamboo (B)
- Sisal (S)

But for making of Geogrid , raw material is to be used

- Polyester (PET)
- Polypropylene (PP)
- High density polyethylene (HPDE)
- PVC

} ***Synthetic Fibers***

- Geo Coir (GC)
- Bamboo (B)
- Sisal (S)

} ***Natural Fibres***

Polyesters(PET): Polyester is synthesised by polymerizing ethylene glycol with dimethyleterephthalate or with terephthalic acid. The fibre has high strength modulus, creep resistance and general chemical inertness due to which it is more suitable for geotextiles. It is attacked by polar solvent like benzyl alcohol, phenol, and meta-cresol. At pH range of 7 to 10, its life span is about 50 years. It possesses high resistance to ultraviolet radiations. However, the installation should be undertaken with care to avoid unnecessary exposure to light.

Polypropylene (PP): Polypropylene is a crystalline thermoplastic produced by polymerizing propylene monomers in the presence of stereo-specific Zeigler- Natta catalytic system. Homo-polymers and copolymers are two types of polypropylene. Homo polymers are used for fibre and yarn applications whereas co-polymers are used for varied industrial applications. Propylene is mainly available in granular form. Both polyethylene and polypropylene fibres are creep prone due to their low glass transition temperature. These polymers are purely hydrocarbons and arechemically inert. They swell by organic solvent and have excellent resistance to diesel and lubricating oils. Soil burial studies have shown that except for low molecular weight component present, neither HDPE nor polyethylene is attacked by micro-organisms.

Polyethylene (PE): Polyethylene can be produced in a highly crystalline form, which is an extremely important characteristic in fibre forming polymer. Three main groups of polyethylene are – Low density polyethylene (LDPE, density 9.2-9.3 g/cc), Linear low density polyethylene (LLDPE, density 9.20-9.45 g/cc) and High density polyethylene (HDPE, density 9.40- 9.6 g/cc).

Natural fibres: The various type of natural fibres available in india are:, Coir, Sisal, Jute, Bamboo. In order to minimize the cost of ply soil, locally available fibres should be considered in design. But at the same time stability, and life of structure should be given prime importance. Most of these fibres have been tested and found to lose their strength when subjected to alternate wetting and drying environment. In view of low strength and lack of durability, natural fibres are not in wide use for reinforcement but preferred for erosion control due to their environment friendliness and biodegradablility. However, some natural fibres like coir are too strong and durable. They can made suitable with proper treatment for reinforcement function in cohesion less soil. Natural fibres have poor resistance to alkaline environment. Almost all natural fibres get damage and loose their strength in 24 hours when given 0.1N solution of sodium hydroxide (Rehsi, 1988). The only exception to this coir.

1.2.3 Definitions, Manufacturing and classification

Geogrid is a type of geosynthetic materials used as reinforcement in civil engineering construction works. These are the Sheet like product with open aperture. Geogrid are the polymeric products which are formed by means of intersecting grids. These have excellent interlocking with soil and have high strength. Geogrids are formed by material ribs that are intersected by their manufacture in two directions: one is the machine direction (MD), which is conducted in the direction of the manufacturing process. The other direction is the cross machine direction (CMD) which is perpendicular to the machine direction shown in figure1.5.

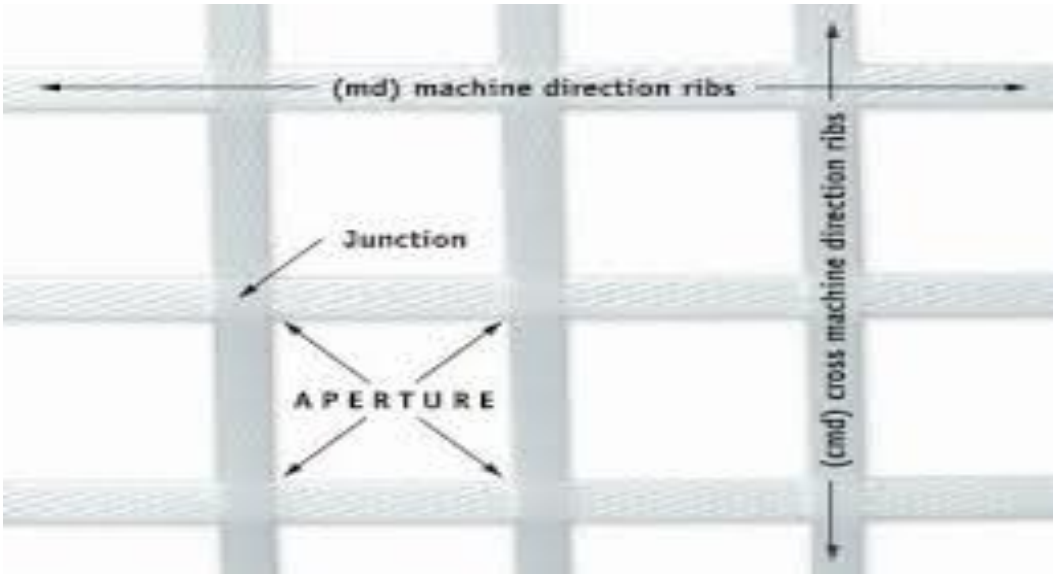

Figure 1.5 Directions in geogrid

For making of geogrid ribs many manufacturing choices are available. Generally there are three types of most used method of manufacturing of geogrids:

(a) Method-1: By Extruding

This manufacturing method of geogrids shown in figure 1.6 which involves the extrusion of a flat sheet of plastic into the desired configuration. The plastic material used may be high density polypropylene or high density polyethylene. Already set punching pattern is placed over the sheet to make holes for the formation of desired grids. The punching of a pattern of holes would result in formation of so- called Apertures. The perforated sheets are then stretched in one direction while it gently heated. The action of stretching the sheet align the polymer's molecules in the direction of stretch, giving the grid a high tensile stiffness in this direction . An alternative form of geogrid may be produced by clamping the uniaxial lattice on stretched side and applying a second stretching on the transverse direction. This gives a biaxial grid with square aperture.

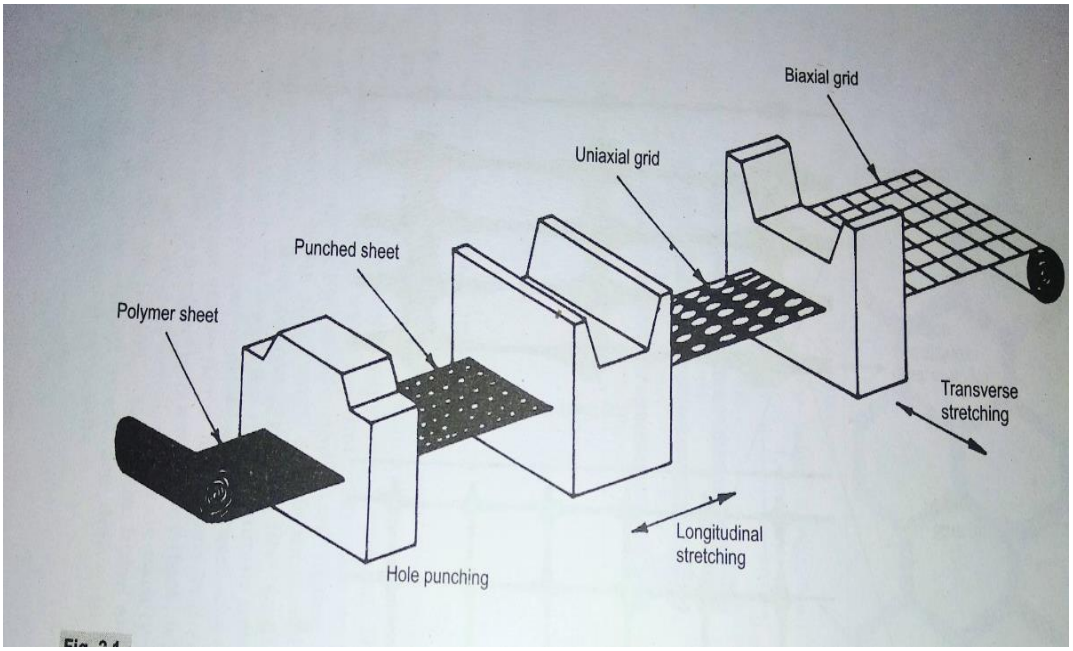

Figure 1.6: Processing of geogrid

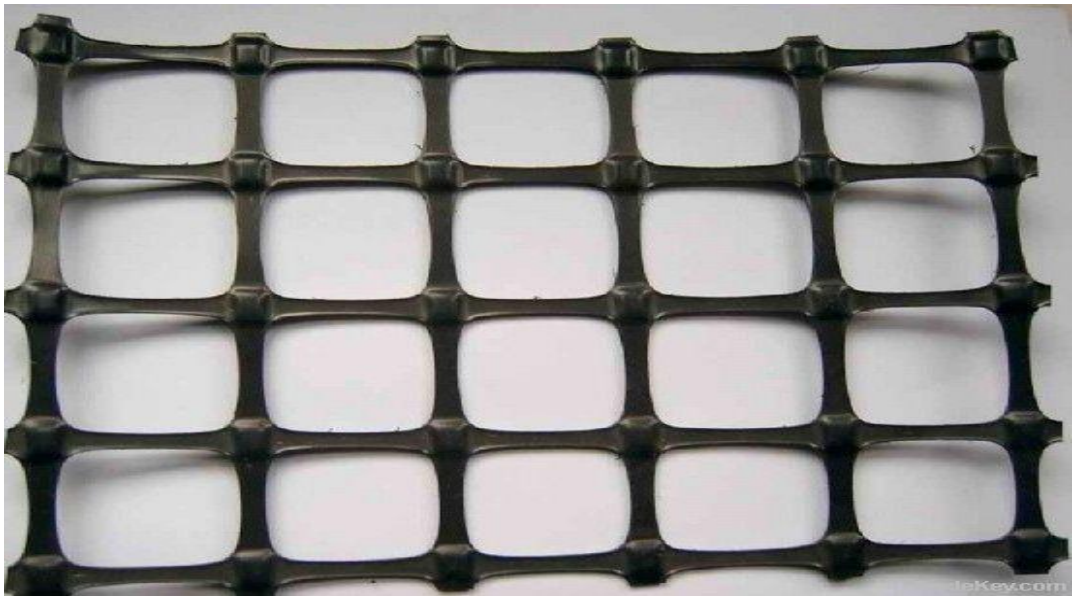

Figure 1.7: Extruded geogrid (www.tradekey.com)

(b) Method-2: By Knitting or Weaving

In this method of geogrid manufacture, single yarn of polyester or polypropylene material undergo either knitting or weaving to form flexible junction forming apertures. These materials are recommended to have high tenacity, to give the geogrid the final desired property.

The product is bought into the market by giving them an additional coating of either bituminous material or a polyvinyl chloride or a latex. This choice varies with the manufacturer of geogrid.

Figure1.8: Knitted geogrid

1.2.4 Type of geogrid

Based on which direction the stretching is done during manufacture, geogrids are classified as :

- Uniaxial Geogrid
- Biaxial Geogrid

(a) Uniaxial geogrid

These geogrids are those geogrid which are formed by stretching in one direction only, that direction is longitudinal direction. So, in this case material possesses high tensile strength in the longitudinal direction than on the transverse direction. Uniaxial geogrid used as reinforcement layer in retaining walls and embankment.

(b) Biaxial Geogrid

Here during the punching of polymer sheets, the stretching is done in both longitudinal and transverse directions. Hence the function of tensile strength is equally given to both longitudinal and transverse directions. Biaxial geogrid used in road bases, below railway track, ground reinforcement etc.

1.2.5 Functions and Working of Geogrids

The main function of geogrid is of holding or capturing the aggregates together. This method of interlocking the aggregates would help in an earthwork that is stabilized mechanically. The apertures in geogrids help in interlocking the aggregates or soil that are placed over them.

(a) Tension membrane effect

This mechanism is based on the concept of vertical stress distribution. This vertical stress is from the deformed shape of membrane as shown in figure1.9. This mechanism was initially considered as the primary mechanism. But later studies proved the lateral restraining mechanism is the major criteria that must be taken into consideration

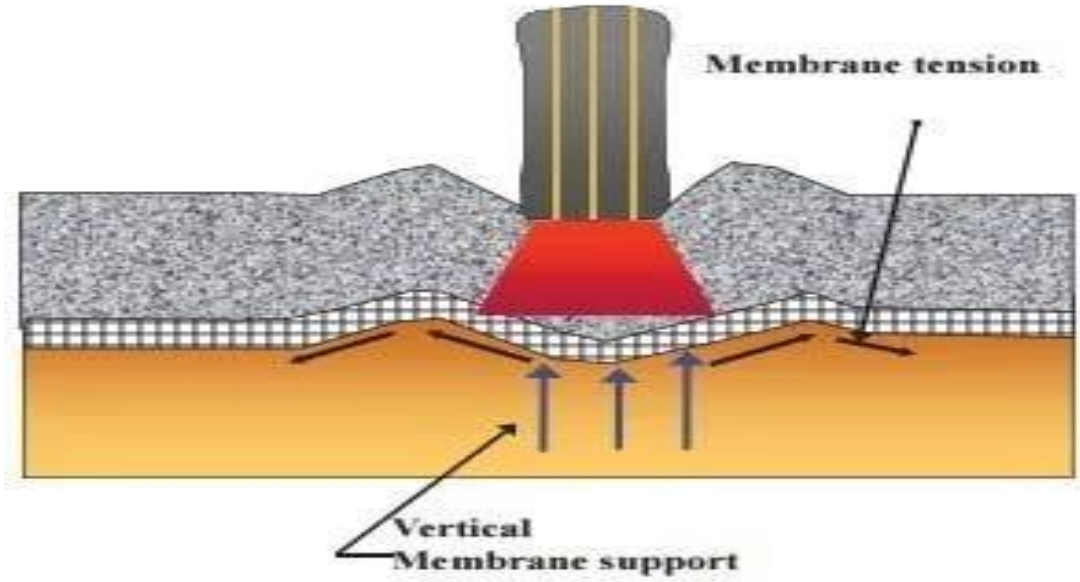

Figure 1.9 Tension membrane effect

(b) Improvement of bearing capacity

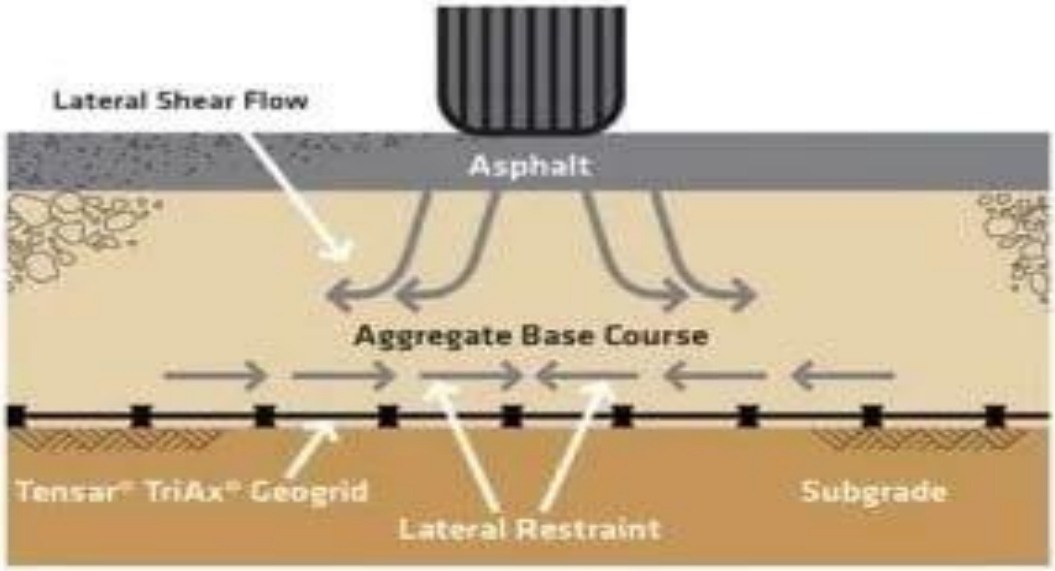

Figure 1.10 Improvement in bearing capacity

One the main mechanism happening after geogrid installation in pavement is the reduction in lateral movement of aggregate. This would result in the elimination of stresses that if exists would have moved to the subgrade.

The geogrid layer possesses sufficient frictional resistance that opposes subgrade lateral movement. This mechanism hence improves the bearing capacity of the layer. Reduction of outward stresses means inward stresses are formed, which is the reason behind the increase in bearing capacity.

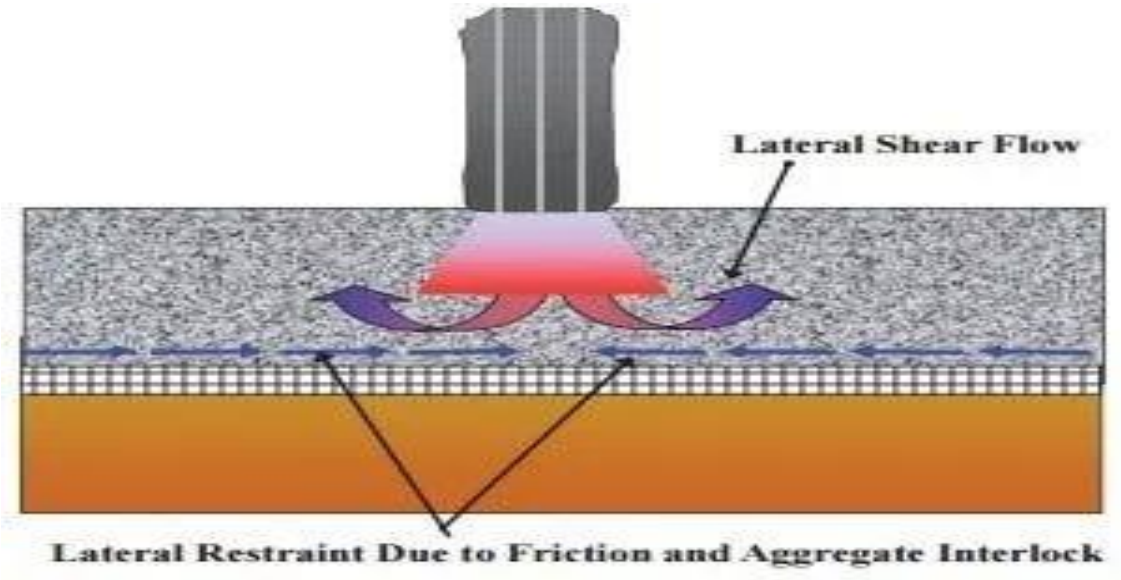

Figure 1.11 Lateral restrain capacity

The stress produced by means of wheel loading coming over the pavement results in lateral movement of aggregates. Which in turn affect the stability of the whole pavement arrangement The geogrid act a restrain against this lateral movement.

1.2.6 Application of Geogrid

(a) Use of geogrid in retaining walls

Generally geogrid is used in the area of backfills of retaining wall. Mainly it holds the soil together and help in stable retaining wall construction. The soil structural reliability is increased by reinforcing the soil by geogrid. This helps in confining the soil backfill and help in distributing the loads. The geogrid solve the problems of soft backfill or sloping ground.

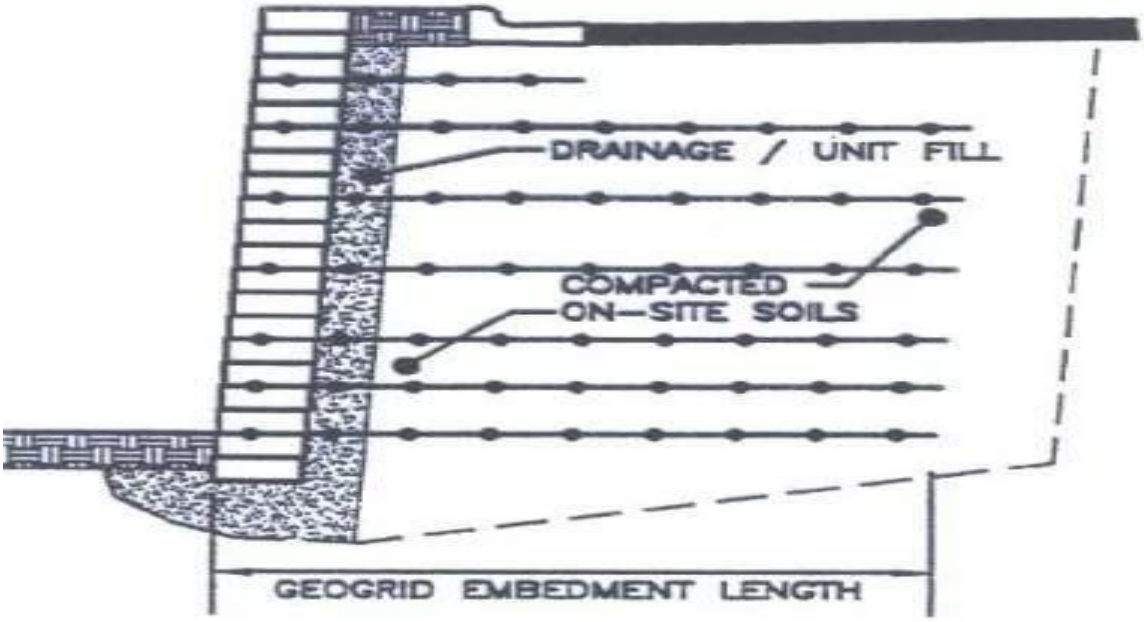

Figure 1.12: A typical arrangement of geogrid in retaining wall

If geogrid length increases then it will help to increasing the mass of structure. This helps in building taller walls. The concept means the makes the whole unit more stiff. The minimum laying depth of geogrid is depend upon the type of soil and the extent of pressure the wall is subjected to from the backfill and other factor.

(b) Usage of geogrid in railway track foundation:

The subgrade which is most important load bearing strata is made solid and strong by using the geogrids. The conventional track foundation consist a minimum ballast depth of 300mm between the underside of sleeper and formation. Ballast generally consist of 50mm single size stone. Where there is possibility of shear failure of subgrade. According to Ayres (1961) track instability occur due to circular shear failure under one of sleeper. Traditional technique use deep sand blankets or sandwich construction of sand layer interrupted by a polyethylene sheet. High strength grids with 5 to 27mm apertures have been used as the upper sandwich layer in conjunction with sand or geotextile. This geogrid keep the ballast away from the geotextile thus avoid the damage , due to provision of combination of geogrid and geotextile track attention for maintenance has reduced considerably, some chances to remove the speed restriction and chance of mud pumping is also reduced and provide excellent rigidity to subgrade of railway track also.

(c) Deep slip repair – In situ Gabions:

When localized slips occurs at the base of embankment then it is possible to apply a partial replacement construction technique which is helpful to stabilise the failure zone of embankment. Spoil material is removed and it is replaced by clean large rock, which is totally encapsulated in the polymeric grid or geogrid to ensure that the stone is firmly held in place. These encapsulated stones resist the movement of parent soil. This type of repair is used to stabilize the small slip. In India and Nepal these slip failures are provided with these type of solution in hilly terrain.

(d) Rock face protection: Geogrid have been used to protect small pieces rock face or friable faces from erosion and avoid the minor rock falls. Grids are sufficiently strong yet flexible enough to confirm to variable topography of the cliff. Before fixing the geogrid the face of protected rock should be cleared from all loose rock and the fixing of geogrid is done with the use of the galvanised rock bolts with huge washers to retain the grid.

(e) Usage of geogrid for off shore protection: Initially we did not able to tackle the power of waves but after sometimes marine engineers are beginning to realise the wisdom of reducing the power of waves before they reach the beach. Generally offshore Gabion structures constructed parallel to the coast are being considered as flexible, permeable energy absorber. These structure consist of rectangular gabions or by using rock filled polymer grid in tubular form. Practically these structures not only does the system reduce the wave energy but also encourage the deposition of sand on leeward side of installation.

(f) Usage of geogrid as gabions or mattress for protection of bank of river: The excessive flow meet during the flood condition in rivers and canal results in excessive damage to bank due to this need for geogrid product in waterways. Grid are fabricated into the gabions or mattress form. Used as a basic building block gabions and mattress provide bank and bed lining to in order to maintain alignment of the canal or river and avoid the erosion.

1.2.7 Advantage of geogrid in civil engineering structures:

The polymer grid structures have become an acceptable component of many civil engineering applications ranging from their inclusion in earthwork to coastal protection. In fact the short coming of many traditional practice and the expense associated with some conventional technique has increased the chances of utilising the geogrid in a wide range if end uses. The geogrid structures have been incorporated in soil masses to improve the physical properties of that soil and

increase the stability. They have been used to protect the surface soil on slopes and in warerways to prevent the erosion and to helpful for vegetation growth. One of the most important property of the geogrid structure is the positive interaction between the grid and surrounding soil. The mechanical interlock achieved when the soil particle become trappedwith in the geogrid apertures, results in an extremely efficient stress transfer from the soil to the geogrid and vice versa. The geogrid can ve installed in any weather condition and geogrid are flexible in nature. Geogrid have the hight durability reducing the maintenance cost.

1.3 PROBLEM STATEMENT

Generally geosynthetics display their beneficial effects only after large settlements. Large settlements are not a desirable aspect for shallow footings, embankments, pavements, etc. For initial settlements, strains in the soil are insufficient to mobilize the significant tensile load in geosynthetic. Thus, there is a need for a technique that may permit the geosynthetic layer to increase the load-bearing capacity of the soil without occurrence of large settlements.

1.4 RESEARCH OBJECTIVE

The main objective of present research are as follows: -

- To determine the effect of prestressed geogrid in reinforcement of soil.
- To determine the optimum depth of geogrid below foundation level at different-2 density.
- To provide environmental friendly and sustainable solution for disposal of slag.

1.5 STUDY LAYOUT

This study is structured as stated below:

Chapter 1 consists of introduction. It states the background to the study, the reasons of carrying out this research, the problem statement and the objective of the study

Chapter 2 reviews the literature related to ferrochrome slag and use of prestressed geogrid

Chapter 3 describes the materials and methods used to achieve the research.

Chapter 4 focuses on the results and analysis of these results.

Chapter 5 presents the summary of the whole research and conclusions derived from this research.

Chapter 6 describes future scopes of the present research.

CHAPTER 2

LITERATURE REVIEW

2.1 INTRODUCTION

This chapter discussed about the literature review for the ferrochrome slag. Then limited study available of characterization of ferrochrome slag is enclosed. Since 2001's various efforts have been made towards characterization and utilization of ferrochrome slag for different engineering purpose. This chapter discusses about the different investigation for effective use of ferrochrome slag in different applications in general. There, specific literature pertains to geotechnical engineering application is presented.

Further this chapter also encloses the literature review on reinforced earth technique. For low levels of settlement, strains in the soil are insufficient to mobilize tensile load in geogrid reinforcement. This may not be a desirable feature for shallow footing where deformation allowed is very limited. To overcome this problem, geogrid can be pre-stressed.

2.2 STUDY ON FERROCHROME SLAG

Lind *et al.*, (2001) investigated that "leaching tests with salt seawater and PH adjusted water reveal low leachability from the slag for most elements. It was also reported that in road construction, there was a low migration of particles from the slag to the underlying soil and that the leaching from the Ferrochrome slag to the groundwater was low for the elements analysed, except for potassium. Thus, found that slag is attractive as construction material due to its excellent technical material properties. However, environmental concerns have been raised about the content and leachability of heavy metals, especially chromium. A potential leachability test (availability test) shows low leaching of chromium.

Kauppi *et al.*, (2007) reported that the structure of the slag is partly crystalline and partly glassy. Significant phases are amorphous glass, Fe-Mg-Cr-Al-spinels, forsterite, Mg-Al-silicate and metal alloy. The ferrochrome slag products are chemically very stable.

Yilmaz *et al.*, (2009) reported the results of experiments, to use ferrochromium slag as an aggregate for granular layers of flexible pavements. The results indicate that the physical and mechanical properties of air-cooled ferrochromium slag are as good as or better than those of natural aggregates. Therefore, FeCr slag and SiFeCr slag have potential to be used as a pavement

base layer material in applications where crushed limestone aggregate materials are traditionally used. It can be used as a base or sub-base material in highway pavements and as an embankment material. The behaviour of granular road material under such repetitive loading should be analysed using repeated load triaxial tests in the laboratory. According to leaching test results, it can be concluded that the ferrochromium slag is not a potential pollutant**.**

Konarbaeva *et al.*, (2010) mineralogical composition of low-carbon ferrochrome slags was studied by means of petrographic analysis. Ferrochrome was produced with ferrosilicon-aluminium used as a reductant. Petrographic analysis of slags indicates the presence of helenite in various forms. Isolated impregnations of mellite, larnite and vitreous phase are distinctly separated which proves the possibility of their separation from helenite phase in further processing.

2.3 LITERATURE REVIEW ON MODEL FOOTING TEST

Aboshi et al. (1984) described the 'Roped Sheet Method' used in Japan to stabilize soft clay. In this method, two layers of canvas or plastic sheets are dragged or rolled out over the area to be stabilized. Ropes placed between the two layers. The ropes are preloaded to 0.5–0.6 kN in order to increase their effectiveness. A stabilizing berm is then placed around the perimeter to fix (anchor) the sheet before spreading the fill.

***Guido et al. (1985*)**: This research was performed to investigate the behaviour of geosynthetic-reinforced sandy soil foundations and to study the effect of different parameters contributing to their performance using laboratory model tests.

The parameters investigated in this study included top layer spacing, number of reinforcement layers, vertical spacing between layers, tensile modulus and type of geosynthetic reinforcement, embedment depth, and shape of footing.The effect of geosynthetic reinforcement on the vertical stress distribution in the sand and the strain distribution along the reinforcement were also investigated.

A series of laboratory model footing tests were conducted on geosynthetic reinforced sand foundation. The model tests were conducted in a1.5m long, 0.91m wide, and 0.91m deep steel test box. The model footings used in the tests were 25.4 mm thick steel plates with dimensions of 152mm×152mm (B×L) for square footings and 152mm×254 mm(B×L) for rectangular footings, which were chosen, based on the dimension of box, to minimize the boundary effect. The load

increments were applied and maintained until the rate of settlement was less than 0.03 mm/min for three minutes consecutively. The load and the corresponding footing settlement were measured by a ring load cell and two dial gauges.

The experimental test results indicated that the magnitude of settlement ratio (s/B) at ultimate bearing capacity is about 7–10% for embedded footings and 4–7% for surface footings on both unreinforced and reinforced sands.

The study came up with the following conclusions: -

- An optimum top layer spacing of 0.33B (B: footing width) for the embedded square model footing (D_f/B=1.0) on geogrid reinforced sand.
- An influence depth of 1.25B for placing geosynthetic reinforcement regardless of the type of reinforcement and embedment depth.
- No optimum vertical spacing for the geogrid reinforced sand tested.
- A reduction of immediate settlement by 20% at all footing pressure levels with two or more layers of geogrid.
- Better performance of geogrid as compared to geotextile for sandy soil foundation.
- A redistribution of the foundation loads over a wider area (i.e., more uniformly) below the reinforced zone.
- A ‘‘surcharge effect’’ brought by the inclusion of geosynthetic reinforcement for surface footing condition.

Guido et al. (1986) Compared the results of laboratory model tests used to study the bearing capacity of geogrid and geotextile-reinforced earth slabs supporting a square footing.

The parameters studied were the coefficient of friction between the geotextile and the soil, pull-out resistance between the geogrid and the soil, depth below the footing of the first layer of reinforcement, vertical spacing of the layers, number of layers, width size of a square sheet of reinforcement, and tensile strength of the reinforcement.

For both geogrids and geotextiles, after an optimum number of layers or width of reinforcement, the bearing capacity did not increase. In addition, the bearing capacity was largest for those geogrid and geotextile reinforced earth slabs where the first layer was close to the footing and the spacing between the layers was the smallest. Bearing capacity increased directly with increasing

reinforcement tensile strength for the geotextile; however, for the geogrid, it depends on aperture size and reinforcement tensile strength.

The experimental study was conducted in a square, stiffened,Plexiglas box 1.22 m wide with a depth of 0.92 m.A square footing 305 mm wide was used, consisting of a 19-mm thick piece of exterior grade plywood stiffened by a3 mm thick steel plate at the top and bottom. A recess was cut into the centre of the top steel plate to accommodate an 89 kNcapacity load ring used to measure the vertical load, which was applied to the footing through the use of a 223 kN capacity hydraulic cylinder and hand pump. the hydraulic cylinder was bolted to a welded frame, which was bolted to the floor and used to jack against. The load was applied in small increments and the resulting footing displacement measured by two dial gages, placed at opposite comers of the footing. These dial gages had a51 mm run with a 25-pm sensitivity. The differential settlement recorded by these gages was very small for all tests performed. Square sheets of geogrid or geotextile were placed concentrically under the square footing, with no sheet being used more than once.

The effect of various parameters on the bearing capacity of a square footing on a geogrid or geotextile reinforced earth slab were studied. The parameters were the following:

- Depth below the footing of the first layer of reinforcement, *u*,expressed in dimensionless form as *u/B*, where *B* is the width of the footing.
- Vertical spacing of the layers of reinforcement.
- Number of layers of reinforcement, N.
- Width size, b, of the square sheet of reinforcement, expressed in dimensionless form as b/ B.
- Tensile strength of the reinforcement.

This paper has discussed a series of laboratory plate loading tests using either geogrids or geotextiles as reinforcement insane. The results have shown that the bearing capacity of anunreinforced earth slab can increase substantially with the insertion of either type of reinforcement. For geotextiles to function properly as reinforcement, friction must develop between the soil and the reinforcement to prevent sliding, whereas for grids, it is the interlocking of the soil through the apertures of the grid that achieves an efficient anchoring effect. Therefore, it has been shown that fixed shear box tests and pull-out tests are required to be run to determine the failure mechanisms of geotextiles and geogrids, respectively.

The study came up with the following conclusions: -

- For both types of reinforcement investigated, geogrids and geotextiles, the BCR decreased with increasing *u/B* up to acritical depth of *u* equal to *B (u/B = 1)*, after which it remained essentially constant.
- For both the geotextile and the geogrid the BCR increased with an increasing number of layers of reinforcement up to an optimum value of N = *3*, after which there was little benefit in increasing the number of layers.

For both the geotextile and the geogrid the BCR increased with increasing b/However, the rate of increase for the two types of reinforcement is very different. For the geogrid reinforced earth slab the BCR increases rapidly with increasing b/B up to value of approximately 2.0, after which there is little change, whereas for the geotextile reinforced earth slab the increase inBCR with increasing b/B is more steady and remains relatively constant at a BCR value of approximately 3.0.

From the test results, it seems that the tensile strength of the grid alone is not a sufficient parameter. The aperture size of the grid must be considered in conjunction with the grid tensile strength.

Khing et al. (1993) conducted model tests on a strip footing supported by a sand layer reinforced with layers of geogrid. Laboratory-model tests were conducted in a steel box measuring 1.1 m (length) × 304.8 mm (width) × 914 mm (depth). The sides of the box were braced with stiffeners to avoid lateral yielding during soil placement and loading of the model foundation. The model foundation used for the tests was made out of hardwood and measured 304.8 mm (length) × 101.6 mm (width) × 25.4 mm (thickness). Since the inside width of the box was equal to the length of the model foundation, a plane-strain condition was generally maintained. A rough-base condition was achieved by cementing a thin layer of sand onto the base of the model foundation with epoxy glue. A 6-35-mm-thick steel plate, having the same plan dimensions as the model foundation and with a groove at the centre, was mounted on the model foundation. The groove was made to ensure that the applied load during the tests would be centric and vertical. The ends of the model foundation and the sides of the model test box were made as smooth as possible to reduce friction during tests.

For conducting the model tests, sand was poured into the test box in25-4-mm-thick layers by using a raining technique. The accuracy of sand placement and consistency of the placement density were checked during raining by placing small cans with known volumes at different locations in

the box. Geogrid layers were placed in the sand at desired values of*u/B* and *h/B*. The model foundation was placed on the surface of the sand bed, and load on the model foundation was applied by a hydraulic jack. The load and the corresponding foundation settlement were measured by a proving ring and two dial gauges placed on each side of the centre line of the foundation.

Three series of tests were conducted, the details of which are given below:

- Variation of bearing capacity with *u/B* (Test Series A) (*u*=the location of the top layer of the reinforcement measured from the bottom of the foundation, u)
- Variation of bearing capacity with *d/B* (Test Series B) (*d*=the depth of reinforcement)
- Variation of bearing capacity with *b/B* (Test Series C) (*b*=the width of each reinforcement layer)

The study came up with the following conclusions:-

- The maximum benefit of geogrid reinforcement in increasing the bearing capacity was obtained when the ratio of the depth of the first reinforcing layer to the foundation width was less than unity.
- For the case of the strip foundation, a reinforcement placed below the foundation at a depth of more than 2.25 times the foundation width did not contribute to any increase in bearing capacity.
- For maximum benefit, the minimum width of the geogrid layers should be about six times the foundation width.
- The bearing-capacity ratio calculated on the basis of the ultimate bearing capacity may be somewhat misleading for the actual foundation design, since most foundations are constructed on the basis of limited settlement. The bearing-capacity ratio calculated on the basis of limited settlement appears to be about 67-70% of the ultimate bearing-capacity ratio.

Omar et al. (1993) presented the results of the laboratory model tests for strip and square foundations supported by sand reinforced with geogrid layers.

The model square foundation used for this study measured76.2 x 76.2 mm. The strip foundation had a width of 76.2 mm and a length of 304.8 mm. They were made out of aluminum plates. Rough bottom condition of the model foundations was achieved by cementing a thin layer of sand using glue. Bearing-capacity tests on the strip foundation was conducted in a box measuring 1.1 m

(length) x 304.8 mm (width) x 914 mm (depth). The inside walls of the box and the edges of the model foundation were polished as much as possible to reduce friction. Tests on the square foundation were conducted in another box having dimensions of 760 x 760 x 760 mm. The sides of both of the boxes were heavily braced to avoid lateral yielding.

In conducting a model test, sand was poured into the test box in 25.4-mm-thick layers using a raining technique. The accuracy of sand placement and the consistency of placement density were checked by placing small cans with known volumes at different locations in the box. Geogrid layers were placed in the sand at desired values of u/B and h/B. The model foundation was placed on the surface of the sand bed. Load to the model foundation was applied by a hydraulic jack. Rotation of the foundation during load application was allowed. The load and the corresponding settlements along the centreline were measured by a proving ring and two dial gauges.

The study came up with the following conclusions: -

- For development of maximum bearing capacity, the effective depth of reinforcement is about 2B for strip foundations and 1.4B for square foundations.
- Maximum width of reinforcement layers required for mobilization of maximum bearing-capacity ratio is about 8B for strip foundations and 4.5B for square foundations.
- The maximum depth of placement of the first layer of geogrid should be less than about B to take advantage of reinforcement.

Shukla and Chandra (1994) Analytically evaluated the effect of prestressing the geosynthetic reinforcement on the settlement behaviour of geosynthetic-reinforced granular fill-soft soil system. They developed foundation model element which has a rough membrane embedded in a granular layer which has been modified to include the prestressing effect in the geosynthetic reinforcement. Parametric studies reveal that the settlement reductions within the loaded region were observed even for low prestress in the reinforcement. They concluded that prestressing the geosynthetic reinforcement is a significant ground improvement technique to enhance the settlement characteristics of the soft soils where the membrane effect of reinforcement is felt.

Yetimoglu et al. (1994) Conducted laboratory model tests to investigate the bearing capacity of rectangular footings on geogrid-reinforced sand.

The study was undertaken to investigate the bearing capacity of rectangular footings on geogrid-reinforced sand by performing laboratory model tests as well as finite-element analyses. The

effects of the depth to the first layer of reinforcement, vertical spacing of reinforcement layers, number of reinforcement layers, and the size of reinforcement sheet on the bearing capacity were investigated.

In this study both experimental and analytical studies were conducted. The parameters investigated include

1. Depth to the first layer of reinforcement u;
2. Vertical spacing of reinforcement layers;
3. Number of reinforcement layers;
4. Size of reinforcement sheet (Br: width of reinforcement sheet in the tests)
5. Stiffness of reinforcement.

In experimental part of test, a series of model loading tests were conducted inside a cubical steel tank of 70 cm by 70 cm in plane and 100 cm in depth. The test footing was a rectangular steel plate 12.5-mm thick, 101.5-mm wide and 127-mm long. The tank was strengthened by a number of channel-shaped steel beams in both vertical and horizontal directions to restrain lateral expansion under loads. Static vertical loads were applied using a 100-kN capacity electrical hydraulic pump. Loads transferred from the pump to a hydraulic jack were carefully recorded by a proving ring installed between the jack and the test footing. The footing was loaded at a constant loading rate until an ultimate bearing state was reached.

The study came up with the following conclusions:-

- For single-layer reinforced sand, there is an optimum embedment depth for the first reinforcement layer at which the bearing capacity is the highest. The tests indicated that the optimum embedment depth was approximately 0.3 of the footing width.
- For multilayer reinforced sand, the highest bearing capacity occurs at an embedment depth of approximately 0.25B. For multilayer reinforced sand, there is an optimum vertical spacing of reinforcement layers. The optimum spacing for the reinforced sand investigated is between 0.2B and 0.4B.
- Increasing reinforcement stiffness beyond a certain value would only result in small increases in the bearing capacity of reinforced sand.

Patra et al. (2005) Conducted laboratory model tests for the ultimate bearing capacity of a strip foundation supported by multi-layered geogrid-reinforced sand.

The model foundation used for this study had a width of 80mm and a length of360 mm. It was made out of mild steel plate with a thickness of25 mm. The bottommost model foundation was made rough by coating it with glue and then rolling it over sand. Bearing capacity tests were conducted in a box measuring 0.8m (length)×0.365m (width)×0.7m (depth). The inside walls of the box and the edgesofthe model were polished to reduce friction as much as possible. The sides of thebox were heavily braced to avoid lateral yielding. Locally available sand dried in anoven was used for the present model tests. The sand used for the tests had 100%passing 1.18mm size sieve and 0% passing 0.075mm size sieve. For all tests, theaverage unit weight and the relative density of compaction were kept at 14.81 kN/m^{3}and 71%, respectively. The average peak friction angle ofthe sand at the testconditions as determined from direct shear tests was 41˚.

Based on the tests, the following conclusion was drawn:

1. For the same soil, geogrid and its configuration, the ultimate bearing capacity and BCR increases with the increase in embedment ratio d_f/B.

Lovisa et al., (2010)Conducted laboratory physical model tests and finite element analyses to study the behaviour of two dimensionally prestressed geotextile-reinforced sand bed supporting a loaded circular footing.

Clean, oven-dried beach sand at 50% relative density was used as a sand bed in the laboratory model tests. The sand was classified as poorly graded sand (SP) as per the Unified Soil Classification System. The angle of internal friction of the sand was determined by direct-shear tests under normal pressures of 15, 27 and 55 kPa. A single layer of woven geotextile (SG40/40) was used to reinforce the sand bed.

Loading tests were carried out on a circular rigid footing fabricated from mild steel. The model footing was 20 mm thick and100 mm in diameter. Three different footing embedment depths of0, 50 and 100 mm were investigated. The prestress applied was 2%of the allowable tensile strength of the geotextile (approximately0.84 kN/m) and was distributed over three pulleys in both x and ydirections.The test tank was constructed from perspex of following dimensions: 0.8 m× 0.8 min plan and 0.6 m high. The steel circular footing was considered rigid due to the high strength and stiffness properties of steel.

The model footing was placed on the surface of the sand bed ata predetermined location in the test tank. A normal compressive load was applied in increments of 0.075 kN to the model footing by

means of a mechanical jack supported against a reaction beam. Load increments were monitored using a load cell. The settlement was measured using two dial gauges located at equal distances from the footing, and averaged to obtain the settlement at the centre of the footing. The test was concluded when the load capacity of the jack was reached, or when failure occurred within the soil as the predefined amount of displacement or tilt of the footing. The test tank was emptied and refilled for each test, to ensure standardised conditions were maintained throughout the investigation.

The study came up with the following conclusions: -

- The addition of prestress to the geotextile reinforcement significantly improved the settlement response and loadbearing capacity of the soil.
- The beneficial effects of geotextile reinforcement without prestress were insignificant beyond a footing embedment depth of 50 mm for low strains (i.e. small displacements). However, the addition of prestress to the geotextile reinforcement improved the settlement response and loadbearing capacity for all footing depths.
- The ultimate bearing capacity of unreinforced sand foundations was in good agreement with the values obtained from Meyerhof bearing capacity equations. The bearing capacity equation modification suggested in literature to include reinforcement also produced theoretical results similar to those obtained from physical model tests.
- The relationship for modulus of subgrade reaction at a certain footing embedment depth suggested in literature, produced results that were in good agreement with those obtained from the physical model tests.
- Results obtained from finite element analysis using the program, PLAXIS, were generally in good agreement with those obtained from physical model tests. This validated the equation in literature, relating the modulus of elasticity to the modulus of subgrade reaction, where the parameter H was approximately2.5–3 times the footing width.
- To achieve the benefits of prestressing the geosynthetic in field conditions, the geosynthetic should be pulled out following the laboratory method in principle, and anchored in trenches surrounding the area to be reinforced before placement of the granular fill over it. The pulling out process may not be easy to simulate in field conditions, especially to have a high prestress in the geosynthetic.

CHAPTER 3

MATERIALS AND METHODOLOGY

3.1 INTRODUCTION

This chapter contains the materials and methods used in research. In this study we determine the effect of pre-tensioning the on single layer reinforcement on the load bearing of reinforced ferrochrome slag consist of strip footing.

3.2 MATERIALS

3.2.1 Ferrochrome slag

In this study the soil which is FERROCHROME SLAG is taken from TATA STEEL PLANT, JAMSHEDPUR 2017 for research purposes. The diagram of soil sample is shown in the figure 3.1 below.

Figure 3.1: Ferrochrome slag

3.2.2 Preparation of Samples

For study point of view the ferrochrome slag was collected from Tata Steel plant in Jamshedpur. The Ferrochrome slag was oven dried in the laboratory at 105˚C for 24hrs and sieved by 4.75mm sieve.

3.2.3 Grain Size Analysis Tests

The particle size grading was carried out as specified in IS 2720-4 (1985).

For ferrochrome slag Grain Size Distribution Curve as per IS 1498: 1970 is shown in fig 3.2.

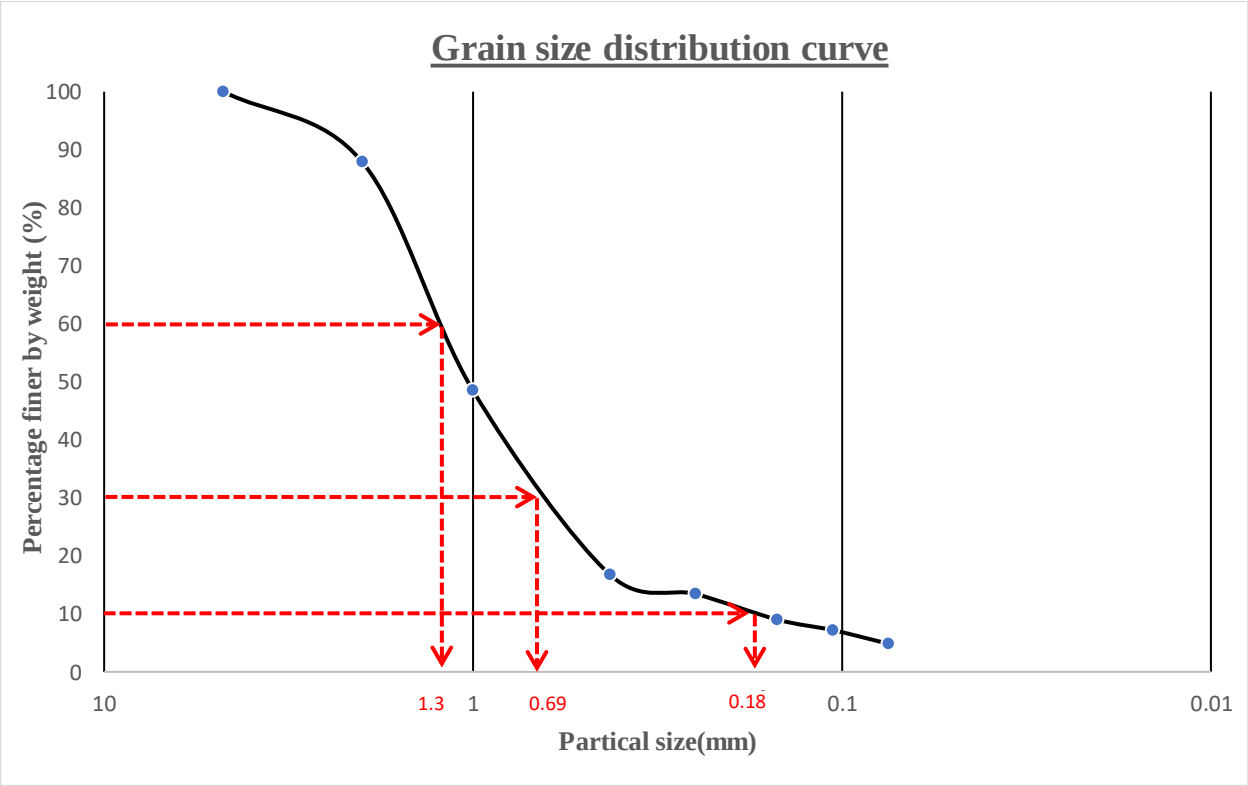

Figure 3.2: Particle size distribution curve

3.2.4 Specific Gravity of Solids

Specific Gravity tests were conducted on ferrochrome slag collected from Tata Steel plant in Jamshedpur as per IS: 2730(Part-3)-1980 .

3.2.5 Direct Shear Test

Direct shear test is a laboratory or field test used to measure the shear strength properties of soil or rock. The test is performed on three or four specimens from a relatively undisturbed soil sample. A specimen is placed in a shear box which has two stacked rings to hold the sample; the contact

between the two rings is at approximately the mid-height of the sample. A confining stress is applied vertically to the specimen, and the upper ring is pulled laterally until the sample fails, or through a specified strain. The load applied and the strain induced is recorded at frequent intervals to determine a stress–strain curve for each confining stress. Several specimens are tested at varying confining stresses to determine the shear strength parameters, the soil cohesion (c) and the angle of internal friction, commonly known as friction angle (φ). The results of the tests on each specimen are plotted on a graph with the peak (or residual) stress on the y-axis and the confining stress on the x-axis. The y-intercept of the curve which fits the test results is the cohesion, and the slope of the line or curve is the friction angle.

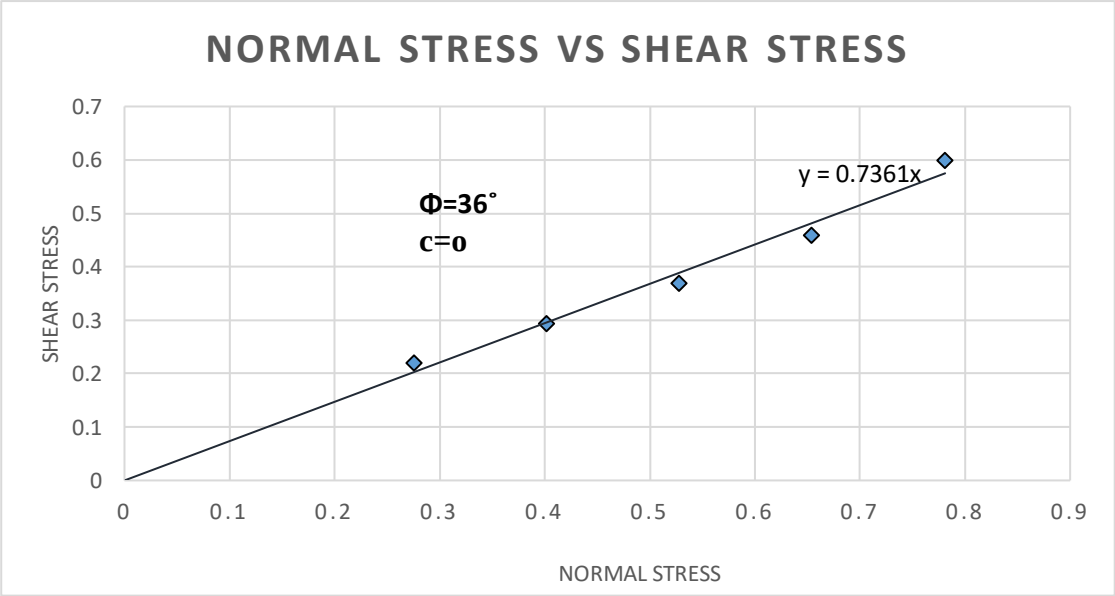

3.2.6 Relative density test

Relative density experiment were done on ferrochrome slag which is collected from Tata Steel plant in Jamshedpur as per IS: 2720-14 (Part-4)-1983.

Basic Geotechnical Properties of ferrochrome slag is taken in lab for study shown below in table 3.1

Table 3.1 Physical properties of ferrochrome slag

PROPERTY	**VALUE**
Colour	Dark black
Specific Gravity	2.70
Gravel content (%)	NIL
Sand content (%)	95.00
Silt and clay content (%)	5.00
Coefficient of uniformity, C_u	7.22
Coefficient of curvature, C_c	2.03
Soil classification as per ISSCS	SP
Maximum dry unit weight (kN/m^3)	14.40
Minimum dry unit weight (kN/m^3)	11.80
Peak friction angle at 60 % relative density (degree)	40.00
Cohesion, c (kPa)	NIL

3.2.7 Geogrid

Knitted polypropylene geogrid (SG-40) manufactured by STRATA INDIA was used in the study. Basic Properties of Geogrid are given below in table 3.2

Table 3.2 Basic properties of geogrid used

PROPERTY	**VALUE**
Geogrid material	Polypropylene, Uniaxial
Type of geogrid	Knitted
Tensile strength (kN/m)	40
Aperture size (mm)	20

3.3 METHODOLOGY

3.3.1 Test setup

The entire setup consists of a test tank and loading system. The inner dimension of the test tank was : 1.0 m in length, 0.51 m in width and 0.70 m in height. The front, back and side faces of the tank were made of steel plates which was welded to stiff channel sections.

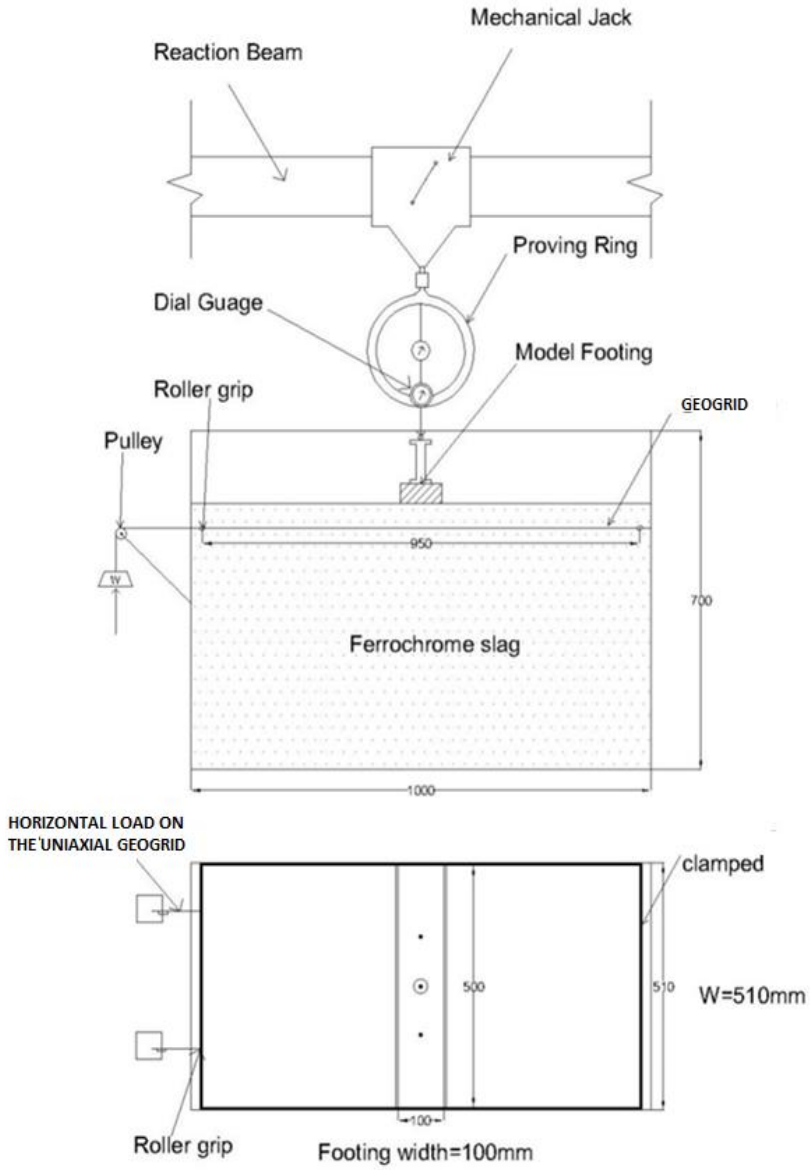

Figure3.3: Elevation and plan of the test setup (dimensions in mm)

The loading system consists of a loading frame and a mechanical jack which hand operated. The loading frame consists of two vertical heavy steel columns and a horizontal crosshead which is act as a reaction frame that supports the mechanical jack. The jack is capable of applying a compressive load of up to 10 tons. The dimension of strip model footing was, 50 cm in length 10

cm in width and 5 cm in thickness was made of seasoned teak wood. The top of the model footing was reinforced with 50 cm long, 6 cm wide and 10 cm high steel I section. A recess was made at the centre of I section to hold a steel ball through which vertical loads were applied to the footing. Load is applied on the footing by the mechanical jack which is fixed in the horizontal crosshead. The base of the footing was made rough by cementing a thin layer of sand using epoxy glue. The pre-calibrated 5 t proving ring was placed between the loading jack and steel ball and this pre-calibrated proving ring measure the how much load act on the model strip footing. Settlement of footing was observed on two dial gauges attached on either side of the loading point at equal distances from the centre. The pre-tension load was applied on the geogrid along the length of the tank across two pulleys. In my experiment geogrid was anchored on one end of the tank and the other end was connected to two pulleys. For uniform distribution of the pre-tensioning force, a roller grip was used. The pre-tension load was applied as a1%, 2% and3% percentage of tensile strength the geogird. Fig.3.2 gives the detailed technical view of the test setup. The following considerations are to be taken while deciding the dimension of the box.

- As per provision of IS 1888-1962, the width of the test pit should not be less than5 times the width of the test plate, so that the failure zones are freely developed without any interference from sides.
- Chumar (1972) has suggested that in case of cohesion less soil, the maximum extension of failure zone is 5B to the sides and 3B below the footing.

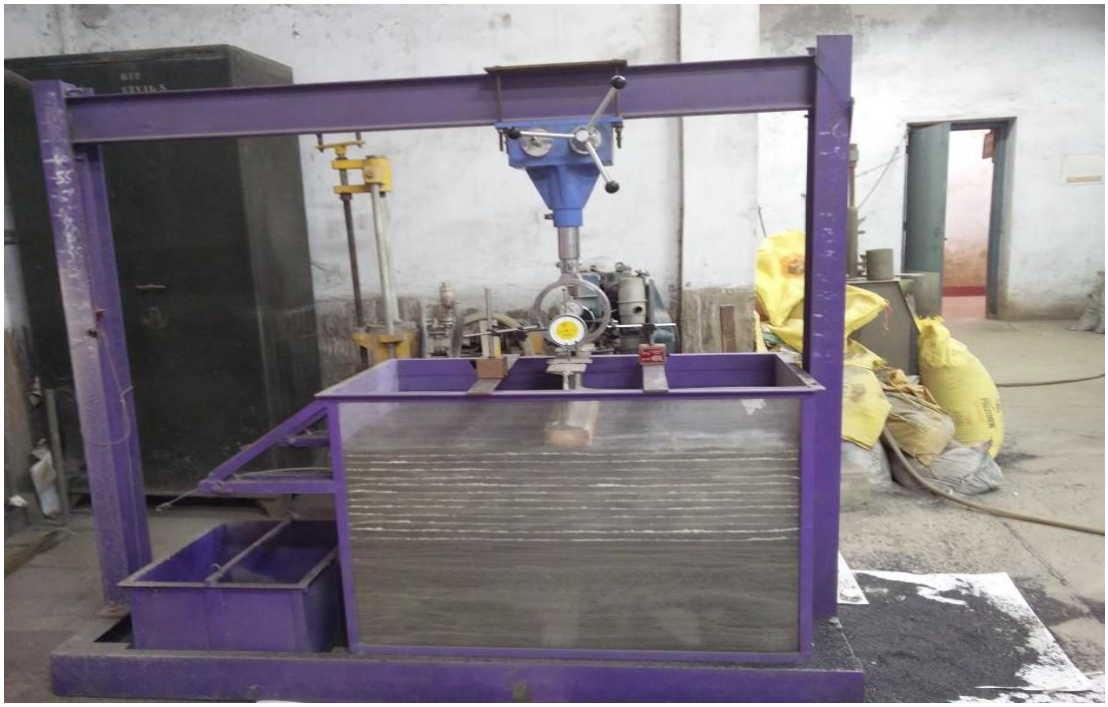

Figure3.4: Test setup for the experiment

3.3.2 Preparation of test bed

To check the results of this analysis have a practical significance, The test is conducted on ferrochrome slag with two relative density to see the behavior of pre-tensioning of geogrid . Thus, two relative densities of 60% and 30% was selected. In order to filling the tank, the raining technique was used to drop the ferrochrome slag in the testing tank at a known height and uniform density. A pouring device with a 5-mm slit was made for raining ferrochrome slag inside the testing tank. To maintain the considered relative density a free fall of ferrochrome slag into the tank is done from the determined height. The height of raining to achieve the desired density was determined previously by performing a series of trials with different heights of raining. Ferrochrome slag was then rained from a pre-calibrated height of 70cm and 45cm. Relative density was constantly maintained at 60% and 30% in all the tests. For checking the relative density which was used to fill the tank the placement density is determined which is achieved by collecting samples in small aluminium cans of known volume placed at different locations during rainfall of ferrochrome slag.

In the case of reinforced test bed, both the position of footing and the position of the geogrid layer was marked on the inner face of the tank. The ferrochrome slag was rained into the tank from the determined height. On reaching the geogrid position, the raining of ferrochrome slag was temporarily stopped and the geogrid was placed on the ferrochrome slag bed (figure 3.4).

Prestensioning load was applied across the two pulleys. After placement of geogrid and application of pre tension force the top of the geogrid was again filled with the ferrochrome slag by using raining technique and this is continued upto the footing level.

Figure3.5: Test arrangement

3.3.3 Test procedure

When test tank was filled up to the footing level then before placing the footing on bed of slag the ferrochrome slag surface was leveled with ruler. Leveling of ferrochrome slag bed is done with great care so that the relative density of the soil was not disturbed. After leveling the surface the model strip footing was placed on the surface and placement of footing was done so accurately so that any eccentricity should not take place because if any eccentricity take place then load is applied on the footing will not concentric. A seating load of 70 g/cm^2 (as per code) was applied for a minute and then released. The dial gauges were attached to the footing. A normal compressive load was applied in increments of 1.0 kN to the model footing by means of a mechanical jack supported against the reaction beam. The settlement of footing was measured by two dial gauge and takes the average of the both dial gauge reading for obtaining the footing settlement at centre. Least count of both dial gauge is 0.01. The test was completed when the excessive tilting of the footing take place or when the load capacity of the jack was reached, or when failure occurred within the soil as the predefined amount of displacement. Now the test tank was emptied and again refilled with accuracy for each test, to ensure standardized conditions were maintained throughout the investigation.

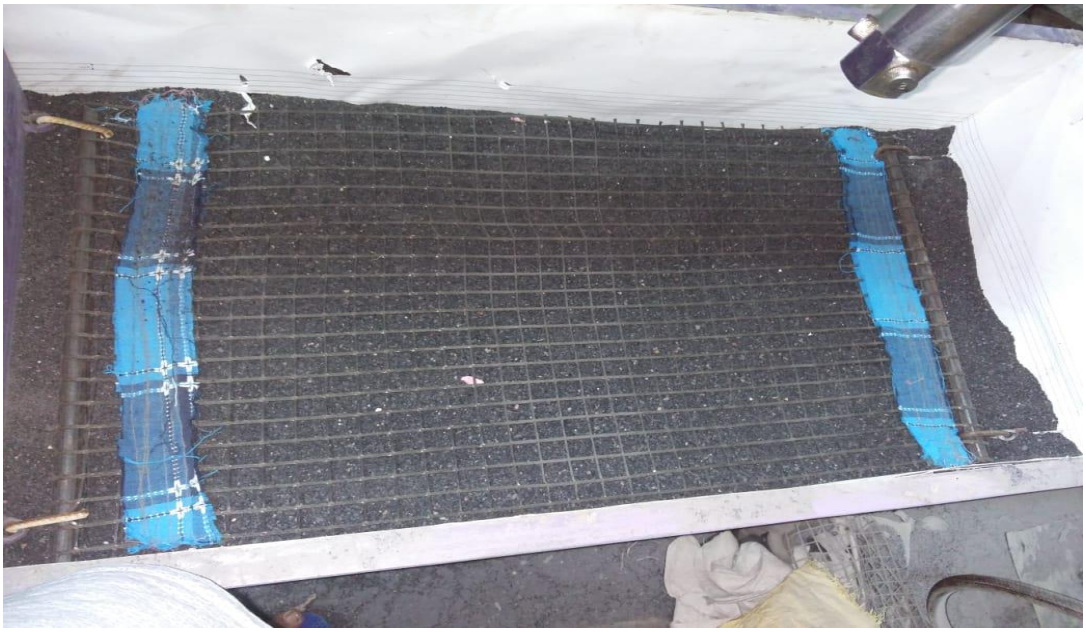

Figure 3.6: Placement of geogrid

3.3.4 Test variables

The width of footing (*B*), width of the geogrid (*b*) and density of the fill were kept constant throughout the entire investigation. Total six different series of tests (i.e. A, B ,C and 1,2,3) were conducted by varying test parameters like the depth of the geogrid layer below the footing level (*u*) and amount of pretension force. The test series A,B and C was carried out for ferrochrome slag having relative density is 60% and the test series 1,2 and 3 was carried out for ferrochrome slag having relative density 30%. Now for Unreinforced condition the test series A and test series 1 were conducted. Test series B was carried on unpretensioned geogrid by varying the depth of the geogrid layer (*u*). Test series 2 was carried out unpretensioned condition by placing the geogrid at the optimum depth which was determined from test series B. The main aim of the test series B was to identify the optimum embedment depth of geogrid layer. The variable parameters was used in this test series are expressed in a non-dimensional form with respect to model footing width (*B*) as *u*/*B*. Test series C and 3 were conducted by varying the pretension force on the geogrid layer which was placed at optimum embedment depth. The Pretensioning force is applied as a percentage of tensile strength of the geogrid used. The main objective of test series C and 3 was to find out the influence of pretensioning force on the overall performance of the footing.

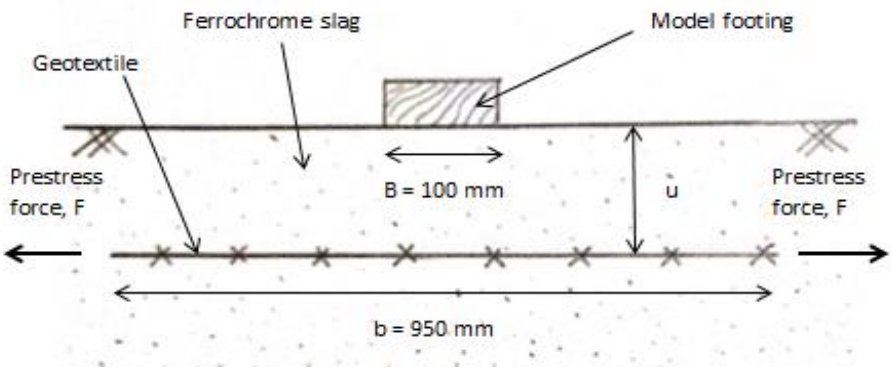

Figure 3.7: Geometry of the prestensioned geogrid-reinforced foundation bed

Table3.3 Series of test at different-2 relative density of slag

Condition	**Medium densely filled**	**Loosely filled**
Unreinforced condition	Test Series (A)	Test Series (1)
Unpretensioned condition	Test series (B) for *u/B* =0.2, 0.3, 0.4, 0.5	Test Series (2) for *u/B*= 0.4
Pretensioned condition	Pretensining of geogrid done at 1%,2%,3%	Pretensoning of geogrid done at 1%,2%,3%

CHAPTER 4

RESULTS AND DISCUSSION

4.1 TEST SERIES A (UNREINFORCED)

Table 4.1: Readings of test series A (Unreinforced)

Proving Ring Divisions	Load (kN)	Load Intensity (kPa)	Dial gauge 1 reading	Settlement 1 (mm)	Dial gauge 2 reading	Settlement 1 (mm)	Average settlement (mm)
0	0	0	0	0	0	0	0
5	0.40	8.51	0	0	60	0.60	0.30
10	0.80	17.03	0	0	200	2.00	1.00
15	1.20	25.54	27	0.27	317	3.17	1.72
20	1.60	34.05	116	1.16	461	4.61	2.88
25	2.00	42.56	208	2.08	598	5.98	4.03
30	2.40	51.07	283	2.83	694	6.94	4.88
35	2.80	59.58	349	3.49	780	7.80	5.64
40	3.20	68.09	415	4.15	875	8.75	6.45
45	3.60	76.61	477	4.77	959	9.59	7.18
50	4.00	85.12	568	5.68	1069	10.69	8.18
55	4.40	93.63	640	6.40	1155	11.55	8.97
60	4.80	102.14	713	7.13	1238	12.38	9.75
65	5.20	110.66	791	7.91	1317	13.17	10.54
70	5.60	119.17	879	8.79	1415	14.15	11.47
75	6.00	127.68	959	9.59	1509	15.09	12.34
80	6.40	136.19	1030	10.3	1589	15.89	13.00
85	6.80	144.70	1111	11.11	1683	16.83	13.97
90	7.20	153.22	1203	12.03	1785	17.85	14.94
95	7.60	161.73	1297	12.97	1877	18.77	15.87
100	8.00	170.24	1399	13.99	1987	19.87	16.93
105	8.40	178.75	1459	14.59	2055	20.55	17.57
110	8.80	187.26	1603	16.03	2198	21.98	19.00
115	9.20	195.78	1729	17.29	2340	23.40	20.34
120	9.60	204.29	1830	18.30	2439	24.39	21.34
125	10.00	212.80	1981	19.81	2589	25.89	22.85
130	10.40	221.31	2098	20.98	2708	27.08	24.03
135	10.80	229.82	2223	22.23	2837	28.37	25.30

140	11.20	238.33	2372	23.72	2978	29.78	26.75
145	11.60	246.85	2523	25.23	3119	31.19	28.21
150	12.00	255.36	2749	27.49	3353	33.53	30.51
155	12.40	263.87	2869	28.69	3469	34.69	31.69
160	12.80	272.38	3185	31.85	3762	37.62	34.73
165	13.20	280.90	3544	35.44	4117	41.17	38.30
170	13.60	289.41	4547	45.47	4943	49.43	47.45
175	14.00	297.92	4846	48.46	5000	50.00	49.23

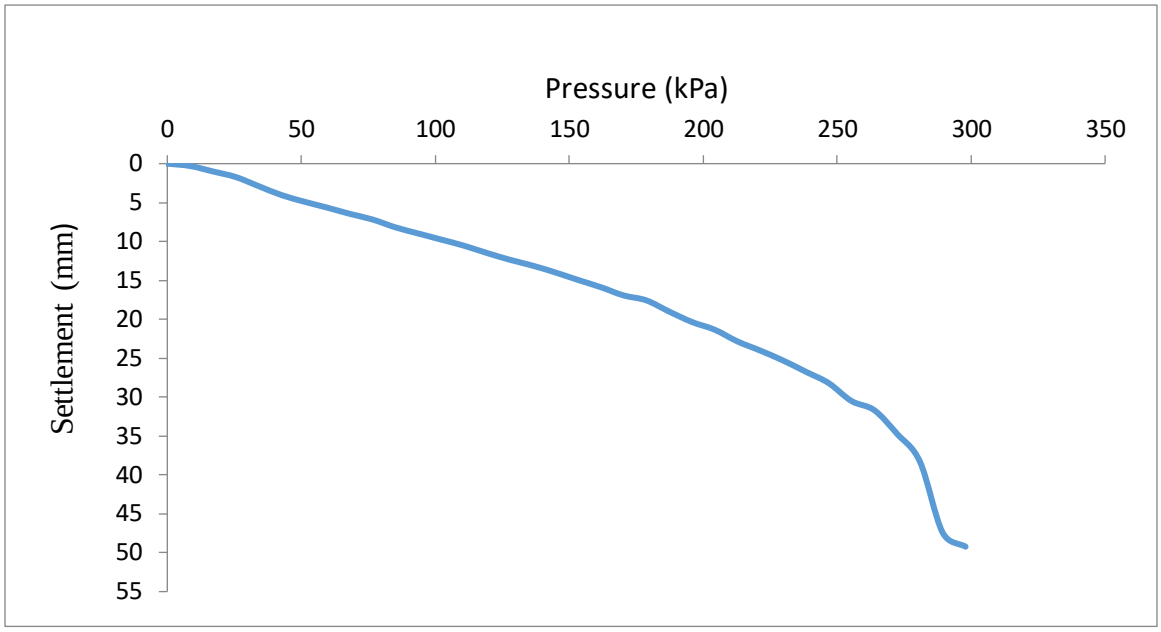

Figure 4.1: Bearing pressure versus normalized settlement curves in unreinforced condition

From figure 4.1 we determine the load carrying capacity of medium densely filled ferrochrome slag corresponding to 5mm settlement 46kPa.

4.2 TEST SERIES B (VARYING DEPTH OF GEOGRID)

4.2.1 Depth of geogrid =0.2B

Table4.2 Readings of test series B (u=0.2B)

Proving Ring Divisions	Load (kN)	Load Intensity (kPa)	Dial gauge 1 reading	Settlement 1 (mm)	Dial gauge 2 reading	Settlement 2 (mm)	Average settlement (mm)
0	0	0	0	0	0	0	0
5	0.40	8.51	4	0.04	0	0	0.02
10	0.80	17.02	61	0.61	60	0.60	0.60

15	1.20	25.54	125	1.25	134	1.34	1.29
20	1.60	34.00	184	1.84	198	1.98	1.91
25	2.00	42.56	247	2.47	265	2.65	2.56
30	2.40	51.07	304	3.04	330	3.30	3.17
35	2.80	59.58	366	3.66	398	3.98	3.82
40	3.20	68.09	405	4.05	465	4.65	4.35
45	3.60	76.61	465	4.65	531	5.31	4.98
50	4.00	85.12	524	5.24	593	5.93	5.58
55	4.40	93.63	578	5.78	646	6.46	6.12
60	4.80	102.14	640	6.40	710	7.10	6.75
65	5.20	110.66	710	7.10	783	7.83	7.46
70	5.60	119.17	753	7.53	832	8.32	7.92
75	6.00	127.68	808	8.08	883	8.83	8.45
80	6.40	136.19	862	8.62	936	9.36	8.99
85	6.80	144.70	928	9.28	995	9.95	9.61
90	7.20	153.22	988	9.88	1053	10.53	10.20
95	7.60	161.73	1041	10.41	1106	11.06	10.73
100	8.00	170.24	1111	11.11	1173	11.73	11.42
105	8.40	178.75	1178	11.78	1237	12.37	12.07
110	8.80	187.26	1233	12.33	1292	12.92	12.62
115	9.20	195.78	1277	12.77	1345	13.45	13.11
120	9.60	204.29	1346	13.46	1405	14.05	13.75
125	10.00	212.80	1426	14.26	1466	14.66	14.46
130	10.40	221.31	1494	14.94	1520	15.20	15.07
135	10.80	229.82	1558	15.58	1572	15.72	15.65
140	11.20	238.34	1611	16.11	1618	16.18	16.14
145	11.60	246.85	1671	16.71	1673	16.73	16.72
150	12.00	255.36	1735	17.35	1733	17.33	17.34
155	12.40	263.87	1798	17.98	1787	17.87	17.92
160	12.80	272.38	1867	18.67	1848	18.48	18.57
165	13.20	280.89	1948	19.48	1908	19.08	19.28
170	13.60	289.40	2044	20.44	1976	19.76	20.10
175	14.00	297.90	2111	21.11	2024	20.24	20.67
180	14.40	306.43	2196	21.96	2072	20.72	21.34
185	14.80	314.94	2302	23.02	2137	21.37	22.19
190	15.20	323.46	2400	24.00	2207	22.07	23.03
195	15.60	331.97	2521	25.21	2282	22.82	24.01
200	16.00	340.48	2653	26.53	2351	23.51	25.02
205	16.40	348.992	2760	27.60	2412	24.12	25.86
210	16.80	357.504	2899	28.99	2483	24.83	26.91
215	17.20	366.016	3034	30.34	2556	25.56	27.95
220	17.60	374.528	3167	31.67	2635	26.35	29.01
225	18.00	383.04	3311	33.11	2711	27.11	30.11

230	18.40	391.552	3452	34.52	2780	27.80	31.16
235	18.80	400.064	3638	36.38	2866	28.66	32.52
240	19.20	408.576	3768	37.68	2932	29.32	33.50
245	19.60	417.088	4010	40.10	3034	30.34	35.22
250	20.00	425.6	4173	41.73	3096	30.96	36.34
255	20.40	434.112	4424	44.24	3181	31.81	38.02
260	20.8	442.62	4729	47.29	3271	32.71	40.00

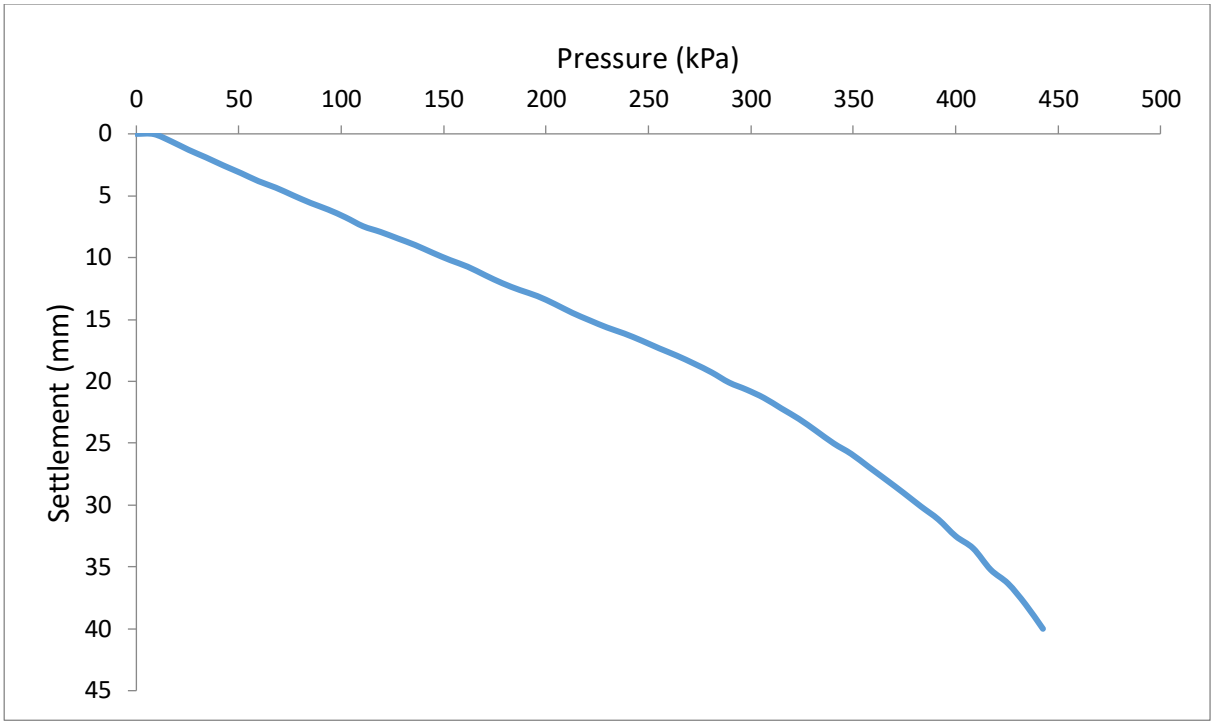

Figure 4.2: Bearing pressure versus normalized settlement curves with geogrid layer at 0.2B

We determined the load carrying capacity of densely filled ferrochrome corresponding to 5mm settlement of footing from the figure 4.2 is 71kPa.

4.2.2 Depth of geogrid =0.3B

Table 4.3 Readings of test series B (u=0.3B)

Proving Ring Divisions	Load (kN)	Load Intensity (kPa)	Dial gauge 2 reading	Settlement 1 (mm)	Dial gauge 2 reading	Settlement 2 (mm)	Average settlement (mm)
0	0	0	0	0	0	0	0
5	0.40	8.51	14	0.14	30	0.30	0.22
10	0.80	17.02	102	1.02	98	0.98	1.00
15	1.20	25.54	181	1.81	166	1.66	1.73
20	1.60	34.05	271	2.71	243	2.43	2.57
25	2.00	42.58	350	3.5	321	3.21	3.35
30	2.40	51.07	423	4.23	395	3.95	4.09
35	2.80	59.58	492	4.92	457	4.57	4.74
40	3.20	68.09	563	5.63	530	5.30	5.46
45	3.60	76.61	627	6.27	598	5.98	6.12
50	4.00	85.12	695	6.95	655	6.55	6.75
55	4.40	93.63	744	7.44	724	7.24	7.34
60	4.80	102.14	817	8.17	795	7.95	8.06
65	5.20	110.65	894	8.94	866	8.66	8.80
70	5.60	119.17	950	9.50	926	9.26	9.30
75	6.00	127.68	1020	10.20	994	9.94	10.07
80	6.40	136.19	1085	10.85	1053	10.53	10.69
85	6.80	144.70	1165	11.65	1130	11.30	11.47
90	7.20	153.21	1223	12.23	1184	11.84	12.03
95	7.60	161.73	1300	13.00	1260	12.60	12.80
100	8.00	170.24	1367	13.67	1336	13.36	13.51
105	8.40	178.75	1424	14.24	1404	14.04	14.14
110	8.80	187.26	1494	14.94	1485	14.85	14.89
115	9.20	195.78	1560	15.60	1560	15.60	15.60
120	9.60	204.29	1618	16.18	1622	16.22	16.20
125	10.00	212.80	1698	16.98	1698	16.98	16.98
130	10.40	221.31	1756	17.56	1755	17.55	17.55
135	10.80	229.82	1844	18.44	1848	18.48	18.46
140	11.20	238.34	1915	19.15	1917	19.17	19.16
145	11.60	246.85	1974	19.74	1983	19.83	19.78
150	12.00	255.36	2033	20.33	2059	20.59	20.46
155	12.40	263.87	2117	21.17	2157	21.57	21.37
160	12.80	272.38	2194	21.94	2226	22.26	22.10
165	13.20	280.89	2300	23.00	2334	23.34	23.17
170	13.60	289.40	2383	23.83	2422	24.22	24.02
175	14.00	297.92	2465	24.65	2516	25.16	24.90

180	14.40	306.43	2557	25.57	2621	26.21	25.89
185	14.80	314.94	2645	26.45	2720	27.20	26.82
190	15.20	323.46	2749	27.49	2840	28.40	27.94
195	15.60	331.97	2820	28.20	2937	29.37	28.78
200	16.00	340.48	2920	29.20	3059	30.59	29.89
205	16.40	348.99	3026	30.26	3193	31.93	31.09
210	16.80	357.50	3160	31.60	3363	33.63	32.61
215	17.20	366.01	3260	32.60	3498	34.98	33.79
220	17.60	374.53	3379	33.79	3669	36.69	35.24
225	18.00	383.04	3490	34.90	3835	38.35	36.62
230	18.40	391.55	3570	35.70	3985	39.85	37.77
235	18.80	400.06	3695	36.95	4213	42.13	39.54
240	19.20	408.57	3818	38.18	4486	44.86	41.52
245	19.60	417.09	3997	39.97	4799	47.99	43.98
250	20.00	425.60	4118	41.18	4998	49.98	45.58

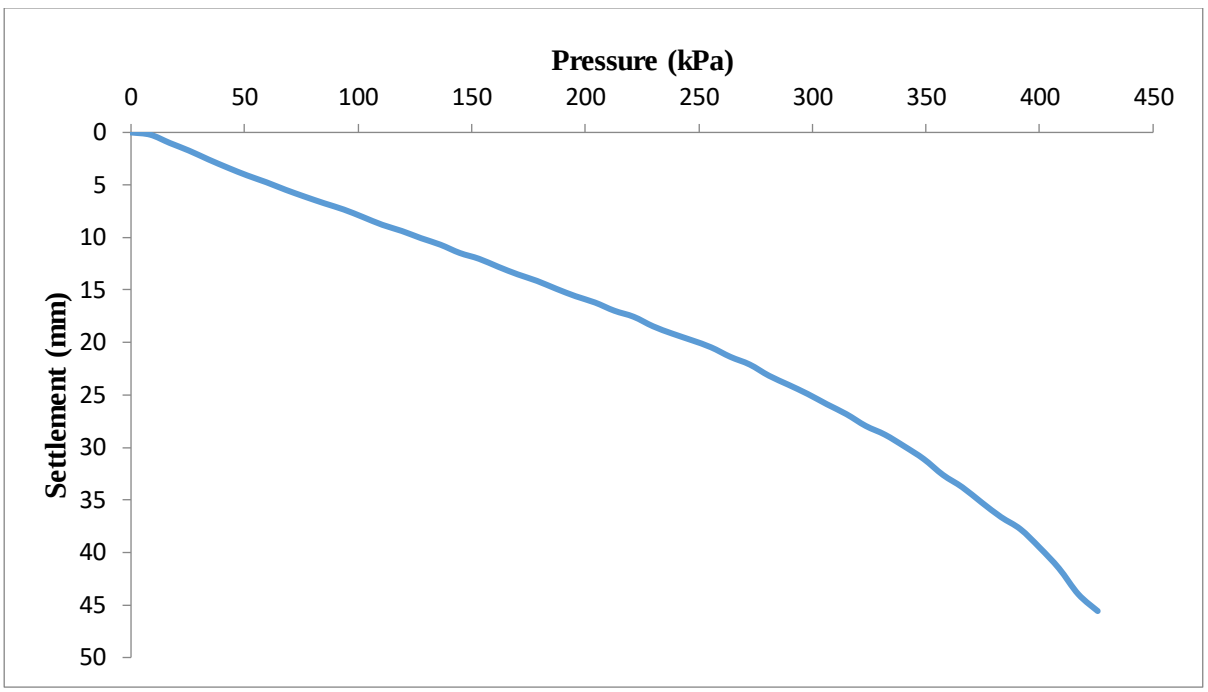

Figure:4.3 Bearing pressure versus normalized settlement curves with geogrid layer at 0.3B

From the figure4.3 the load carrying capacity of slag is 59kPa.

4.2.3 Depth of geogrid =0.4B

Table 4.4 Readings of test series B (u=0.4B)

Proving Ring Divisions	Load (kN)	Load Intensity (kPa)	Dial gauge 1 reading	Settlement 1 (mm)	Dial gauge 2 reading	Settlement 2 (mm)	Average settlement (mm)
0	0	0	0	0	0	0	0
5	0.40	8.51	20	0.20	14	0.14	0.17
10	0.80	17.02	45	0.45	51	0.51	0.48
15	1.20	25.54	75	0.75	84	0.84	0.79
20	1.60	34.05	108	1.08	134	1.34	1.21
25	2.00	42.56	163	1.63	200	2.00	1.81
30	2.40	51.07	210	2.10	255	2.55	2.32
35	2.80	59.58	279	2.79	333	3.33	3.06
40	3.20	68.09	343	3.43	399	3.99	3.71
45	3.60	76.61	387	3.87	441	4.41	4.14
50	4.00	85.12	458	4.58	507	5.07	4.82
55	4.40	93.63	509	5.09	556	5.56	5.32
60	4.80	102.14	572	5.72	610	6.10	5.91
65	5.20	110.66	627	6.27	658	6.58	6.42
70	5.60	119.17	710	7.10	734	7.34	7.22
75	6.00	127.68	757	7.57	781	7.81	7.69
80	6.40	136.19	797	7.97	815	8.15	8.06
85	6.80	144.70	857	8.57	870	8.70	8.63
90	7.20	153.22	908	9.08	916	9.16	9.12
95	7.60	161.73	963	9.63	947	9.47	9.55
100	8.00	170.24	1028	10.28	1032	10.32	10.30
105	8.40	178.75	1087	10.87	1090	10.90	10.885
110	8.80	187.26	1151	11.51	1148	11.48	11.495
115	9.20	195.78	1211	12.11	1209	12.09	12.10
120	9.60	204.29	1265	12.65	1271	12.71	12.68
125	10.00	212.80	1331	13.31	1325	13.25	13.28
130	10.40	221.31	1409	14.09	1399	13.99	14.04
135	10.80	229.82	1456	14.56	1443	14.43	14.49
140	11.20	238.33	1510	15.10	1495	14.95	15.02
145	11.60	246.85	1574	15.74	1555	15.55	15.64
150	12.00	255.36	1642	16.42	1621	16.21	16.31
155	12.40	263.87	1709	17.09	1675	16.75	16.92
160	12.80	272.38	1761	17.61	1735	17.35	17.48
165	13.20	280.89	1838	18.38	1805	18.05	18.21
170	13.60	289.41	1914	19.14	1875	18.75	18.94
175	14.00	297.92	1994	19.94	1944	19.44	19.69

180	14.40	306.43	2066	20.66	2015	20.15	20.40
185	14.80	314.94	2150	21.50	2095	20.95	21.22
190	15.20	323.46	2228	22.28	2164	21.64	21.96
195	15.60	331.97	2305	23.05	2229	22.29	22.67
200	16.00	340.48	2400	24.00	2310	23.10	23.55
205	16.40	348.99	2489	24.89	2376	23.76	24.32
210	16.80	357.50	2595	25.95	2465	24.65	25.30
215	17.20	366.01	2691	26.91	2540	25.40	26.15
220	17.60	374.53	2798	27.98	2627	26.27	27.12
225	18.00	383.04	2916	29.16	2715	27.15	28.15
230	18.40	391.55	3030	30.30	2796	27.96	29.13
235	18.80	400.06	3140	31.40	2878	28.78	30.09
240	19.20	408.58	3268	32.68	2958	29.58	31.13
245	19.60	417.09	3375	33.75	3050	30.50	32.12
250	20.00	425.60	3519	35.19	3125	31.25	33.22
255	20.40	434.11	3715	37.15	3213	32.13	34.64
260	20.80	442.62	3879	38.79	3334	33.34	36.06
265	21.20	451.13	4050	40.50	3426	34.26	37.38
270	21.60	459.65	4301	43.01	3577	35.77	39.39
275	22.00	468.16	4655	46.55	3669	36.69	41.62
277	22.16	471.56	4688	46.88	3823	38.23	42.55
278	22.24	473.27	4843	48.43	3836	38.36	43.39
275	22.00	468.16	4890	48.90	3912	39.12	44.01
276	22.08	469.86	4924	49.24	3920	39.20	44.22
277	22.16	471.56	4955	49.55	3933	39.33	44.44
275	22	468.16	5000	50.00	3940	39.40	44.70

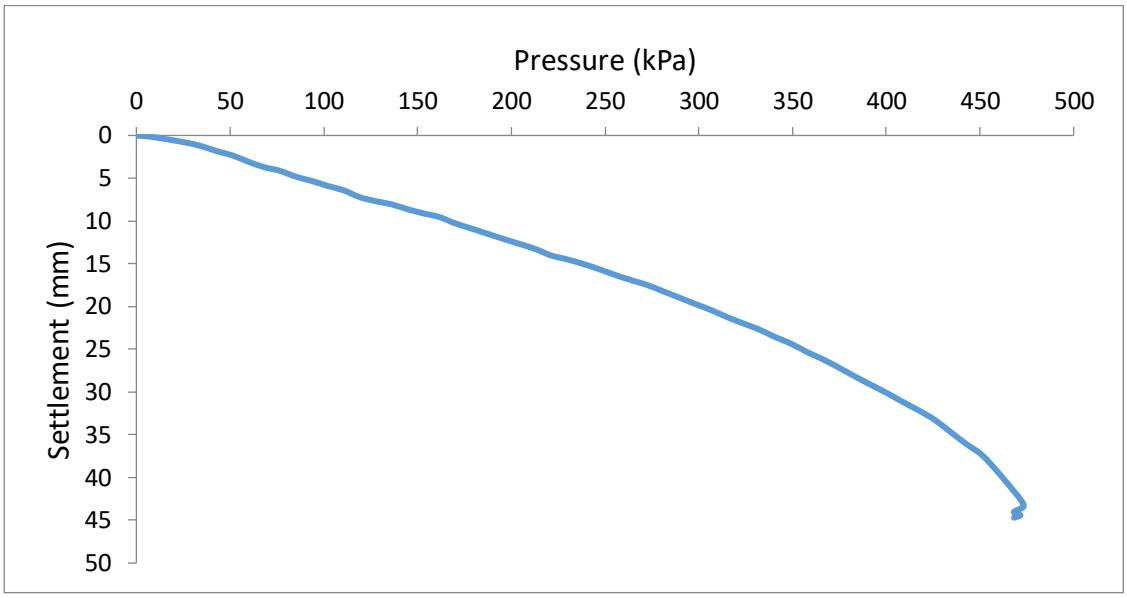

Figure 4.4 Bearing pressure versus normalized settlement curves with geogrid layer at 0.4B

The load carrying capacity of ferrochrome slag corresponding to 5mm settlement in case of relative density 60% is 86kPa.

4.2.4 Depth of geogrid =0.5B

Table 4.5 Readings of test series B (u=0.5B)

Proving Ring Divisions	Load (kN)	Load Intensity (kPa)	Dial gauge 1 reading	Settlement 1 (mm)	Dial gauge 2 reading	Settlement 2 (mm)	Average settlement (mm)
0	0	0	0	0	0	0	0
5	0.40	8.51	40	0.40	40	0.40	0.40
10	0.80	17.02	61	0.61	60	0.60	0.60
15	1.20	25.54	120	1.20	100	1.00	1.10
20	1.60	34.05	214	2.14	280	2.80	2.47
25	2.00	42.56	255	2.55	462	4.62	3.58
30	2.40	51.07	315	3.15	560	5.60	4.37
35	2.80	59.58	383	3.83	681	6.81	5.32
40	3.20	68.09	438	4.38	824	8.24	6.31
45	3.60	76.61	491	4.91	945	9.45	7.18
50	4.00	85.12	537	5.37	1057	10.57	7.97
55	4.40	93.63	585	5.85	1174	11.74	8.79
60	4.80	102.14	635	6.35	1279	12.79	9.57
65	5.20	110.66	694	6.94	1372	13.72	10.33
70	5.60	119.17	741	7.41	1467	14.67	11.04
75	6.00	127.68	794	7.94	1549	15.49	11.71
80	6.40	136.19	863	8.63	1642	16.42	12.52
85	6.80	144.70	920	9.20	1729	17.29	13.24
90	7.20	153.22	972	9.72	1805	18.05	13.88
95	7.60	161.73	1030	10.30	1898	18.98	14.64
100	8.00	170.24	1095	10.95	1975	19.75	15.35
105	8.40	178.75	1148	11.48	2050	20.50	15.99
110	8.80	187.26	1225	12.25	2150	21.50	16.87
115	9.20	195.78	1283	12.83	2220	22.20	17.51
120	9.60	204.29	1354	13.54	2306	23.06	18.30
125	10.00	212.80	1438	14.38	2414	24.14	19.26
130	10.40	221.31	1486	14.86	2479	24.79	19.82
135	10.80	229.82	1529	15.29	2541	25.41	20.35
140	11.20	238.34	1618	16.18	2639	26.39	21.28
145	11.60	246.85	1693	16.93	2725	27.25	22.09
150	12.00	255.36	1768	17.68	2818	28.18	22.93

155	12.40	263.87	1845	18.45	2913	29.13	23.79
160	12.80	272.38	1919	19.19	3004	30.04	24.61
165	13.20	280.89	1993	19.93	3096	30.96	25.44
170	13.60	289.41	2077	20.77	3190	31.90	26.33
175	14.00	297.92	2155	21.55	3278	32.78	27.16
180	14.40	306.43	2245	22.45	3377	33.77	28.11
185	14.80	314.94	2330	23.30	3475	34.75	29.02
190	15.20	323.46	2431	24.31	3595	35.95	30.13
195	15.60	331.97	2529	25.29	3715	37.15	31.22
200	16.00	340.48	2647	26.47	3834	38.34	32.40
205	16.40	348.99	2741	27.41	3924	39.24	33.32
210	16.80	357.50	2833	28.33	4025	40.25	34.29
215	17.20	366.02	2950	29.50	4142	41.42	35.46
220	17.60	374.53	3050	30.50	4266	42.66	36.58
225	18.00	383.04	3160	31.60	4379	43.79	37.69
230	18.40	391.55	3278	32.78	4488	44.88	38.83
235	18.80	400.06	3372	33.72	4582	45.82	39.77
240	19.20	408.57	3473	34.73	4702	47.02	40.87
245	19.60	417.09	3573	35.73	4810	48.1	41.91
250	20.00	425.60	3695	36.95	4925	49.25	43.10

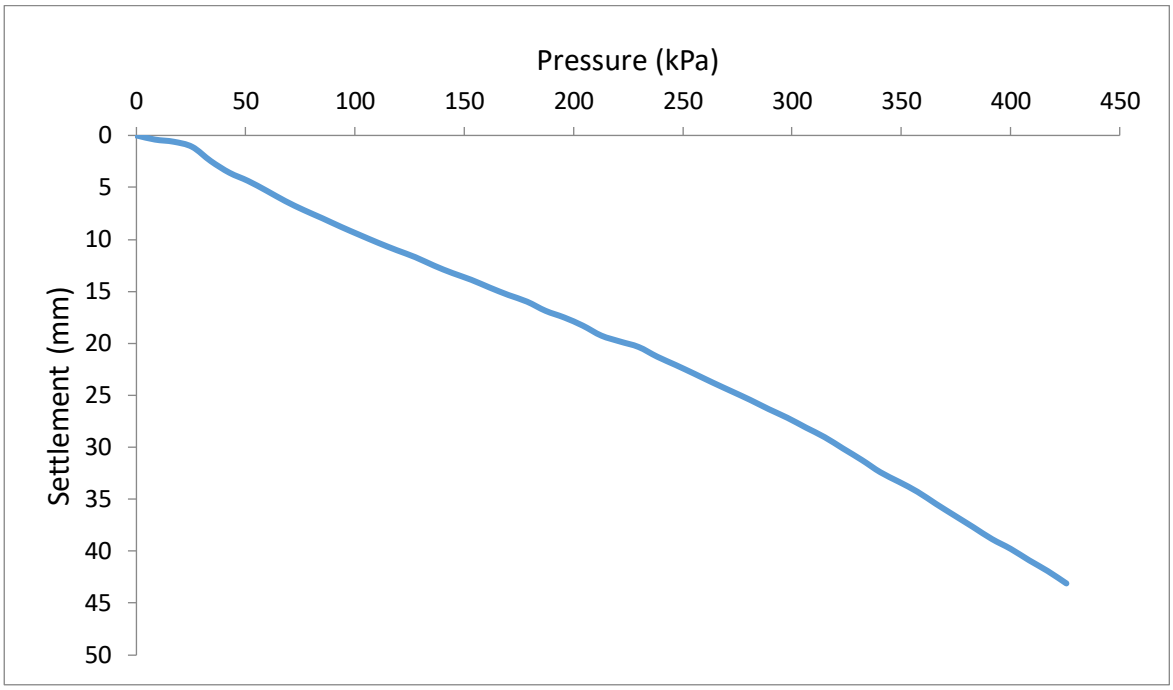

Figure: 4.5 Bearing pressure versus normalized settlement curves with geogrid layer at 0.5B

4.2.5 Optimum depth of geogrid

From comparison curve (figure 4.6), it can be inferred that the optimum depth of geogrid 0.4B because the load carrying capacity of ferrochrome slag in case of 0.4B is maximum in comparison to 0.2B, 0.3B, 0.5B.

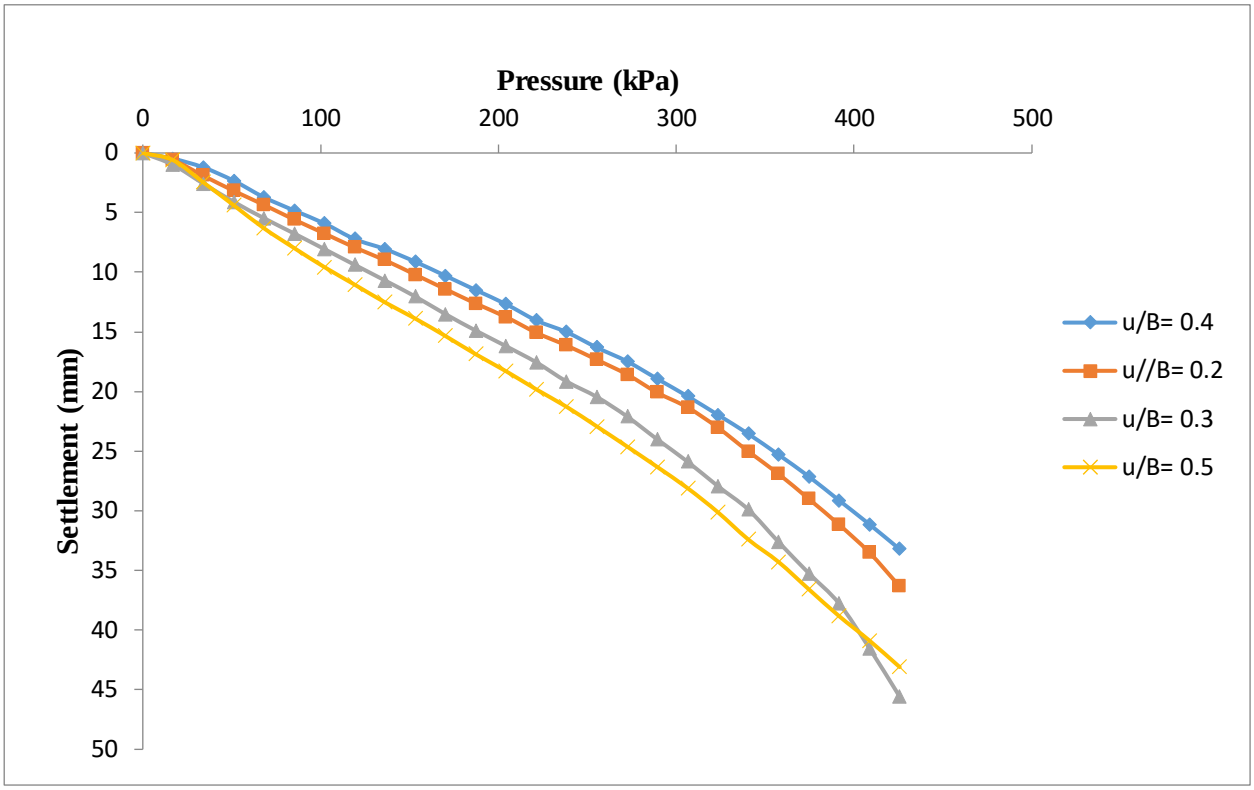

Figure 4.6: Comparison curve of test series B

4.3 TEST SERIES C (PRETENSION CONDITION) :

4.3.1 Pretensioning at 1%

Table 4.6 Readings of test series C (1% pretension)

Proving Ring Divisions	Load (kN)	Load Intensity (kPa)	Dial gauge1 reading	Settlement 1 (mm)	Dial gauge2 reading	Settlement 2 (mm)	Average settlement (mm)
0	0	0	0	0	0	0	0
5	0.40	8.51	0	0.00	20	0.20	0.10
10	0.80	17.02	0	0.00	78	0.78	0.39
15	1.20	25.54	0	0.00	135	1.35	0.67
20	1.60	34.05	10	0.10	191	1.91	1.00
25	2.00	42.56	58	0.58	243	2.43	1.50

30	2.40	51.07	103	1.03	293	2.93	1.90
35	2.80	59.58	152	1.52	352	3.52	2.52
40	3.20	68.09	200	2.00	408	4.08	3.04
45	3.60	76.61	239	2.39	459	4.59	3.49
50	4.00	85.12	295	2.95	518	5.18	4.06
55	4.40	93.63	347	3.47	578	5.78	4.62
60	4.80	102.14	400	4.00	632	6.32	5.16
65	5.20	110.66	451	4.51	691	6.91	5.71
70	5.60	119.17	498	4.98	741	7.41	6.19
75	6.00	127.68	550	5.50	795	7.95	6.72
80	6.40	136.19	593	5.93	838	8.38	7.15
85	6.80	144.70	638	6.38	887	8.87	7.62
90	7.20	153.22	689	6.89	935	9.35	8.12
95	7.60	161.73	744	7.44	990	9.90	8.67
100	8.00	170.24	795	7.95	1040	10.40	9.17
105	8.40	178.75	848	8.48	1092	10.92	9.70
110	8.80	187.26	913	9.13	1152	11.52	10.32
115	9.20	195.78	966	9.66	1207	12.07	10.86
120	9.60	204.29	1013	10.13	1252	12.52	11.32
125	10.00	212.80	1061	10.61	1303	13.03	11.82
130	10.40	221.31	1115	11.15	1357	13.57	12.36
135	10.80	229.82	1162	11.62	1410	14.10	12.86
140	11.20	238.34	1213	12.13	1464	14.64	13.38
145	11.60	246.85	1270	12.70	1516	15.16	13.93
150	12.00	255.36	1330	13.30	1578	15.78	14.54
155	12.40	263.87	1377	13.77	1620	16.20	14.98
160	12.80	272.38	1430	14.30	1678	16.78	15.54
165	13.20	280.89	1483	14.83	1731	17.31	16.07
170	13.60	289.41	1528	15.28	1791	17.91	16.59
175	14.00	297.92	1580	15.80	1850	18.50	17.15
180	14.40	306.43	1628	16.28	1906	19.06	17.67
185	14.80	314.94	1690	16.90	1968	19.68	18.29
190	15.20	323.46	1739	17.39	2028	20.28	18.83
195	15.60	331.96	1803	18.03	2089	20.89	19.46
200	16.00	340.48	1875	18.75	2165	21.65	20.20
205	16.40	348.99	1935	19.35	2227	22.27	20.81
210	16.80	357.50	2007	20.07	2298	22.98	21.52
215	17.20	366.02	2074	20.74	2372	23.72	22.23
220	17.60	374.53	2134	21.34	2434	24.34	22.84
225	18.00	383.04	2215	22.15	2525	25.25	23.70
230	18.40	391.55	2277	22.77	2591	25.91	24.34
235	18.80	400.06	2352	23.52	2663	26.63	25.07
240	19.20	408.57	2425	24.25	2733	27.33	25.79

245	19.60	417.09	2497	24.97	2807	28.07	26.52
250	20.00	425.60	2577	25.77	2884	28.84	27.30
255	20.40	434.11	2638	26.38	2953	29.53	27.95
260	20.80	442.62	2723	27.23	3040	30.40	28.81
265	21.20	451.14	2797	27.97	3107	31.07	29.52
270	21.60	459.65	2800	28.00	3200	32.00	30.00
275	22.00	468.16	2872	28.72	3267	32.67	30.69
280	22.40	476.67	2950	29.50	3338	33.38	31.44
285	22.80	485.18	3056	30.56	3432	34.32	32.44
290	23.20	493.69	3158	31.58	3519	35.19	33.38
295	23.60	502.20	3277	32.77	3606	36.06	34.41
300	24.00	510.72	3377	33.77	3681	36.81	35.29

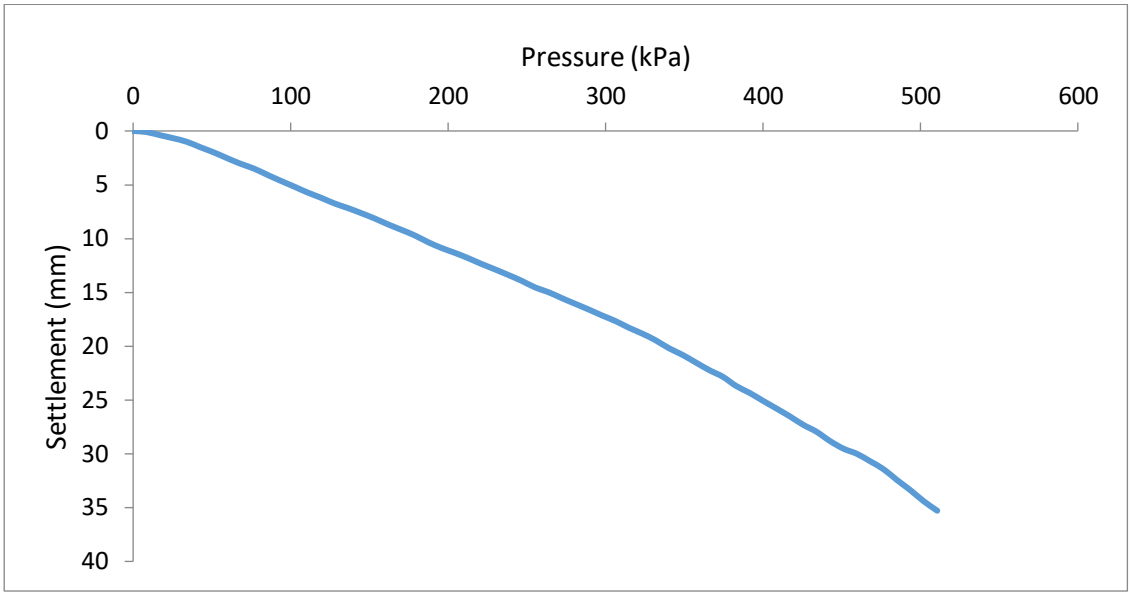

Figure 4.7 Bearing pressure versus normalized settlement curves with 1% pre-tension force

4.3.2 Pretensioning at 2%

Table 4.7 Readings of test series C (2% pretensioned)

Proving Ring Divisions	Load (kN)	Load Intensity (kPa)	Dial gauge 1 reading	Settlement 1 (mm)	Dial gauge 2 reading	Settlement 2 (mm)	Average settlement (mm)
0	0	0	0	0	0	0	0
5	0.40	8.51	0	0	0	0	0
10	0.80	17.02	5	0.05	10	0.10	0.07
15	1.20	25.54	20	0.20	30	0.30	0.25
20	1.60	34.05	35	0.35	40	0.40	0.37

25	2.00	42.56	50	0.50	59	0.59	0.54
30	2.40	51.07	90	0.90	80	0.80	0.85
35	2.80	59.58	115	1.15	125	1.25	1.2
40	3.20	68.09	145	1.45	170	1.70	1.57
45	3.60	76.61	185	1.85	195	1.95	1.90
50	4.00	85.12	220	2.20	240	2.40	2.30
55	4.40	93.63	260	2.60	285	2.85	2.72
60	4.80	102.14	305	3.05	330	3.30	3.17
65	5.20	110.66	340	3.40	375	3.75	3.57
70	5.60	119.17	380	3.80	415	4.15	3.97
75	6.00	127.68	430	4.30	445	4.45	4.37
80	6.40	136.19	450	4.50	485	4.85	4.67
85	6.80	144.70	488	4.88	525	5.25	5.06
90	7.20	153.21	505	5.05	555	5.55	5.30
95	7.60	161.72	530	5.30	585	5.85	5.57
100	8.00	170.24	580	5.80	615	6.15	5.97
105	8.40	178.75	605	6.05	655	6.55	6.30
110	8.80	187.26	650	6.50	690	6.90	6.70
115	9.20	195.78	680	6.80	710	7.10	6.95
120	9.60	204.29	705	7.05	750	7.50	7.27
125	10.00	212.80	740	7.40	785	7.85	7.62
130	10.40	221.31	775	7.75	825	8.25	8.00
135	10.80	229.82	800	8.00	870	8.70	8.35
140	11.20	238.33	855	8.55	920	9.20	8.87
145	11.60	246.85	910	9.10	950	9.50	9.30
150	12.00	255.36	967	9.67	993	9.93	9.80
155	12.40	263.87	1025	10.25	1021	10.21	10.23
160	12.80	272.38	1080	10.80	1035	10.35	10.57
165	13.20	280.89	1135	11.35	1090	10.90	11.12
170	13.60	289.41	1180	11.80	1139	11.39	11.59
175	14.00	297.92	1233	12.33	1190	11.90	12.11
180	14.40	306.43	1279	12.79	1233	12.33	12.56
185	14.80	314.94	1320	13.20	1278	12.78	12.99
190	15.20	323.46	1355	13.55	1350	13.50	13.52
195	15.60	331.97	1400	14.00	1440	14.00	14.20
200	16.00	340.48	1464	14.64	1510	15.10	14.87
205	16.40	348.99	1438	14.38	1645	16.45	15.41
210	16.80	357.50	1483	14.83	1721	17.21	16.02
215	17.20	366.01	1528	15.28	1763	17.63	16.45
220	17.60	374.52	1589	15.89	1810	18.10	16.99
225	18.00	383.04	1614	16.14	1898	18.98	17.56

230	18.40	391.55	1654	16.54	1938	19.38	17.96
235	18.80	400.06	1709	17.09	1978	19.78	18.43
240	19.20	408.58	1750	17.50	2012	20.12	18.81
245	19.60	417.08	1805	18.05	2044	20.44	19.24
250	20.00	425.60	1875	18.75	2074	20.74	19.74
255	20.40	434.11	1940	19.40	2109	21.09	20.24
260	20.80	442.62	2016	20.16	2149	21.49	20.82
265	21.20	451.13	2064	20.64	2192	21.92	21.28
270	21.60	459.65	2109	21.09	2232	22.32	21.70
275	22.00	468.16	2154	21.54	2274	22.74	22.14
280	22.40	476.67	2200	22.00	2319	23.19	22.59
285	22.80	485.18	2253	22.53	2368	23.68	23.10
290	23.20	493.69	2299	22.99	2410	24.10	23.54
295	23.60	502.20	2344	23.44	2450	24.50	23.97
300	24.00	510.72	2373	23.73	2491	24.91	24.32
305	24.40	519.23	2423	24.23	2528	25.28	24.75
310	24.80	527.74	2450	24.50	2561	25.61	25.05

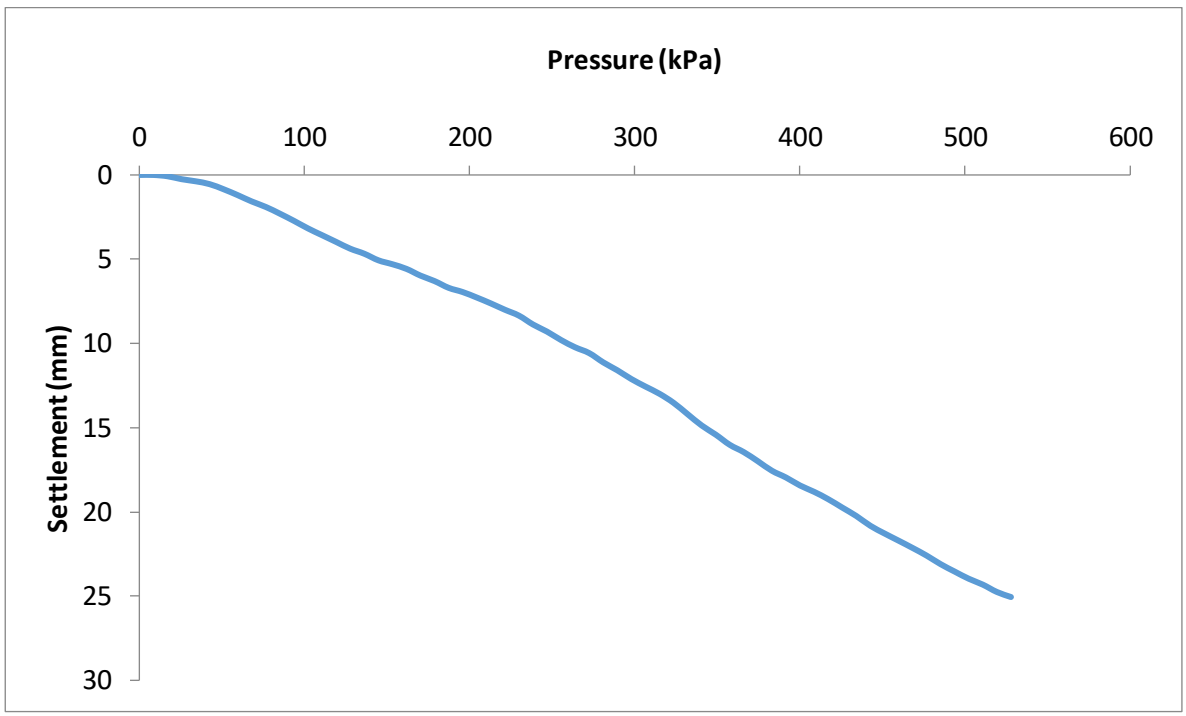

Figure 4.8 Bearing pressure versus normalized settlement curves with 2% pre-tension force

4.3.3 Pretensioning at 3%

Table 4.8 Readings of test series C (3% pretensioned)

Proving Ring Divisions	Load (kN)	Load Intensity (kPa)	Dial gauge 1 reading	Settlement 1 (mm)	Dial gauge 2 reading	Settlement 2 (mm)	Average settlement (mm)
0	0	0	0	0	0	0	0
5	0.40	8.51	10	0.10	22	0.22	0.16
10	0.80	17.02	50	0.50	55	0.55	0.52
15	1.20	25.54	90	0.90	95	0.95	0.92
20	1.60	34.05	130	1.30	130	1.30	1.30
25	2.00	42.56	175	1.75	160	1.60	1.67
30	2.40	51.07	212	2.12	200	2.00	2.06
35	2.80	59.58	250	2.50	235	2.35	2.42
40	3.20	68.09	292	2.92	275	2.75	2.83
45	3.60	76.61	330	3.30	305	3.05	3.17
50	4.00	85.12	370	3.70	345	3.45	3.57
55	4.40	93.63	405	4.05	370	3.70	3.87
60	4.80	102.14	445	4.45	405	4.05	4.25
65	5.20	110.66	485	4.85	440	4.40	4.62
70	5.60	119.17	520	5.20	475	4.75	4.97
75	6.00	127.68	570	5.70	525	5.25	5.47
80	6.40	136.19	635	6.35	589	5.89	6.12
85	6.80	144.70	676	6.76	632	6.32	6.54
90	7.20	153.22	727	7.27	679	6.79	7.03
95	7.60	161.79	791	7.91	743	7.43	7.67
100	8.00	170.24	837	8.37	784	7.84	8.10
105	8.40	178.75	876	8.76	830	8.30	8.53
110	8.80	187.26	935	9.35	880	8.80	9.07
115	9.20	195.78	983	9.83	932	9.32	9.57
120	9.60	204.29	1024	10.24	977	9.77	10.00
125	10.00	212.80	1072	10.72	1020	10.20	10.46
130	10.40	221.31	1122	11.22	1065	10.65	10.93
135	10.80	229.82	1164	11.64	1172	11.72	11.68
140	11.20	238.33	1204	12.04	1222	12.22	12.13
145	11.60	246.85	1258	12.58	1272	12.72	12.65
150	12.00	255.36	1301	13.01	1324	13.24	13.12
155	12.40	263.87	1357	13.57	1360	13.60	13.58
160	12.80	272.38	1407	14.07	1415	14.15	14.11
165	13.20	280.89	1457	14.57	1458	14.58	14.57

170	13.60	289.41	1510	15.10	1504	15.04	15.07
175	14.00	297.92	1553	15.53	1555	15.55	15.54
180	14.40	306.43	1596	15.96	1612	16.12	16.04
185	14.80	314.94	1639	16.39	1652	16.52	16.45
190	15.20	323.46	1691	16.91	1706	17.06	16.98
195	15.60	331.97	1737	17.37	1755	17.55	17.46
200	16.00	340.48	1791	17.91	1804	18.04	17.97
205	16.40	348.99	1850	18.50	1864	18.64	18.57
210	16.80	357.50	1911	19.11	1931	19.31	19.21
215	17.20	366.01	1981	19.81	2006	20.06	19.93
220	17.60	374.53	2056	20.56	2069	20.69	20.62
225	18.00	383.04	2125	21.25	2140	21.40	21.32
230	18.40	391.55	2199	21.99	2203	22.03	22.01
235	18.80	400.06	2266	22.66	2283	22.83	22.74
240	19.20	408.58	2344	23.44	2363	23.63	23.53
245	19.60	417.08	2422	24.22	2434	24.34	24.28
250	20.00	425.60	2498	24.98	2504	25.04	25.01
255	20.40	434.11	2573	25.73	2570	25.70	25.71
260	20.80	442.62	2644	26.44	2633	26.33	26.38

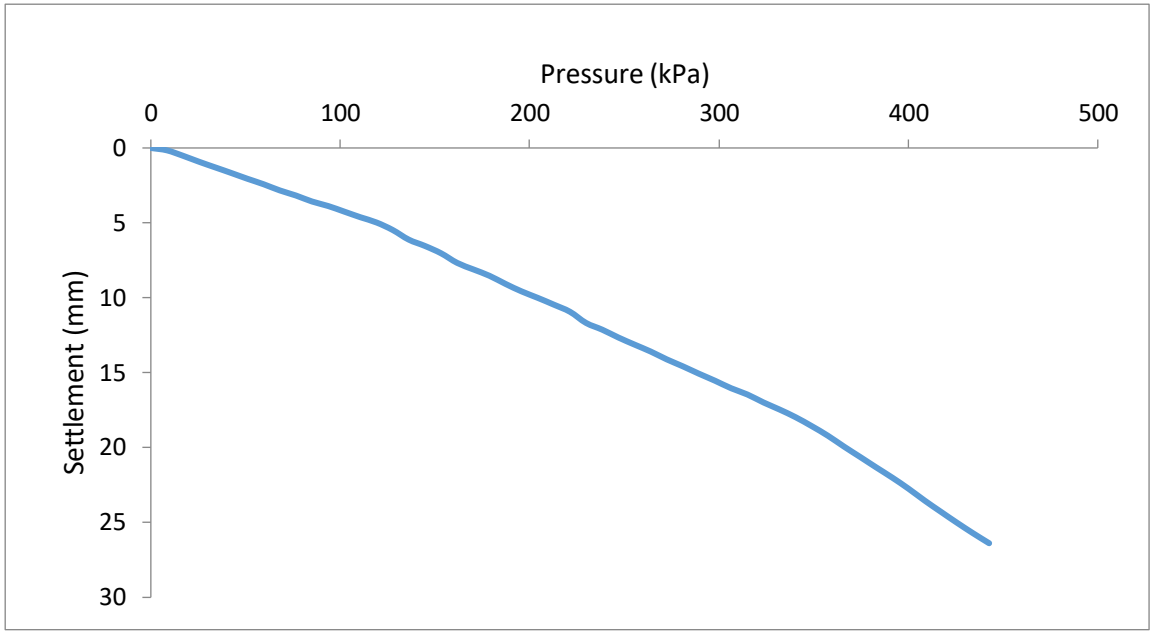

Figure 4.9 Bearing pressure versus normalized settlement curves with 3% pre-tension force

4.3.4 Comparison curve for test series C

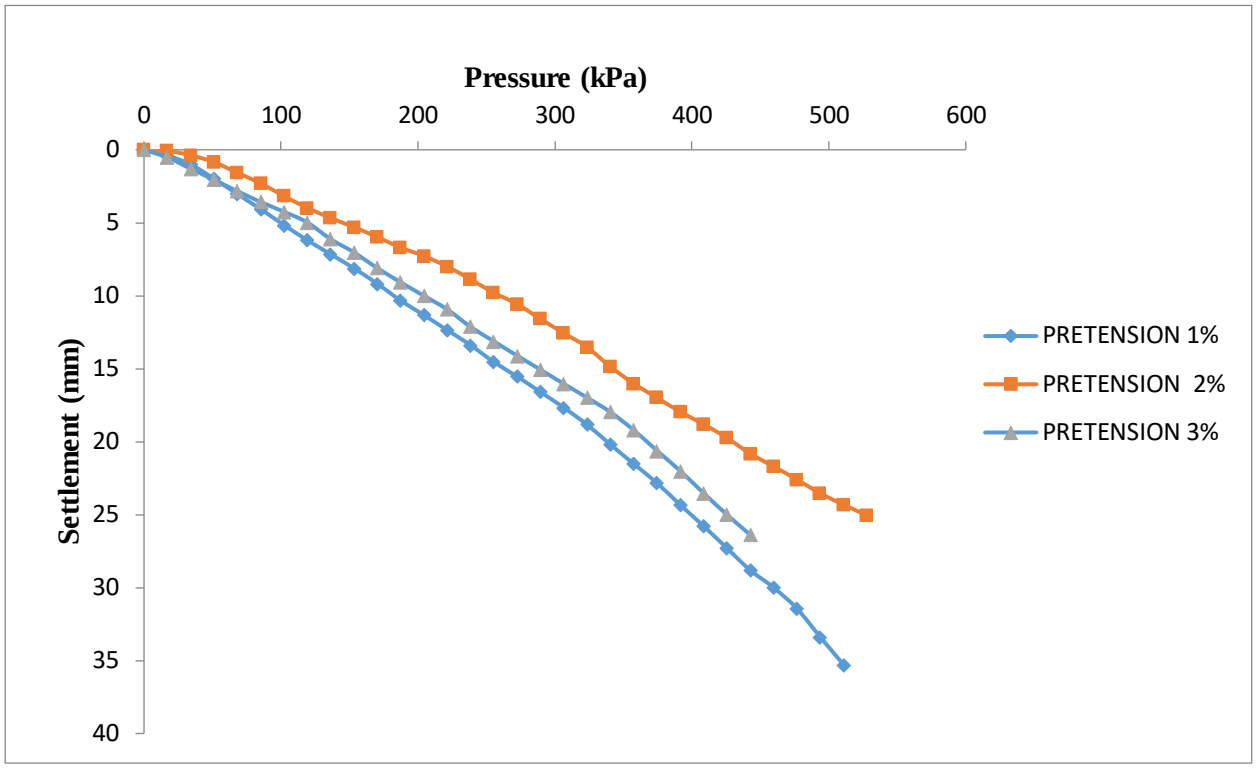

Fig4.10 Bearing pressure versus normalized settlement curves with varying pretension force

4.4 OVERALL COMPARISION

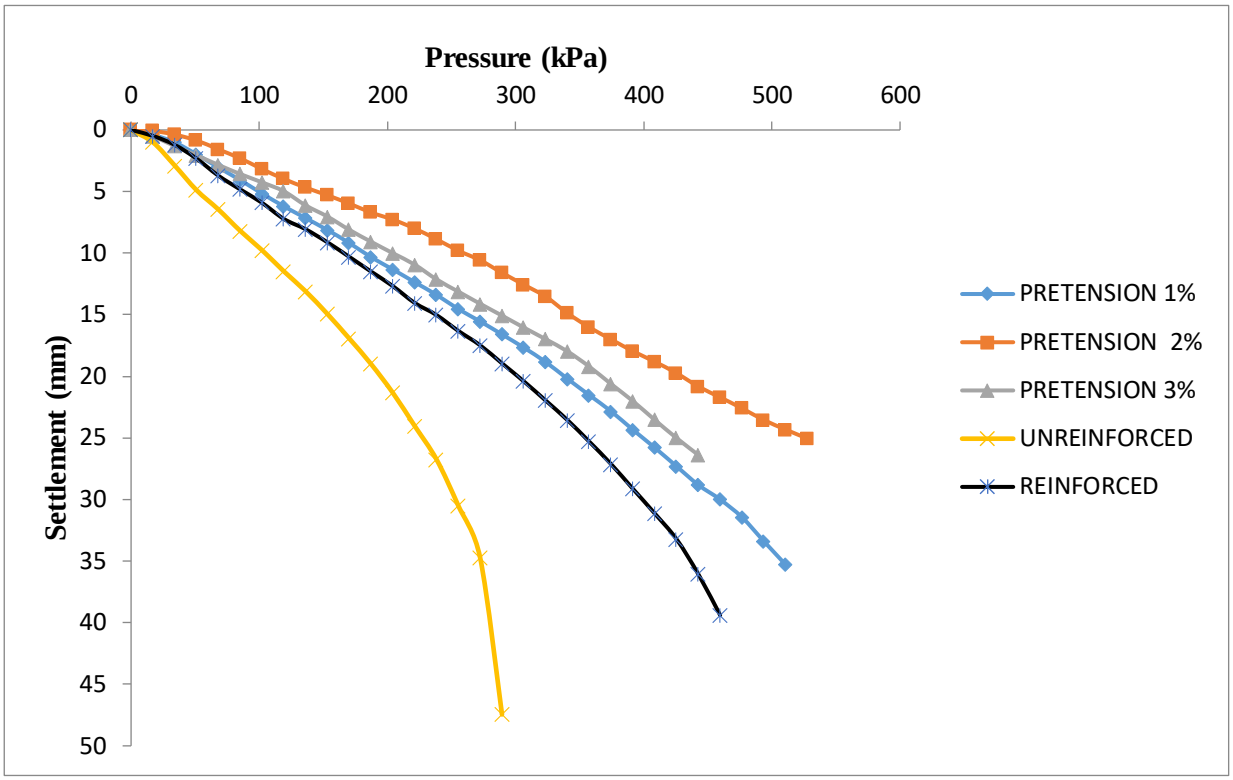

Figure 4.11 Bearing pressure versus normalized settlement curve for test series A,B,C

The result obtained from the experimental program shown in figure 4.1 to 4.11. These graphs show the effect of geogrid by the variation of the placement of geogrid on ferrochrome slag and the effect of pretensioning of geogrid. From the comparison curve of Test series B (fig 4.6) the bearing capacity of ferrochrome slag for u/B= 0.2, u/B= 0.3 u/B=0.4 and u/B= 0.5 at the 5mm settlement are 72kPa, 66kPa, 85kPa, 63kPa respectively is obtained. So it is found that the optimum depth of geogrid(act as reinforcement) is u/B = 0.4. Now geogrid was pretensioned to 1%, 2% and 3% of its tensile strength at the optimum depth of reinforcement. The bearing capacity at a given settlement of ferrochrome slag at 1%,2% and 3% pretensioning are 97kPa,144kPa, and 118kPa respectively. So it is find that at 2% pretensioning of geogrid maximum load carrying capacity is achieved when compare to other case of 1% and 3% of pretensioning.

4.5 IMPROVEMENT FACTOR

This is the improvement factor for medium dense filled soil.

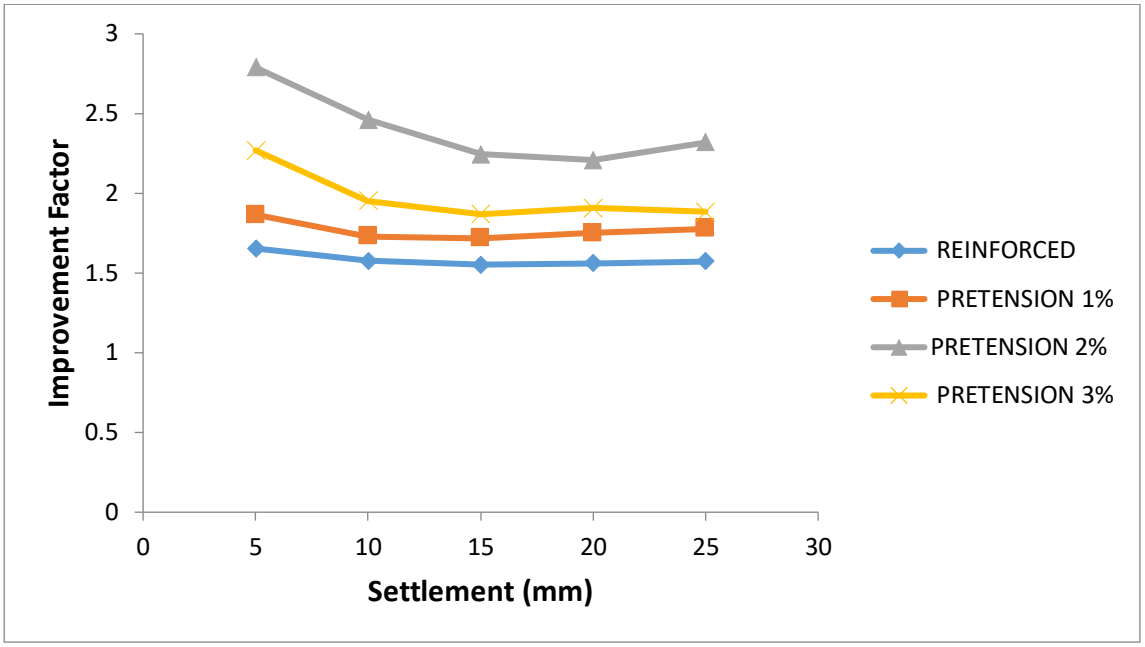

Figure 4.12: Improvement factor versus settlement curve

Allowable bearing capacity ratio (BCR_s) is defined as the ratio of q and q_R , where q is load-bearing capacity values for unreinforced and q_R reinforced foundations, respectively, at the same settlement, s:

$$BCR_s = \frac{q_R}{q}$$

Percentage reduction in settlement (%):

$$PRS(\%) = \frac{S_u \pm S_r or S_p}{S_u} \times 100$$

Where S_r, S_p and S_u are the settlement of the reinforced, pretension reinforced and unreinforced soil respectively at a given bearing pressure.

Allowable bearing capacity ratio corresponding 5mm settlement was calculated for all test series.

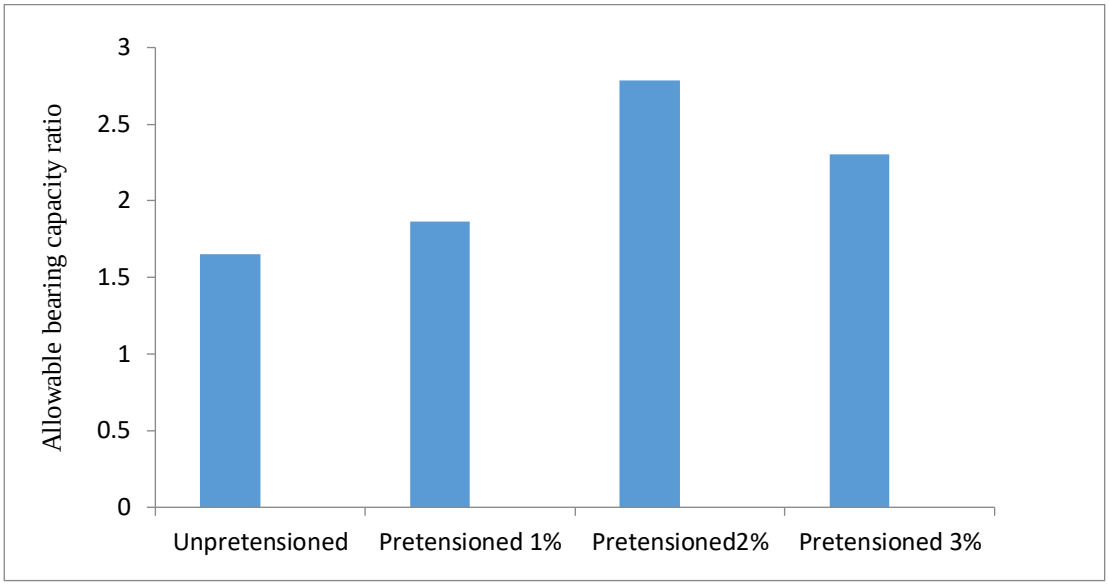

Figure 4.13Variation in allowable bearing capacity ratio

From the figure 4.12 and 4.13 it is found that the after simply reinforcing the soil with geogrid without pretensioning the improvement in load carrying capacity of ferrochrome slag is 1.65 times of the unreinforced condition whereas after the pretensioning the improvement in load carrying capacity corresponding to 5 mm settlement is 2.79 times of unreinforced condition so this data states that pre-tensioning with geogrid is more beneficial in comparison to the simply reinforced with geogrid.

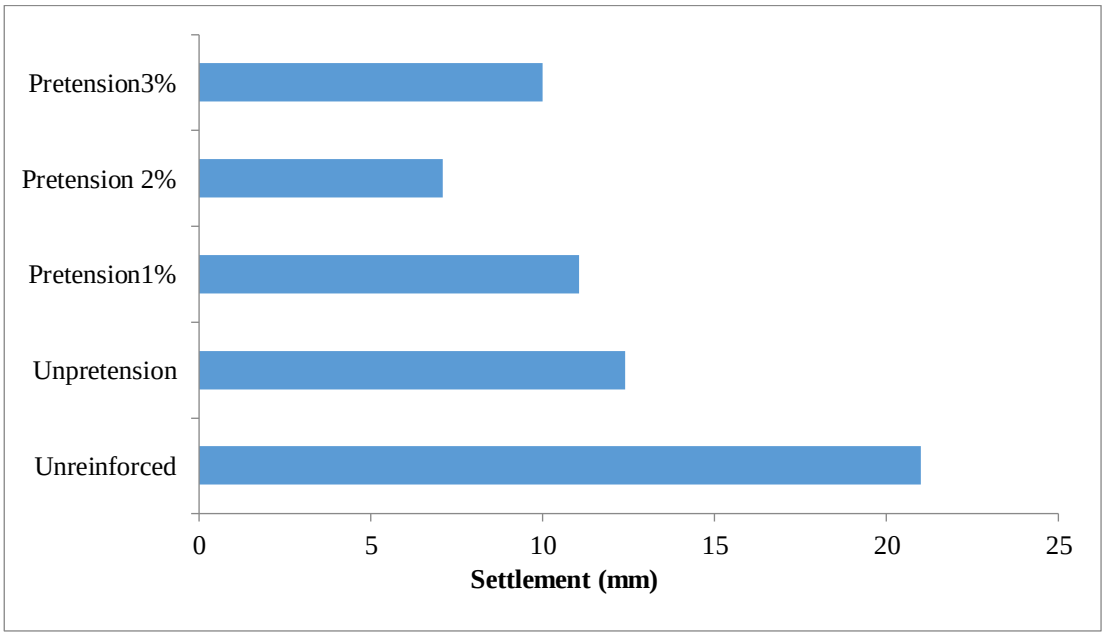

Figure 4.14: Settlement curve corresponding to 200kPa pressure

It is the evident from the nature of the above fig4.14 that obtained settlement is minimum for 2% pre-tensioning, corresponding to 200kPa pressure.

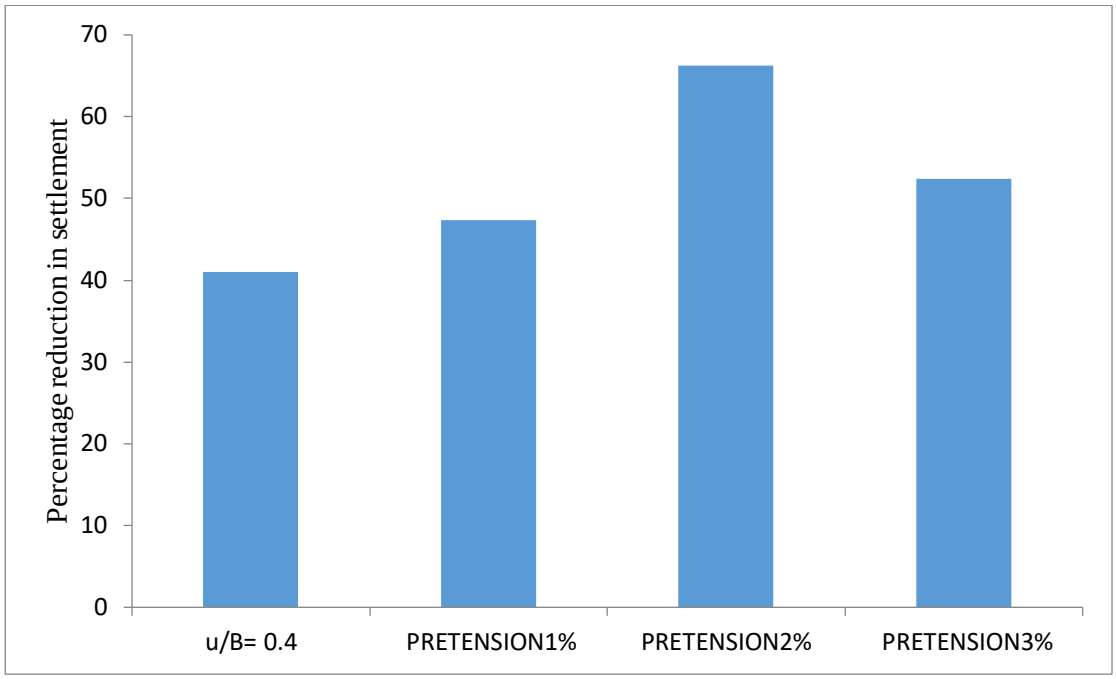

Figure 4.15 Percentage reduction in settlement of footing for Test series B,C

From the fig 4.15 obtained result it is evident that the PRS for 2% pretension showed maximum value of 66.19% and hence it is identified that 2% pretension is the optimum for PRS consideration, corresponding to 200kPa pressure.

4.6 TEST SERIES 1 (UNREINFORCED):

Table 4.9 Readings of test series 1 (Unreinforced)

Proving Ring Divisions	Load (kN)	Load Intensity (kPa)	Dial gauge 1 reading	Settlement 1 (mm)	Dial gauge 2 reading	Settlement 1 (mm)	Average settlement (mm)
0	0	0	0	0	0	0	0
5	0.40	8.51	20	0.20	55	0.55	0.37
10	0.80	17.02	65	0.65	134	1.34	0.99
15	1.20	25.54	160	1.60	198	1.98	1.79
20	1.60	34.05	250	2.50	285	2.85	2.67
25	2.00	42.56	362	3.62	347	3.47	3.54
30	2.40	51.07	481	4.81	429	4.29	4.55
35	2.80	59.58	536	5.36	505	5.05	5.20
40	3.20	68.09	647	6.47	565	5.65	6.07
45	3.60	76.61	710	7.10	629	6.29	6.69
50	4.00	85.12	800	8.00	690	6.90	7.45
55	4.40	93.63	905	9.05	750	7.50	8.27
60	4.80	102.14	996	9.96	844	8.44	9.20
65	5.20	110.66	1012	10.12	943	9.43	9.77
70	5.60	119.17	1105	11.05	1053	10.53	10.79
75	6.00	127.68	1200	12.00	1155	11.55	11.77
80	6.40	136.19	1294	12.94	1265	12.65	12.79
85	6.80	144.70	1396	13.96	1406	14.06	14.01
90	7.20	153.21	1550	15.50	1518	15.18	15.34
95	7.60	161.73	1738	17.38	1615	16.15	16.76
100	8.00	170.24	1910	19.10	1758	17.58	18.34
105	8.40	178.75	2083	20.83	1908	19.08	19.95
110	8.80	187.26	2272	22.72	2046	20.46	21.59
115	9.20	195.78	2443	24.43	2189	21.89	23.16
120	9.60	204.29	2634	26.34	2344	23.44	24.89
125	10.00	212.80	2835	28.35	2484	24.84	26.59
130	10.40	221.31	3031	30.31	2614	26.14	28.22
135	10.80	229.82	3232	32.32	2777	27.77	30.04
140	11.20	238.34	3462	34.62	2941	29.41	32.01
145	11.60	246.85	3702	37.02	3112	31.12	34.07
150	12.00	255.36	3952	39.52	3262	32.62	36.07
155	12.40	263.87	4314	43.14	3429	34.29	38.71
160	12.80	272.38	4519	45.19	3580	35.8	40.49

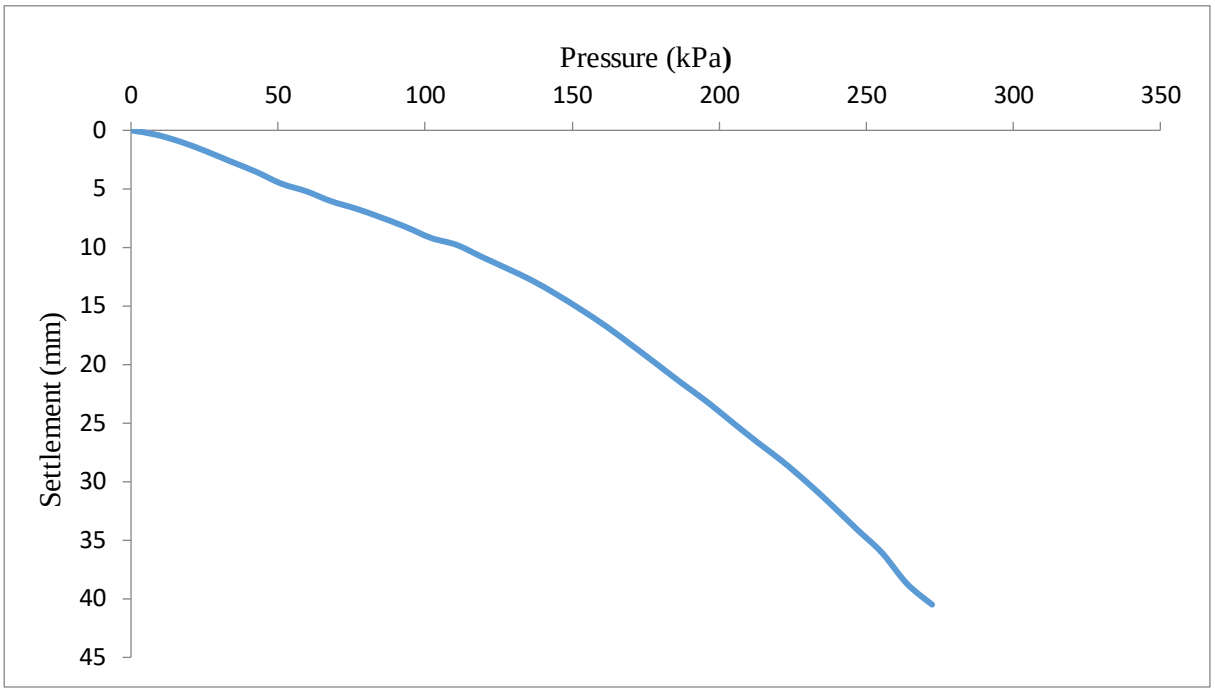

Figure 4.16 Bearing pressure versus normalized settlement curves in unreinforced condition for loosely filled soil

4.7 TEST SERIES 2 (REINFORCED):

Table: 4.10 Readings of test series 2for u/B=0.4

Proving Ring Divisions	Load (kN)	Load Intensity (kPa)	Dial gauge 1 reading	Settlement 1 (mm)	Dial gauge 2 reading	Settlement 2 (mm)	Average settlement (mm)
0	0	0	0	0	0	0	0
5	0.40	8.51	10	0.10	15	0.15	0.12
10	0.80	17.02	92	0.92	50	0.50	0.71
15	1.20	25.54	180	1.80	100	1.00	1.40
20	1.60	34.05	240	2.40	156	1.56	1.98
25	2.00	42.56	320	3.20	213	2.13	2.66
30	2.40	51.07	398	3.98	290	2.90	3.44
35	2.80	59.58	471	4.71	354	3.54	4.12
40	3.20	68.09	553	5.53	433	4.33	4.93
45	3.60	76.61	619	6.19	500	5.00	5.59
50	4.00	85.12	698	6.98	565	5.65	6.31
55	4.40	93.63	775	7.75	635	6.35	7.05

60	4.80	102.14	840	8.40	701	7.01	7.70
65	5.20	110.66	928	9.28	770	7.70	8.49
70	5.60	119.17	998	9.98	832	8.32	9.15
75	6.00	127.68	1064	10.64	890	8.90	9.77
80	6.40	136.19	1139	11.39	953	9.53	10.46
85	6.80	144.70	1230	12.30	1031	10.31	11.30
90	7.20	153.22	1310	13.10	1092	10.92	12.01
95	7.60	161.73	1390	13.90	1159	11.59	12.74
100	8.00	170.24	1463	14.63	1230	12.30	13.46
105	8.40	178.75	1529	15.29	1285	12.85	14.07
110	8.80	187.26	1596	15.96	1350	13.50	14.73
115	9.20	195.78	1663	16.63	1409	14.09	15.36
120	9.60	204.28	1738	17.38	1468	14.68	16.03
125	10.00	212.89	1846	18.46	1553	15.53	16.99
130	10.40	221.31	1928	19.28	1623	16.23	17.75
135	10.80	229.82	2005	20.05	1680	16.80	18.42
140	11.20	238.34	2080	20.80	1739	17.39	19.09
145	11.60	246.85	2200	22.00	1832	18.32	20.16
150	12.00	255.36	2292	22.92	1896	18.96	20.94
155	12.40	263.87	2383	23.83	1954	19.54	21.68
160	12.80	272.38	2483	24.83	2024	20.24	22.53
165	13.20	280.89	2585	25.85	2090	20.90	23.37
170	13.60	289.41	2708	27.08	2172	21.72	24.40
175	14.00	297.92	2803	28.03	2237	22.37	25.20
180	14.40	306.43	2905	29.05	2303	23.03	26.04
185	14.80	314.94	3013	30.13	2373	23.73	26.93
190	15.20	323.46	3143	31.43	2455	24.55	27.99
195	15.60	331.97	3255	32.55	2529	25.29	28.92
200	16.00	340.48	3381	33.81	2605	26.05	29.93
205	16.40	348.99	3494	34.94	2680	26.80	30.87
210	16.80	357.50	3610	36.10	2746	27.46	31.78
215	17.20	366.01	3780	37.80	2829	28.29	33.04
220	17.60	374.53	3890	38.90	2903	29.03	33.96
225	18.00	383.04	4030	40.30	2980	29.80	35.05
230	18.40	391.55	4135	41.35	3049	30.49	35.92

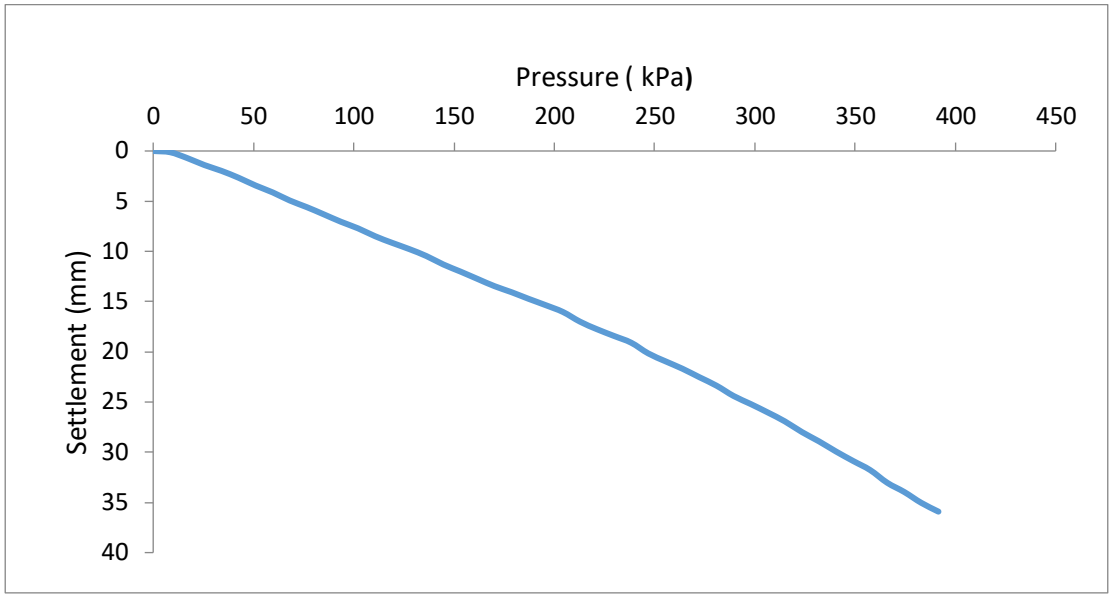

Figure 4.17: Bearing pressure versus normalized settlement curves for u/B=0.4

4.8 TEST SERIES 3 (PRETENSION CONDITION)

4.8.1 Pretension at 1%

Table: 4.11 Readings of test series 3 (1% pretension)

Proving Ring Divisions	Load (kN)	Load Intensity (kPa)	Dial gauge 2 reading	Settlement 1 (mm)	Dial gauge 2 reading	Settlement 2 (mm)	Average settlement (mm)
0	0	0	0	0	0	0	0
5	0.40	8.51	0	0	16	0.16	0.08
10	0.80	17.02	7	0.07	93	0.93	0.50
15	1.20	25.54	65	0.65	159	1.59	1.12
20	1.60	34.05	149	1.49	216	2.16	1.82
25	2.00	42.56	227	2.27	278	2.78	2.52
30	2.40	51.07	312	3.12	346	3.46	3.29
35	2.80	59.58	393	3.93	408	4.08	4.00
40	3.20	68.09	457	4.57	460	4.60	4.58
45	3.60	76.61	532	5.32	517	5.17	5.24
50	4.00	85.12	604	6.04	570	5.70	5.87
55	4.40	93.63	680	6.80	627	6.27	6.53
60	4.80	102.14	747	7.47	680	6.80	7.13
65	5.20	110.66	820	8.20	739	7.39	7.79
70	5.60	119.17	889	8.89	791	7.91	8.40
75	6.00	127.69	947	9.47	841	8.41	8.94

80	6.40	136.19	1016	10.16	897	8.97	9.56
85	6.80	144.70	1086	10.86	955	9.55	10.20
90	7.20	153.22	1157	11.57	1005	10.05	10.81
95	7.60	161.73	1224	12.24	1059	10.59	11.41
100	8.00	170.24	1304	13.04	1125	11.25	12.14
105	8.40	178.75	1360	13.60	1170	11.70	12.65
110	8.80	187.26	1425	14.25	1223	12.23	13.24
115	9.20	195.78	1489	14.89	1270	12.70	13.79
120	9.60	204.29	1562	15.62	1325	13.25	14.43
125	10.00	212.80	1618	16.18	1375	13.75	14.96
130	10.40	221.31	1697	16.97	1441	14.41	15.69
135	10.80	229.82	1760	17.60	1490	14.90	16.25
140	11.20	238.34	1823	18.23	1532	15.32	16.77
145	11.60	246.85	1890	18.90	1578	15.78	17.34
150	12.00	255.36	1955	19.55	1630	16.30	17.92
155	12.40	263.87	2102	21.02	1679	16.79	18.90
160	12.80	272.38	2310	23.10	1743	17.43	20.26
165	13.20	280.89	2368	23.68	1784	17.84	20.76
170	13.60	289.41	2438	24.38	1833	18.33	21.35
175	14.00	297.92	2519	25.19	1875	18.75	21.97
180	14.40	306.43	2599	25.99	1927	19.27	22.63
185	14.80	314.94	2668	26.68	1972	19.72	23.20
190	15.20	323.46	2753	27.53	2028	20.28	23.95
195	15.60	331.97	2831	28.31	2076	20.76	24.53
200	16.00	340.48	2912	29.12	2133	21.33	25.22
205	16.40	348.99	3005	30.05	2190	21.9	25.97
210	16.80	357.50	3073	30.73	2244	22.44	26.58
215	17.20	366.02	3168	31.68	2297	22.97	27.32
220	17.60	374.53	3244	32.44	2340	23.40	27.92
225	18.00	383.04	3335	33.35	2390	23.90	28.62
230	18.40	391.55	3408	34.08	2438	24.38	29.23
235	18.80	400.06	3500	35.00	2492	24.92	29.96
240	19.20	408.58	3590	35.90	2556	25.56	30.73
245	19.60	417.09	3678	36.78	2604	26.04	31.41
250	20.00	425.60	3794	37.94	2656	26.56	32.25
255	20.40	434.11	3885	38.85	2702	27.02	32.93
260	20.80	442.62	3957	39.57	2745	27.45	33.51
265	21.20	451.14	4057	40.57	2791	27.91	34.24
270	21.60	459.65	4154	41.54	2838	28.38	34.96
275	22.00	468.16	4282	42.82	2895	28.95	35.88
280	22.40	476.67	4353	43.53	2930	29.30	36.41
285	22.80	485.18	4487	44.87	2985	29.85	37.36
290	23.20	493.69	4604	46.04	3032	30.32	38.18

295	23.60	502.21	4728	47.28	3082	30.82	39.05

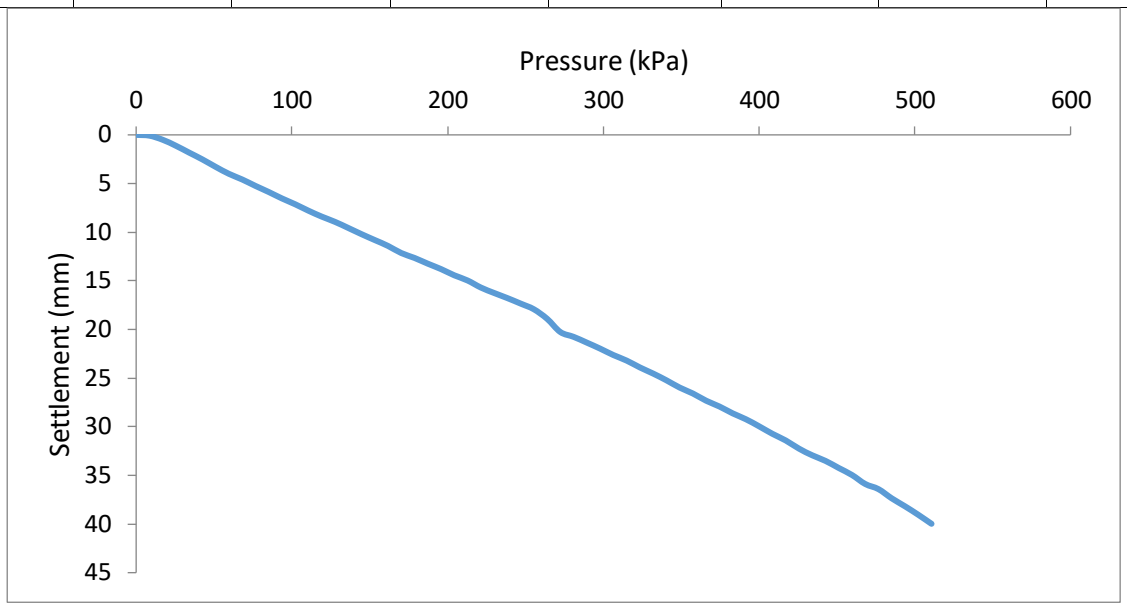

Figure 4.18 :Bearing pressure versus normalized settlement curves for pretension 1%

4.8.2 Pretensioning at 2%

Table 4.12: Readings of test series 3 (2% pretension)

Proving Ring Divisions	Load (kN)	Load Intensity (kPa)	Dial gauge 1 reading	Settlement 1 (mm)	Dial gauge 2 reading	Settlement 1 (mm)	Average settlement (mm)
0	0	0	0	0	0	0	0
5	0.40	8.51	0	0.00	55	0.55	0.27
10	0.80	17.02	0	0.00	149	1.49	0.74
15	1.20	25.54	0	0.00	246	2.46	1.23
20	1.60	34.05	0	0.00	311	3.11	1.55
25	2.00	42.56	0	0.00	387	3.87	1.93
30	2.40	51.07	0	0.00	471	4.71	2.35
35	2.80	59.58	0	0.00	534	5.34	2.67
40	3.20	68.09	0	0.00	609	6.09	3.04
45	3.60	76.61	0	0.00	673	6.73	3.36
50	4.00	85.12	0	0.00	738	7.38	3.69
55	4.40	93.63	0	0.00	811	8.11	4.05
60	4.80	102.14	0	0.00	868	8.68	4.34
65	5.20	110.66	0	0.00	923	9.23	4.61
70	5.60	119.17	0	0.00	984	9.84	4.92
75	6.00	127.68	0	0.00	1046	10.46	5.23
80	6.40	136.19	0	0.00	1107	11.07	5.53

85	6.80	144.71	0	0.00	1167	11.67	5.83
90	7.20	153.22	0	0.00	1228	12.28	6.14
95	7.60	161.73	31	0.31	1296	12.96	6.63
100	8.00	170.24	83	0.83	1356	13.56	7.19
105	8.40	178.75	136	1.36	1418	14.18	7.77
110	8.80	187.26	174	1.74	1473	14.73	8.23
115	9.20	195.78	219	2.19	1527	15.27	8.73
120	9.60	204.29	265	2.65	1581	15.81	9.23
125	10.00	212.80	302	3.02	1632	16.32	9.67
130	10.40	221.31	354	3.54	1693	16.93	10.23
135	10.80	229.82	400	4.00	1741	17.41	10.70
140	11.20	238.34	450	4.50	1798	17.98	11.24
145	11.60	246.85	497	4.97	1870	18.70	11.83
150	12.00	255.36	562	5.62	1943	19.43	12.52
155	12.40	263.87	613	6.13	2004	20.04	13.08
160	12.80	272.38	661	6.61	2078	20.78	13.69
165	13.20	280.89	700	7.00	2125	21.25	14.12
170	13.60	289.41	736	7.36	2181	21.81	14.58
175	14.00	297.92	779	7.79	2239	22.39	15.09
180	14.40	306.43	846	8.46	2317	23.17	15.81
185	14.80	314.94	897	8.97	2397	23.97	16.47
190	15.20	323.45	942	9.42	2459	24.59	17.00
195	15.60	331.97	1005	10.05	2543	25.43	17.74
200	16.00	340.48	1052	10.52	2613	26.13	18.32
205	16.40	348.99	1090	10.90	2668	26.68	18.79
210	16.80	357.50	1150	11.50	2759	27.59	19.54
215	17.20	366.01	1193	11.93	2823	28.23	20.08
220	17.60	374.52	1253	12.53	2905	29.05	20.79
225	18.00	383.04	1314	13.14	2988	29.88	21.51
230	18.40	391.55	1360	13.60	3060	30.60	22.10
235	18.80	400.06	1412	14.12	3135	31.35	22.73
240	19.20	408.57	1454	14.54	3206	32.06	23.30
245	19.60	417.09	1510	15.10	3290	32.90	24.00
250	20.00	425.60	1552	15.52	3357	33.57	24.54
255	20.40	434.11	1608	16.08	3431	34.31	25.19
260	20.80	442.62	1655	16.55	3513	35.13	25.84
265	21.20	451.14	1706	17.06	3598	35.98	26.52
270	21.60	459.65	1754	17.54	3679	36.79	27.16
275	22.00	468.16	1793	17.93	3754	37.54	27.73
280	22.40	476.67	1857	18.57	3863	38.63	28.60
285	22.80	485.18	1903	19.03	3951	39.51	29.27
290	23.20	493.69	1951	19.51	4051	40.51	30.01
295	23.60	502.21	1998	19.98	4141	41.41	30.69

300	24.00	510.72	2046	20.46	4243	42.43	31.44
305	24.40	519.23	2106	21.06	4353	43.53	32.29
310	24.80	527.74	2158	21.58	4435	44.35	32.96
315	25.20	536.26	2215	22.15	4534	45.34	33.74
320	25.60	544.77	2288	22.88	4668	46.68	34.78

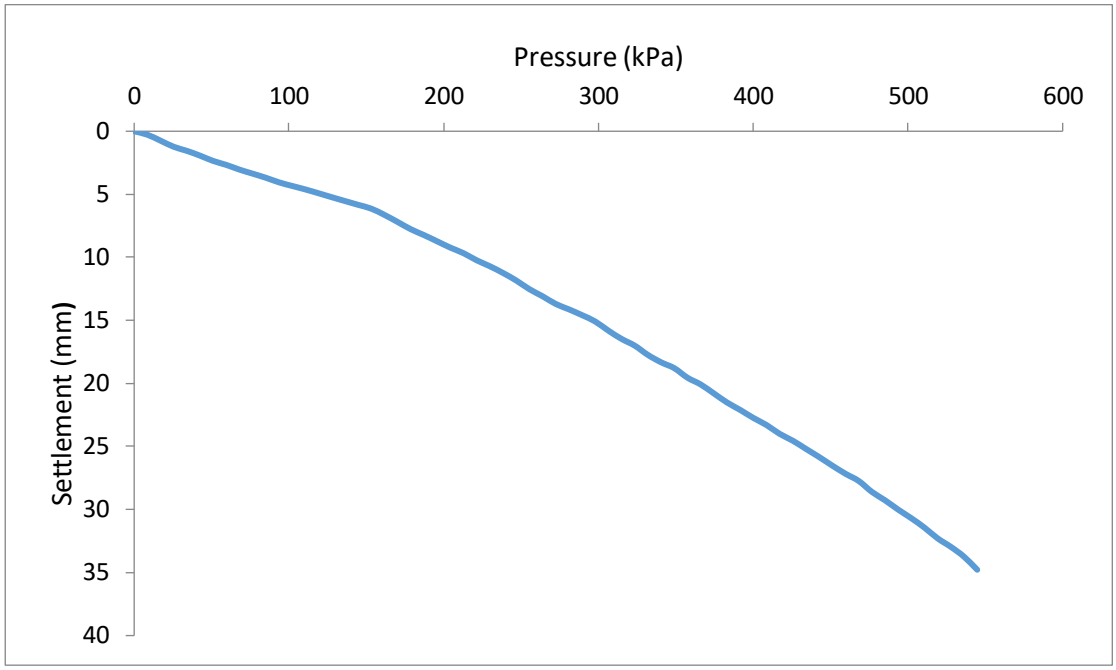

Figure 4.19 Bearing pressure versus normalized settlement curves for pretension 2%

4.8.3 Pretensioning at 3%

Table 4.13: Readings of test series c (3% pretension)

Proving Ring Divisions	Load (kN)	Load Intensity (kPa)	Dial gauge 1 reading	Settlement 1 (mm)	Dial gauge 1 reading	Settlement 1 (mm)	Average settlement (mm)
0	0	0	0	0	0	0	0
5	0.40	8.51	0	0.00	0	0.00	0.00
10	0.80	17.02	29	0.29	20	0.20	0.24
15	1.20	25.54	45	0.45	41	0.41	0.43
20	1.60	34.05	90	0.90	55	0.55	0.72
25	2.00	42.56	140	1.40	70	0.70	1.05
30	2.40	51.07	170	1.70	92	0.92	1.31
35	2.80	59.58	205	2.05	114	1.14	1.59
40	3.20	68.09	296	2.96	120	1.20	2.08

45	3.60	76.61	368	3.68	140	1.40	2.54
50	4.00	85.12	450	4.50	172	1.72	3.11
55	4.40	93.63	525	5.25	235	2.35	3.80
60	4.80	102.14	582	5.82	276	2.76	4.29
65	5.20	110.66	652	6.52	331	3.31	4.91
70	5.60	119.17	735	7.35	391	3.91	5.63
75	6.00	127.68	804	8.04	439	4.39	6.21
80	6.40	136.19	888	8.88	486	4.86	6.87
85	6.80	144.70	951	9.51	538	5.38	7.44
90	7.20	153.22	1025	10.25	597	5.97	8.11
95	7.60	161.73	1100	11.00	647	6.47	8.73
100	8.00	170.24	1173	11.73	704	7.04	9.38
105	8.40	178.75	1233	12.33	750	7.50	9.91
110	8.80	187.26	1306	13.06	804	8.04	10.55
115	9.20	195.78	1380	13.80	848	8.48	11.14
120	9.60	204.28	1447	14.47	898	8.98	11.72
125	10.00	212.80	1513	15.13	937	9.37	12.25
130	10.40	221.31	1586	15.86	992	9.92	12.89
135	10.80	229.82	1660	16.60	1048	10.48	13.54
140	11.20	238.34	1728	17.28	1100	11.00	14.14
145	11.60	246.85	1803	18.03	1149	11.49	14.76
150	12.00	255.36	1867	18.67	1195	11.95	15.31
155	12.40	263.87	1946	19.46	1245	12.45	15.95
160	12.80	272.38	2033	20.33	1294	12.94	16.63
165	13.20	280.89	2103	21.03	1341	13.41	17.22
170	13.60	289.41	2191	21.91	1400	14.00	17.95
175	14.00	297.92	2266	22.66	1452	14.52	18.59
180	14.40	306.43	2341	23.41	1508	15.08	19.24
185	14.80	314.94	2411	24.11	1551	15.51	19.81
190	15.20	323.45	2507	25.07	1610	16.10	20.58
195	15.60	331.97	2594	25.94	1665	16.65	21.29
200	16.00	340.48	2693	26.93	1722	17.22	22.07
205	16.40	348.99	2781	27.81	1781	17.81	22.81
210	16.80	357.50	2877	28.77	1841	18.41	23.59
215	17.20	366.02	2962	29.62	1893	18.93	24.27
220	17.60	374.53	3048	30.48	1946	19.46	24.97
225	18.00	383.04	3145	31.45	2001	20.01	25.73
230	18.40	391.55	3238	32.38	2059	20.59	26.48
235	18.80	400.06	3308	33.08	2100	21.00	27.04
240	19.20	408.58	3437	34.37	2159	21.59	27.98
245	19.60	417.09	3536	35.36	2209	22.09	28.72
250	20.00	425.60	3666	36.66	2271	22.71	29.68
255	20.40	434.11	3760	37.60	2319	23.19	30.39

260	20.80	442.62	3853	38.53	2365	23.65	31.09
265	21.20	451.14	3932	39.32	2404	24.04	31.68
270	21.60	459.65	4085	40.85	2558	25.58	33.21
275	22.00	468.16	4177	41.77	2605	26.05	33.91
280	22.40	476.67	4200	42.00	2670	26.70	34.35
285	22.80	485.18	4308	43.08	2721	27.21	35.14
290	23.20	493.69	4412	44.12	2772	27.72	35.92
295	23.60	502.21	4533	45.33	2820	28.20	36.76
300	24.00	510.72	4673	46.73	2876	28.76	37.74
305	24.40	519.23	4791	47.91	2927	29.27	38.59
310	24.80	527.74	4800	48.00	2976	29.76	38.88

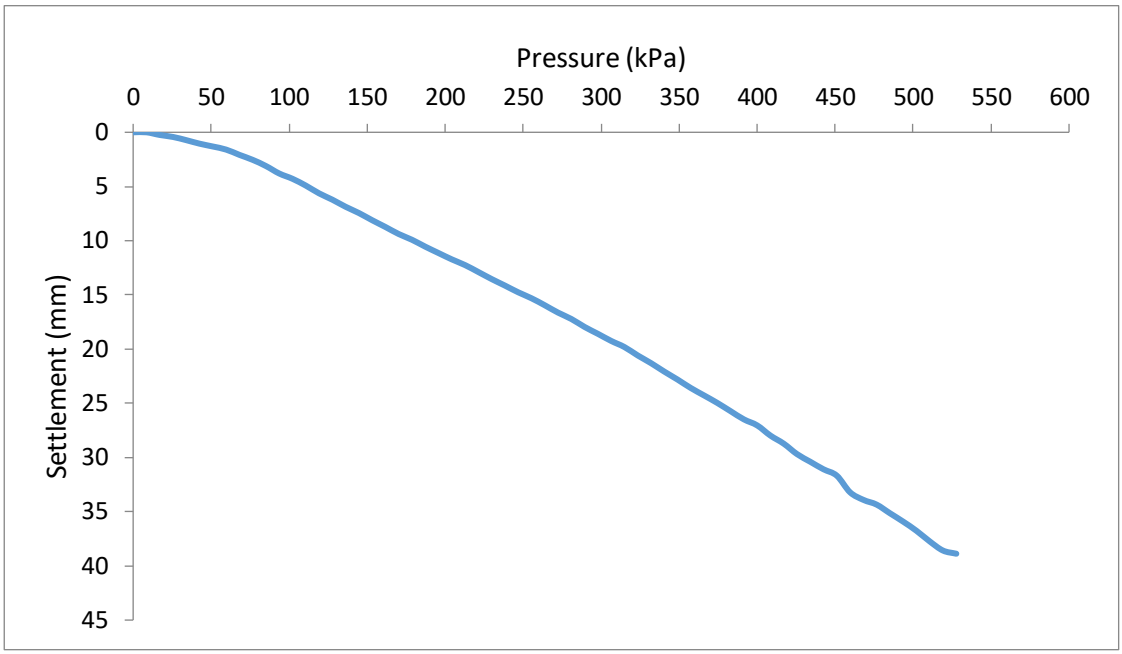

Figure 4.20 Bearing pressure versus normalized settlement curves for pretension 3%

4.8.4 Comparison curve for test series 3

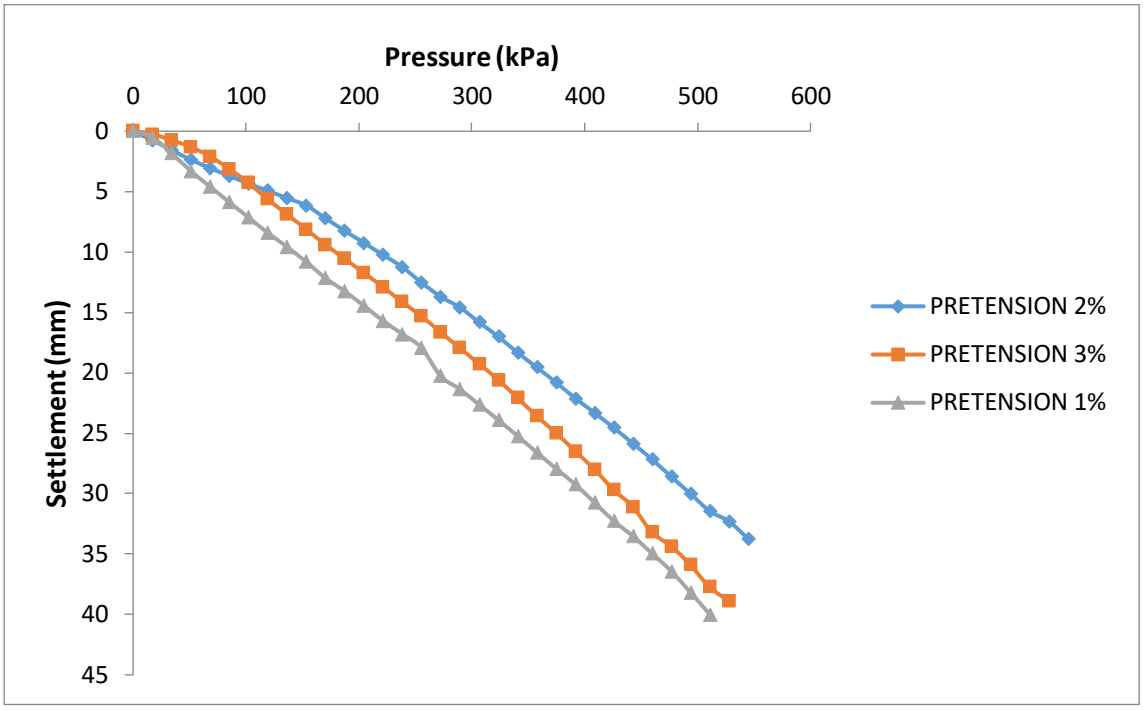

Figure 4.21: Comparison curve for test series 3

4.9 OVERALL COMPARISION FOR LOOSELY FILLED FERRCHROME SLAG

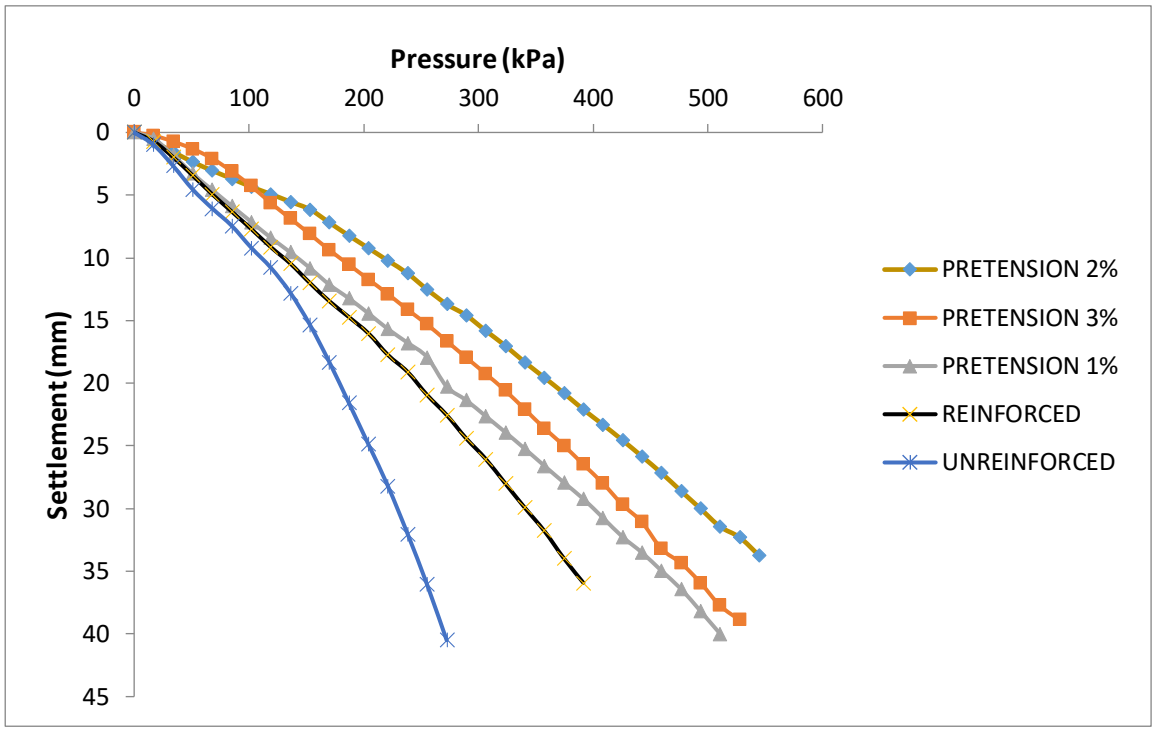

Figure: 4.22 Overall comparison curve for test series 1, 2 & 3

Geogrid was pretensioned to 1%, 2% and 3% of its tensile strength at the optimum depth of reinforcement. The bearing capacity corresponding to 5mm settlement of ferrochrome slag at 1%,2% and 3% pre-tensioning are 72kPa,116kPa, and 108kPa respectively. So it is find that at 2% pretensioning of geogrid maximum load carrying capacity is achieved when compare to other case of 1% and 3% of pretensioning.

4.10 IMPROVEMENT FACTOR

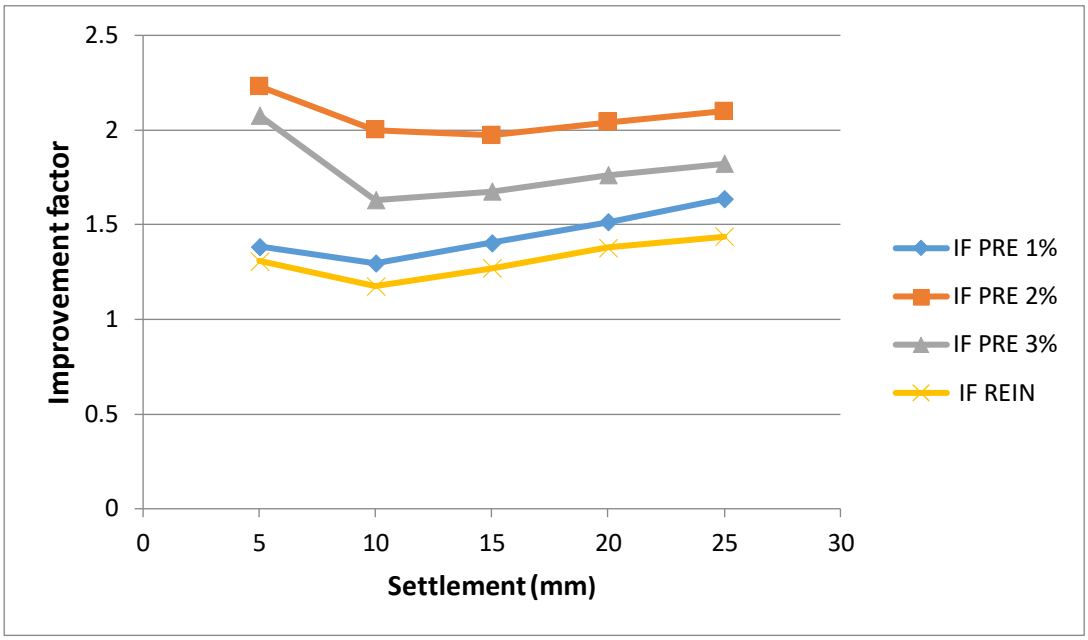

Figure 4.23: Improvement factor v/s settlement curve

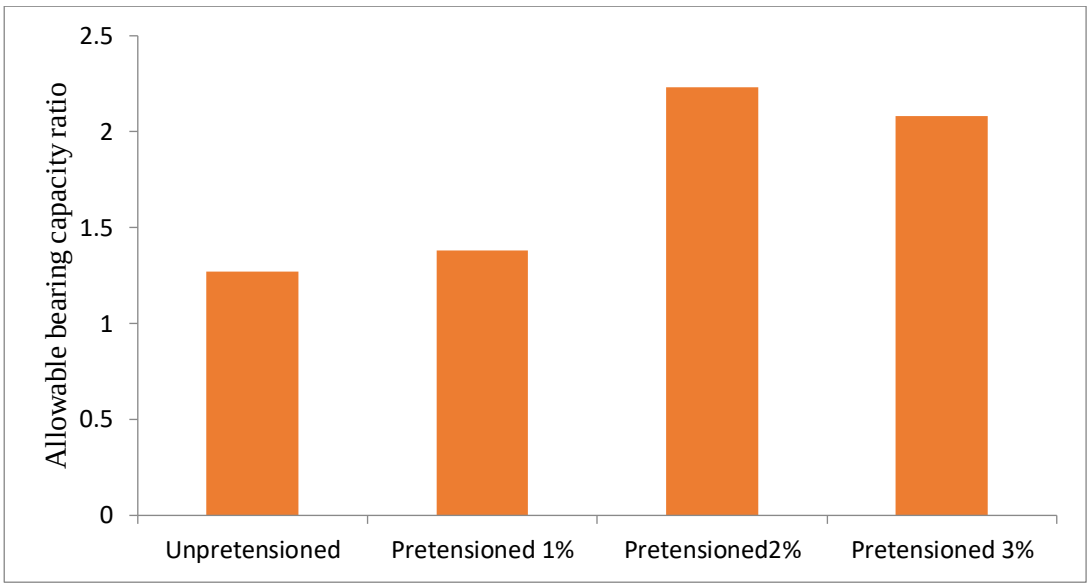

Figure 4.24: Allowable bearing capacity curve corresponding to 5mm settlement

From figure4.23 and 4.24 it is found that the after simply reinforcing the soil with geogrid without pre-tensioning the improvement in load carrying capacity of loosely filled ferrochrome slag is 1.31 times of the unreinforced condition whereas after the pretensioning the improvement in load carrying capacity corresponding to 5mm settlement is 2.23 times of unreinforced which is maximum value compare to 1% and 3% pretensioning of geogrid. This indicates that the 2% pretensioning is more effective in comparison to all for improving the load carrying capacity of ferrochrome slag. Figure 4.24 indicate that the improvement of ferrochrome slag corresponding to 5mm settlement whereas figure 4.23 indicate the improvement in pressure of ferrochrome slag for every instant of settlement.

When I compare the data of ferrochrome slag of loosely filled and medium dense then I found that the improvement in bearing capacity of ferrochrome slag in case of medium densely filled in more in comparison to the loosely filled ferrochrome slag in both unpretensioned condition and pre-tensioned condition.

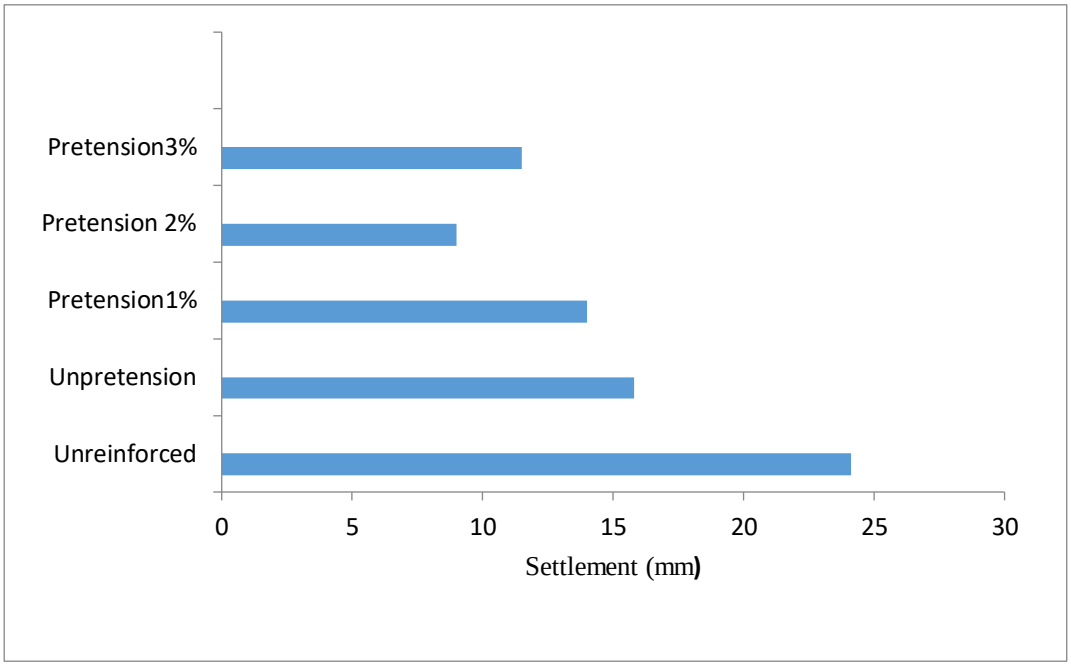

Figure 4.25: Settlement curve corresponding to 200kPa pressure

It is the evident from the nature of the above fig4.25 that obtained settlement is minimum for 2% pre-tensioning, corresponding to 200kPa pressure.

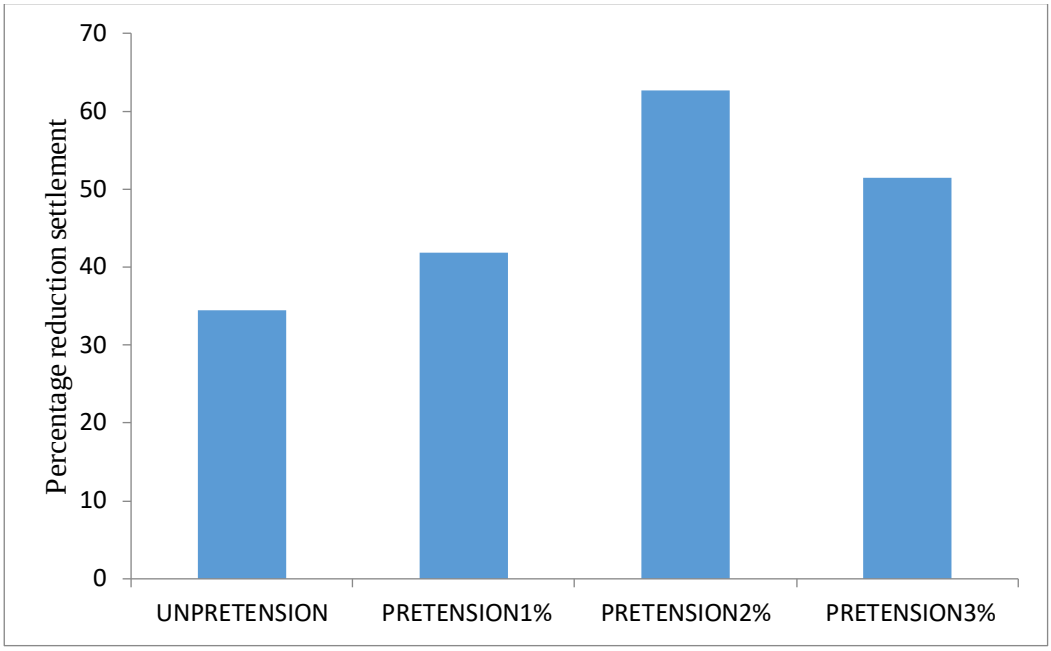

Figure 4.26 Percentage reduction in settlement of footing for Test series 2,3

From the fig 4.15 obtained result it is evident that the PRS for 2% pretension showed maximum value of 62.65% and hence it is identified that 2% pretension is the optimum for PRS consideration, corresponding to 200kPa pressure.

CHAPTER -5

CONCLUSIONS

The improvements in settlement behavior and load-bearing capacity of a geogrid-reinforced ferrochrome foundation were investigated using experimental and method. While the beneficial effects of pretensioning the geogrid prior to loading have been suggested in literature, no numerical or experimental analyses have been conducted to date to quantify these effects except Lovisa et al., (2010) . Thus, a physical model test with one layer of pretension geogrid as reinforcement was developed. Based on the test results obtained and analysis conducted, the following conclusions can be drawn:

1. The addition of pretension to the geogrid reinforcement significantly improved the settlement response and load bearing capacity of the soil.
2. The beneficial effects of geogrid reinforcement without pretension were insignificant for low strains (i.e. small displacements). However, the addition of pretension to the geogrid reinforcement improved the settlement response and load bearing capacity.
3. In unpretensioned system, there is marginal increase in allowable bearing capacity ratio at a low settlement of 5mm. With addition of prestress force, the allowable bearing capacity ratio at the same settlement increases significantly.
4. In unpretensioned condition, the amount of improvement is less even at higher settlement whereas in case of pretensioned condition the improvement is much higher at lower settlement ratio.

REFERENCES

1. Adams, M.T., Collin, J.G., 1997. Large model spread footing load tests on geosynthetic reinforced soil foundations. Journal of Geotechnical Engineering, ASCE 123 (1),66–72.
2. Andrawes, K.Z., McGown, A., Wilson-Fahmy, R.F., Mashhour, M.M., 1982. The finite element method of analysis applied to soil-geotextile systems. In: Proceedings of the Second International Conference of Geotextiles, LasVegas,USA, vol.3, 695–700.
3. Bowles, J.E., 1977. Foundation Analysis and Design, second ed. McGraw-Hill, New York. Das, B.M., 1999. Shallow Foundations: Bearing Capacity and Settlement. CRC Press.
4. Duncan, M., Chang, C.Y., 1970. Nonlinear analysis of stress and strain in soil. Journal of Soil Mechanics and Foundations, ASCE 96 (5), 1629–1653.
5. Guido, V.A., Biesiadecki, G.L., Sullivan, M.J., 1985. Bearing capacity of a geotextilereinforced foundation. In: Proceedings of 11th International Conference on Soil Mechanics and Foundation Engineering, San Francisco, USA, 1777–1780.
6. Guido, V.A., Chang, D.K., Sweeney, M.A., 1986. Comparison of geogrid and geotextile reinforced slabs. Canadian Geotechnical Journal 23, 435–440.
7. Huang, C.C., Menq, F.Y., 1997. Deep footing and wide-slap effects on reinforced sandy ground. Journal of Geotechnical and Geoenvironmental Engineering, ASCE 123 (1), 30–36.
8. Ismail, I., Raymond, G.P., 1995. Geosynthetic reinforcement of granular layered soil. In: Proceedings of Geosynthetics ’95 Conference, Nashville, TN, vol. 1. Industrial Fabrics Association International, Roseville, MN, USA, pp. 317–330.
9. Khing, K.H., Das, B.M., Puri, V.K., Cook, E.E., Yen, S.C., 1993. The bearing capacity of a strip foundation on geogrid-reinforced sand. Geotextiles and Geomembranes 12 (4), 351–361.
10. Koerner, R.M., 2005. Designing with Geosynthetics, fifth ed. Prentice Hall, New Jersey, USA.
11. Kurian, N., Beena, K.S., Kumar, R.K., 1997. Settlement of reinforced sand in foundations. Journal of Geotechnical Engineering 123 (9), 818–827.
12. Madhav, M.R., Poorooshasb, H.B., 1988. A new model for geosynthetic-reinforced soil. Computers and Geotechnics 6, 277–290.

13. Meyerhof, G.G., 1963. Some recent research on bearing capacity of foundations. Canadian Geotechnical Journal 1 (1), 16–26.
14. Milligan, G.W.E., Love, J.P., 1984. Model testing of geogrids under an aggregate layer in soft ground. In: Proceedings of the Symposium on Polymer. Grid Reinforcement in Civil Engineering, ICE, London.
15. Omar, M.T., Das, B.M., Puri, V.K., Yen, S.C., 1993. Ultimate bearing capacity of shallow foundations on sand with geogrid reinforcement. Canadian Geotechnical Journal 30, 545–549.
16. Patra, C.R., Das, B.M., Atalar, C., 2005. Bearing capacity of embedded strip foundation on geogrid-reinforced sand. Geotextiles and Geomembranes 23, 454–462.
17. Rowe, R.K., Soderman, K.L., 1987. Stabilization of very soft soils using high strength geosynthetics: the role of finite element analyses. Geotextiles and Geomembranes 6, 53–80.
18. Selvadurai, A.P.S., 1979. Elastic Analysis of Soil-Foundation Interaction. Elsevier Scientific Publishing Company, New York.
19. Shin, E.C., Das, B.M., 2000. Experimental study of bearing capacity of a strip foundation on geogrid-reinforced sand. Geosynthetic International 7 (1), 59–71.
20. Shukla, S.K., 2002. Geosynthetics and their Applications. Thomas Telford, London.
21. Shukla, S.K., Yin, J.H., 2006. Fundamentals of Geosynthetic Engineering. Taylor and Francis, London.
22. Shukla, S.K., 1995. Foundation model for reinforced granular fill – soft soil system and its settlement response. Ph.D. thesis, Department of Civil Engineering, Indian Institute of Technology, Kanpur, India.
23. Shukla, S.K., Chandra, S., 1994a. A generalized mechanical model for geosynthetic reinforced foundation soil. Geotextiles and Geomembranes 13, 531–543.
24. Shukla, S.K., Chandra, S., 1994b. A generalized mechanical model for geosynthetic reinforced foundation soil. Geotextiles and Geomembranes 13, 813–825.
25. Sitharam, T.G., Sireesh, S., 2004. Model studies of embedded circular footing on geogrid-reinforced sand beds. Ground Improvement 8 (2), 69–75.
26. Teng, W.C., 1962. Foundation Design. Prentice-Hall, Englewood Cliffs, N.J. Terzaghi, K., 1955. Evaluation of coefficients of subgrade reaction. Geotechnique 5(4), 297–326.

27. Yetimoglu, T., Wu, J.T.H., Saglamer, A., 1994. Bearing capacity of rectangular footingson geogrid-reinforced sand. Journal of Geotechnical Engineering, ASCE 120 (12),2083–2099.

List of Publication

Kumar, A., Choudhary, A.K. and Shukla S.K. "**Behaviour of strip footing resting on pretensioned geogrid-reinforced ferrochrome slag subgrade**" Abstract ID TH-05-007 accepted for full length paper submission. Full length paper is under review for consideration at Indian Geotechnical Conference 2018, to be held on 13-15 December, 2018, at IISc Bengaluru , India (Under Review) .